Study of Traveling Waves in a Nonlinear Continuum Dimer Model

Huaiyu Li

Submitted in partial fulfillment of the
requirements for the degree of
Doctor of Philosophy
under the Executive Committee
of the Graduate School of Arts and Sciences

COLUMBIA UNIVERSITY

2023

© 2023

Huaiyu Li

All Rights Reserved

Abstract

Study of Traveling Waves in a Nonlinear Continuum Dimer Model

Huaiyu Li

We study a system of semilinear hyperbolic PDEs which arises as a continuum approximation of the discrete nonlinear dimer array model of SSH type of Hadad, Vitelli and Alú in [1]. We classify the system's traveling waves, and study their stability properties. We focus on pulse solutions (solitons) on a nontrivial background and moving domain wall solutions (kinks and antikinks), corresponding to heteroclinic orbits for a reduced two-dimensional dynamical system. We further present analytical results on: nonlinear stability and spectral stability of supersonic pulses, and the spectral stability of moving domain walls. Our result for nonlinear stability is expressed in terms of appropriately weighted H^1-norms of the perturbation, which captures the phenomenon of *convective stabilization*; as time advances, the traveling wave "outruns" the growing disturbance excited by an initial perturbation. We use our analytical results to interpret phenomena observed in numerical simulations. The results for (linear) spectral stability are studied in appropriately-weighted L^2-norms.

Table of Contents

Acknowledgments . . . iv

Dedication . . . vi

Introduction and Overview . . . 1

Chapter 1: Physical Motivations and Problem Setup . . . 7

- 1.1 Linear SSH model . . . 7
- 1.2 HVA model . . . 9
- 1.3 Basic properties . . . 12
- 1.4 Overview of phenomena motivating this work . . . 13
  - 1.4.1 Convective stability and weighted spaces . . . 13
- 1.5 Summary of results . . . 15
- 1.6 Future directions, open questions . . . 16
  - 1.6.1 Spectral stability with respect to other, less constrained, norms . . . 16
  - 1.6.2 Nonlinear stability with respect to more general perturbations . . . 16
  - 1.6.3 Nonlinear stability of kinks . . . 17
  - 1.6.4 Periodic solutions . . . 17
  - 1.6.5 Relation between discrete and continuum models . . . 18
- 1.7 Notation and conventions . . . 18

Chapter 2: Traveling wave solutions 22

2.1 Basic properties of system (2.0.3) 22

2.2 Homoclinic traveling wave solutions; pulses and kinks 24

2.3 Convergence rate of heteroclinic orbits to asymptotic equilibria 27

2.4 A complete list of the bounded traveling wave solutions 28

Chapter 3: Nonlinear dynamics around traveling wave solutions 32

3.1 Local and global well-posedness 32

3.2 Proof of PROPOSITION 3.1 34

3.2.1 Self-mapping properties 35

3.2.2 Lipschitz properties on L^2 39

3.2.3 Lipschitz properties on H^1 39

3.3 Well-posedness results 41

3.4 Finite propagation speed 44

Chapter 4: Nonlinear convective stability of supersonic pulses 50

Chapter 5: Linearized stability analysis 55

5.1 Linearized spectral stability analysis of pulses and kinks; qualitative discussion . . 55

5.1.1 Exponentially weighted spaces 56

5.1.2 Linearized perturbation equation in a moving frame with speed $c \geq 0$ . . . 57

5.2 Spectral stability of equilibria 58

5.2.1 The trivial equilibrium 59

5.2.2 Nontrivial equilibria 60

Chapter 6: Strategy for studying TWS stability 65

6.1 Sketch of proof of PROPOSITION 6.1 66

Chapter 7: Supersonic pulses 73

7.1 Essential spectrum for supersonic pulses 74

7.2 Discrete spectrum for supersonic pulses 77

7.3 Remarks on instability of subsonic pulses and antikinks 80

Chapter 8: Spectral stability of kinks 82

8.1 Essential spectrum for kinks 82

8.2 Neutral spectral stability of Non-moving ($c = 0$) kinks 84

8.3 Spectral stability of moving kinks ($0 \leq c < 1$) 90

Conclusion or Epilogue 102

Appendix A: Numerical schemes for simulation 103

A.1 Dynamical simulation 103

References 106

Acknowledgments

I owe an immense debt of gratitude to my advisor, Professor Michael I. WEINSTEIN, for his support, trust, and guidance throughout and beyond my five-year doctoral journey. His mentorship has helped me strive to become a proficient researcher in the field of applied mathematics. In addition to his invaluable academic guidance, without which the results in this thesis would not have been possible, it was Michael who rekindled my hope and restored my confidence, during the harshest initial months of the Covid-19 pandemic. He encouraged me to keep my hopes alive and helped me maintain my strength, in the darkest hour of my years in the US as an international student.

I'd also like to express my sincere gratitude to the other members of my defense committee, Prof. DU Qiang, Prof. REN Kui, Dr. Amir SAGIV, and Dr. Andrew HOFSTRAND, for their expertise and invaluable feedback. I have had the privilege of working closely with Andrew on various projects during his three-year post-doctoral appointment at SEAS. His critical insights on developing numerical simulations were crucial for identifying key structures of the system the present work evolves around.

I am also grateful to my collaborators, peers and colleagues, Prof. Andrea Alù, Prof. Yakir HADAD, Prof. Alejandro ACEVES, Dr. ZHANG Lu, Dr. Ivan MITEVSKI, XU Zirui, Jonah CHABAN, Remy KASSEM, Jackson TURNER, Isabelle BUNGE, CHENG Yan, Dr. Alexander B. WATSON, Dr. Joseph KRAISLER, and Dr. LAI Chen-Chih. Their invaluable suggestions, profound insights, and stimulating discussions have not only deepened my understanding of the projects I've been involved in, but have also reinforced my pride in being a humble member of the applied mathematics community.

I have been fortunate to have the steadfast companionship of my dear friends over the years. I extend my heartfelt thanks to Dr. LI Weiyi, LI Boting, GUO Xufei, Dr. SUN Guanhao, Dr. SUN Xin, WANG Shiya, Dr. ZHOU Yang, ZHANG Xin, KONG Xiangyi, DONG Yinan, Dr. BAI Peiliang, Dr. MENG Tingyang, Dr. WANG Yuxiang, Dr. CHEN Dianteng, Dr. LI Shaokun, YIN Bingyu, CHAO Chun-lin, FEI Fan, ZHUANG Wei, HUANG Yuheng, Dr. ZHANG Kaijin, Dr. DENG Lingjia, Dr. HE Yilei, Mrs. Cara MITEVSKI and Dr. Ivan MITEVSKI. The memories of our shared moments will forever remain dear to me - from our lively strolls through the streets of NYC, to the countless hours spent laughing and reminiscing about the past while envisioning our futures. Thanks to my endearing furry friends, Sandy and Mia, *felibus catis domesticis*, and Xingxing, *cani lupi familiari*, for their loving cuddles.

I would like to send my gratitude to Dr. Nonso ENEKWECHI from Columbia's Counseling and Psychological Service, as well as Dr. Graham KAVANAGH. Their professional guidance and support have helped me manage the escalating stress as I neared the completion of my program.

I thank the City of New York, for its efficient public transportation and other services, and the staff of the Columbia University Public Safety team, for ensuring the security of our campus.

I have been supported partly by NSF grant DMS-1908657 and also Simons Foundation Math + X Investigator Award # 376319 awarded to Prof. Michael I. WEINSTEIN.

Throughout these lengthy years, despite our separation across the hemispheres, the love, support, and unwavering belief of my family have remained a constant. Their faith in me extends beyond what any earthly language can adequately express. To my father and mother, I want to convey my boundless love and pride. The prospect of our impending reunion in our subtropical hometown, after far too many years apart, fills me with immense joy.

I dedicate this thesis to my beloved Lao Lao, my late grandmother. May you rest in blissful peace.

献给姥姥。

Introduction and Overview

The present work studies a nonlinear hyperbolic system of PDEs with a rich family of traveling wave solutions (TWSs). Our study is inspired by work of Hadad, Vitelli and Alù (HVA) [1], and also an earlier work of Hadad et al.[2]. There, they introduce a nonlinear variant of the *discrete and linear* Su-Schrieffer-Heeger (SSH) dimer model. The linear SSH model was first introduced in the context of condensed matter physics, in Su et al.[3], to study topological properties of polyacetylene chains. The linear SSH model exhibit topological transitions, related to the closing and reopening of a spectral gap in its band structure. This transition is parametrized by the ratio of the chain's intra-cell to inter-cell coupling coefficients; the spectral gap closes when the ratio is unity. In [1], the authors (HVA) generalized it to a model of an electric array of coupled *nonlinear* circuit elements. In the same work, a continuum model was introduced to describe the dynamic of envelopes modulating Bloch waves at the (linear) band crossing wave number. They found traveling pulse solutions (solitons) and traveling domain wall solutions (kinks). They also reported on numerical simulations of the time evolution of the the *discrete system*, with initial data sampled from continuum solitons and kinks. The continuum model can be nondimensionalized and scaled to become (1.0.1), which we study in this thesis.

In this thesis, we present analytical results for the system (1.0.1)*, on* $\mathbb{R}_y \times \mathbb{R}_t$ *governing a real-valued unknown*

$$b(y,t) = \begin{bmatrix} u(y,t) & v(y,t) \end{bmatrix}^{\mathsf{T}}$$

We focus on the nonlinear stability and spectral stability analysis of heteroclinic traveling wave *solutions.*

The present work is organized as follows:

1. We start with CHAPTER 1, discussing motivations behind this work. In SECTION 1.1, we briefly discuss the SSH model, in particular, how it has different topological phases. In SECTION 1.2, we review the experimental setup of the HVA model, which exhibits *intensity-induced* topological phase transition. We then present the mathematical framework of our study of (1.0.1). In SECTION 1.3, we list assumptions on the nonlinearity profile $\mathcal{N}(r^2)$, consistent with the original nonlinearity used by Hadad et al. in [1]. In PROPOSITION 1.2, the discrete symmetries of (1.0.1) are displayed. These discrete symmetries are shared by the system's traveling wave solutions (PROPOSITION 2.1) and their linearized spectra (THEOREM 6.7). In SECTION 1.4, we summarize observed phenomena of convective stability of the traveling wave solutions of system (1.0.1). A rigorous proof of nonlinear convective stability of supersonic pulses (THEOREM 4.1). We also discuss open questions and future directions not addressed in the present work, as well as different directions which hopefully can bifurcate from the currently available results, in SECTION 1.6.

2. In CHAPTER 2 we present a complete classification of the **traveling wave solutions** (TWS) of (1.0.1). In particular, we solve for the profiles of the traveling wave solutions in a reference frame traveling with speed $c \neq \pm 1$, where the spatial coordinate is denoted $x = y - ct$. Phase plane analysis can then be applied to the resulting 2-real-dimensional dynamical system (2.0.3), whose properties are summarized in SECTION 2.1. The traveling wave solutions then can be identified with the orbits of (2.0.3). These orbits are connected subsets of *level sets* of a conserved quantity E_c, see (2.1.1). The only homoclinic orbits of (2.0.3) are *fixed points*. Non-fixed point TWSs have two speed regimes, $|c| > 1$ (**supersonic**) and $|c| < 1$ (**subsonic**). We restrict our study to TWSs given by the heteroclinic orbits of (2.0.3), which asymptote to different equilibria/fixed points. Although periodic TWSs (wave trains) exist, we do not address their stability properties in this thesis.

We then introduce the discrete symmetries on the family of traveling wave solutions in PROPOSITION 2.1 to greatly compress work on their classification. We then focus on *supersonic pulses* and *kinks* in SECTION 2.2. In SECTION 2.3, we calculate the convergence rates of their profiles to their asymptotic equilibria at $\pm\infty$. These results are crucial in understanding the role of translation modes in linear stability analysis of supersonic pulses and kinks. Lastly we give in SECTION 2.4 an exhaustive list of all possible traveling wave solutions of (1.0.1), and display a "phase diagram" FIGURE 2.4 showing the type of TWS given on the E_c - c plane.

3. Let $b_*(y,t) = b_*(y-ct)$ denote a generic TWS. In CHAPTER 3 we study the nonlinear dynamics of perturbations on $b_*(y-ct)$. As mentioned above, we focus on heteroclinic TWSs. The profile of such a TWS asymptotes to a nonzero equilibria either as $x \to \infty$, as $x \to \infty$, or both. It is therefore challenging to provide an functional analytic framework for studying $b_*(y-ct) + B(y,t)$, where $B(y,t)$ is the perturbation on the TWS, observed in the lab frame. Instead, we restrict $B(y,t)$ itself to be decaying at $x = \pm\infty$, study its dynamic stability via the nonlinear PDE system for it. This equation is given in (3.4.1) in the lab frame. Local and global-in-time wellposedness results are presented in THEOREM 3.3 of SECTION 3.3. Here and in CHAPTER 4, the nonlinearity $\mathcal{N}(r^2)$ is assumed to be **saturable**, see SECTION 1.3. The hyperbolicity of system (3.4.1) gives rise to finite propagation speed of data, as summarized in PROPOSITION 3.4.

4. In CHAPTER 4, we prove the first major result, THEOREM 4.1, on the nonlinear convective stability of supersonic pulses. Intuitively speaking, if one is to travel with a *supersonic* pulse $b_*(x)$ with the speed $|c| > 1$ it travels at, however large the initial perturbation on b_* is, the profile of the pulse on $[R, \infty)$, where $R \in \mathbb{R}$ fixed but arbitrary, will eventually restore to almost the same as an unperturbed pulse, as long as the initial perturbation decays fast enough *in the direction in which it travels*. In other words, a supersonic pulse always outrun sufficiently rapidly decaying initial perturbations. The proof of THEOREM 4.1

consists of two previous results. The first one is that data of (3.4.1) propagates with finite speed, and the second is the *a priori* exponential rate of growth of data given in the wellposedness result THEOREM 3.3.

5. The rest of this work starting from CHAPTER 5 concerns the linear spectral stability analysis of heteroclinic TWSs. For the linear stability theory, we *no longer require* $\mathcal{N}(r^2)$ to be saturable. The spectral stability analysis is carried out in the reference frame traveling with same speed c of the TWS $b_*(x = y - ct)$, which we call *comoving* reference frames. In SECTION 5.1, motivated by the phenomena seen from the numerical simulations discussed in SECTION 1.4 and previous works, we introduce a class of weights, $W(x) = e^{w(x)}$, in SECTION 5.1.1, and associated weighted L^2 and H^1 function spaces, where convective stability can be appropriately accounted for. The resulting spaces are denoted L^2_w, H^1_w etc. In SECTION 5.1.2, we linearize the nonlinear equation (3.4.1) of perturbation B, and obtain its linearized version $\partial_t B = L_* B$. To study the linear stability of b_* in the weighted space L^2_w, it is equivalent to study the *unweighted* L^2-spectral theory of conjugated linear operators $L_{*,w}$, see DEFINITION 5.1. The **spectral stability** of b_* in L^2_w is equivalent to $\sigma(L_{*,w})$ being contained in the closed left-half complex plane. In SECTION 5.2 we study the spectral stability of equilibria, both trivial and nontrivial, in appropriately weighted spaces with weight $W(x) \sim e^{ax}$ and summarize the result in PROPOSITION 5.6. This result helps us to locate the *essential spectrum*, in the following chapters, of pulses and kinks.

6. In CHAPTER 6 we describe our strategy to study the spectral stability of TWSs. For a general operator L on a Banach space, in particular a Hilbert space, its spectrum $\sigma(L)$ can be decomposed uniquely into essential and discrete spectra. The operators $L_{*,w}$ have the property that their coefficients asymptote exponentially to constants as $x \to \pm\infty$. This holds because $b_*(x)$ asymptotes to its equilibria as $x \to \pm\infty$. As a result, the left- and right-asymptotic operators of $L_{*,w}$ are constant-coefficient. Moreover, they are exactly the weight-conjugated operators of the equilibria whose spectra we characterized in SECTION

5.2. PROPOSITION 6.1 enables us to systematically bound the *essential spectrum* of $L_{*,w}$ simply by bounding the spectra of its asymptotic operators. This is a well-established result and we only provide a sketch for its proof. In the next two chapters we will apply PROPOSITION 6.1 to the cases of supersonic pulses and kinks to locate their essential spectra, and to investigate whether it is possible to choose a weight $W(x) = e^{w(x)}$, so that b_* is spectrally stable in L^2_w space equipped with it. Concluding this chapter, we remark with THEOREM 6.7 that the weight-conjugated linearized operators of TWSs associated with certain discrete symmetries are identical, upon suitably transforming weights as well. This greatly simplifies our study of spectral stability. In particular, we only need study those TWSs with $c \geq 0$, and the result for $c < 0$ TWSs follows directly.

7. In CHAPTER 7 we study the spectral stability of supersonic pulses. We summarize the result in THEOREM 7.1, which says supersonic pulses are spectrally stable in L^2_a for some a. Here, $L^2_a := L^2(\mathbb{R}.e^{\alpha x}\,\mathrm{d}x)$. The proof consists of two parts. First, we locate the essential spectrum with the help of PROPOSITION 6.1, in SECTION 7.1; see PROPOSITION 7.3. Then, in SECTION 7.2 results from ODE theory on the growth rate of solutions of ODE preclude the existence of discrete spectrum of $L_{*,a}$ of a supersonic pulse, *to the right* of its essential spectrum; see PROPOSITION 7.4. We also briefly remark on the *instability* of *subsonic* pulses and antikinks, in SECTION 7.3. This instability result is a direct consequence of PROPOSITION 6.1 In fact, there are no such exponential type weight $W(x) = e^{w(x)}$, that such solutions (even at least one of their asymptotic equilibria as $x \to \pm\infty$) are spectrally stable.

8. The last chapter, CHAPTER 8, concludes the spectral stability of kinks, under the rather mild concavity requirement that the nonlinearity $\mathcal{N}(s)$ (where $s = r^2$) be concave for $s \in [0, 1]$. This requirement is met by, for example, $\mathcal{N}(r^2) = 1 - r^{2m}$ where $m = 1, 2, \cdots$. Kink solutions are *heteroclinic* orbits of dynamical system (2.0.3) that connect the trivial equilibrium to some nontrivial equilibria on the unit circle. Again applying PROPOSITION 6.1, PROPOSITION 8.1 gives us the condition of the weight w for a kink with speed $c \geq 0$ is

spectrally stable in L^2_w. We first treat the case $c = 0$, that of a non-moving kink, in SECTION 8.2, with more detail. In fact a nonmoving kink can be only made neutrally spectrally stable, namely, the spectrum of its weight-conjugated operator $L_{*,w}$ is entirely on the imaginary axis. This result is summarized in THEOREM 8.3. The method we use is to transform the eigenvalue problem $L_{*,w}B = \lambda B$ into locating the bound states of a linear Schrödinger operator (LEMMA 8.6). In this case we can conclude the zero eigenvalue is the only element of the point spectrum. On the other hand, in SECTION 8.3 we generalize the approach used in SECTION 8.2, and are able to conclude the nonexistence of *unstable* eigenvalues, when the essential spectrum of $L_{*,w}$ is contained in the closed left-half plane. The result for the spectral stability of a general kink ($|c| < 1$) is given by THEOREM 8.8 Towards the proof of this result, the crux of our method is to find an appropriate linear transformation (PROPOSITION 8.11), so that the resulting transformed problem can again be reduced to a generalized eigenvalue problem (8.3.28) given by second-order ordinary differential operator; this transformation is not as straightforward as the non-moving case and (8.3.28) is highly nonlinear in λ, the eigenvalue. In this case, the present work does not preclude the existence of stable and neutral eigenvalues apart from the neutral $\lambda = 0$, but is enough for us to conclude, with nonlinearity being concave, the spectral stability for a general kink.

Chapter 1: Physical Motivations and Problem Setup

We study a system of semi-linear hyperbolic PDEs:

$$\begin{aligned} u_t &= v_y + \mathcal{N}\big(u^2+v^2\big)v \\ v_t &= u_y - \mathcal{N}\big(u^2+v^2\big)u \end{aligned} \tag{1.0.1}$$

governing the time evolution of a real-valued unknown $b(y,t) = \begin{bmatrix} u(y,t) & v(y,t) \end{bmatrix}^{\mathsf{T}}$. The properties of the nonlinearity, $\mathcal{N}(\cdot)$ are discussed below in SECTION 1.3. We extensively account for the motivation behind (1.0.1) in SECTION 1.1.

1.1 Linear SSH model

The Su-Schrieffer-Heeger (SSH) model is one of the earliest and models in condensed matter physics which exhibit what physicists refer to as *topological phase transition*. In a series of paper by Su, Schrieffer and Heeger [3] [4][5], introduced and studied a model for *trans*-polyacetylene $(\mathrm{CH})_x$ chain. The SSH model describes, under *tight-binding* approximation of the π-electrons [3][6] and in *single-electron* picture[7], a chain of atoms on which a single delocalized electron "hops" back and forth, and on each of the atoms there is only one available orbital. Schematically, the SSH model describes the evolution of a state $|a\rangle$. See FIGURE 1.2. The bulk Hamiltonian is

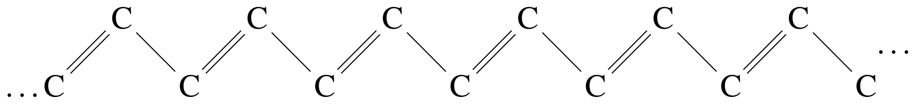

Figure 1.1: Dimerized polyacetylene chain with alternating single and double bonds.

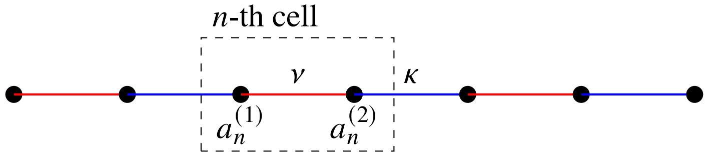

Figure 1.2: A schematic dimer chain in the SSH model

given by

$$H = \sum_{n\in\mathbb{Z}} \nu\big(|n,1\rangle\langle n,2| + |n,2\rangle\langle n,1|\big) + \kappa\big(|n+1,1\rangle\langle n,2| + |n-1,2\rangle\langle n,1|\big) \tag{1.1.1}$$

where $\nu, \kappa > 0$ and the summation is only formal. Here we have used the Dirac bra-ket notation [8] where $|n,1\rangle$ is the state/orbital on site-1 of the n-th cell, and $\langle n,2|$ is the orthogonal projection onto site-2 of the n-th cell, etc. Let the state vector be $|a\rangle$ and $a_n^{(1)} = \langle n,1|a\rangle$, $a_n^{(2)} = \langle n,2|a\rangle$, we have

$$\begin{aligned} \mathrm{i}\dot{a}_n^{(1)} &= \nu a_n^{(2)} + \kappa a_{n-1}^{(2)} \\ \mathrm{i}\dot{a}_n^{(2)} &= \nu a_n^{(1)} + \kappa a_{n+1}^{(1)} \end{aligned} \tag{1.1.2}$$

By Floquet-Bloch theory, the generalized eigenfunctions of this system is of the form $a_n(k) \sim e^{\mathrm{i}kn}A$, where $k \in \left[-\frac{\pi}{\Delta}, \frac{\pi}{\Delta}\right)$ where Δ is the lattice constant. Now the dispersion relation is given by solving

$$\det\begin{bmatrix} -\omega(k) & \nu + \kappa e^{-\mathrm{i}k\Delta} \\ \nu + \kappa e^{\mathrm{i}k\Delta} & -\omega(k) \end{bmatrix} = 0$$

whence

$$\omega(k) = \pm\left|\nu + \kappa e^{\mathrm{i}k\Delta}\right| = \pm\sqrt{\nu^2 + \kappa^2 + 2\nu\kappa\cos\left(k\Delta\right)} \tag{1.1.3}$$

The union of the images of $\omega(k)$ gives the **band** of system (1.1.2). If $\nu \neq \kappa$, it is impossible that the bands touch, namely the band gap closes, since it would require $\nu + \kappa e^{\mathrm{i}k\Delta} = 0$. So the band gap closes if and only if $\nu = \kappa$ at $k = \pm\frac{\pi}{\Delta}$, and the Bloch wave $a \sim e^{\pm\mathrm{i}\pi}B \sim (-1)^n B$ is "alternating" in amplitude; moreover, the energy at which the gap closes is $\omega(\pm\pi/\Delta) = 0$. See FIGURE 1.3, where the graphs of $\omega(k)$ with different choices of κ, while keeping ν constant, are plotted.

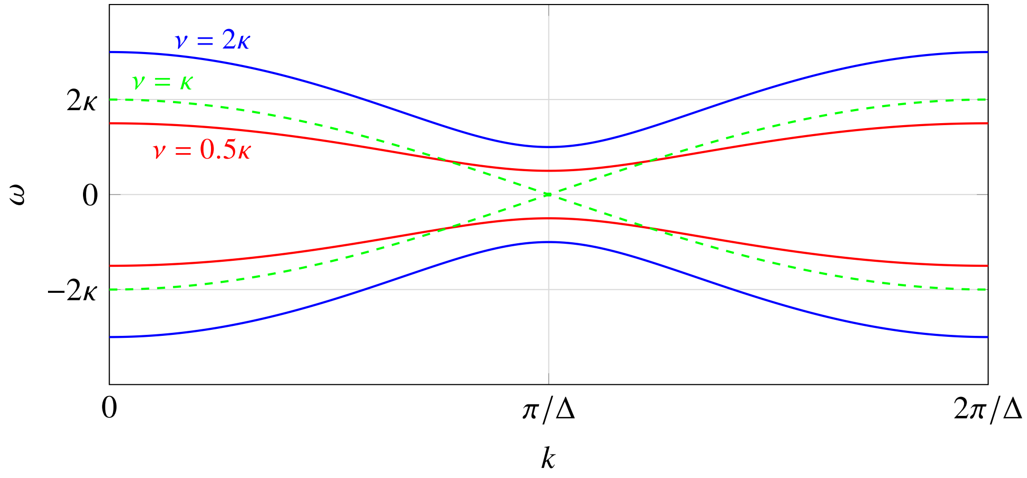

Figure 1.3: Dispersion relation of linear SSH model for different choices of ν and κ

1.2 HVA model

In [1], the *intracell* coupling ν of SSH system (1.1.2) is replaced with an amplitude-dependent nonlinear coupling coefficient:

$$\begin{aligned} -\mathrm{i}\dot{a}_n^{(1)} &= \omega_0 a_n^{(1)} + \nu\left(\left|a_n^{(2)} - a_n^{(1)}\right|^2\right) a_n^{(2)} + \kappa a_{n-1}^{(2)} \\ -\mathrm{i}\dot{a}_n^{(2)} &= \omega_0 a_n^{(2)} + \nu\left(\left|a_n^{(2)} - a_n^{(1)}\right|^2\right) a_n^{(1)} + \kappa a_{n+1}^{(1)} \end{aligned} \tag{1.2.1}$$

where ω_0 is the "self-resonance" frequency, or on-site energy of the hopping electron in the linear SSH model. $\nu(A_n^2)$ where $A_n = \left|a_n^{(2)} - a_n^{(1)}\right|$ is monotonically decreasing from $\nu_0 > \kappa$ to $\nu_\infty < \kappa$. We call this the **HVA model**. See FIGURE 1.4 for a schematic plot of the HVA model, analogous to FIGURE 1.2 for the (linear) SSH model. Experimentally, this system is realized by a chain of electric circuits, see FIGURE 1.4.

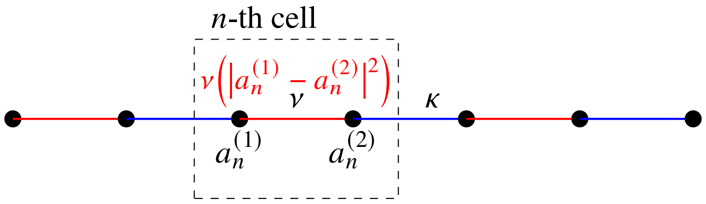

The infinite-dimensional dynamical system (1.2.1) is the original form which models the non-

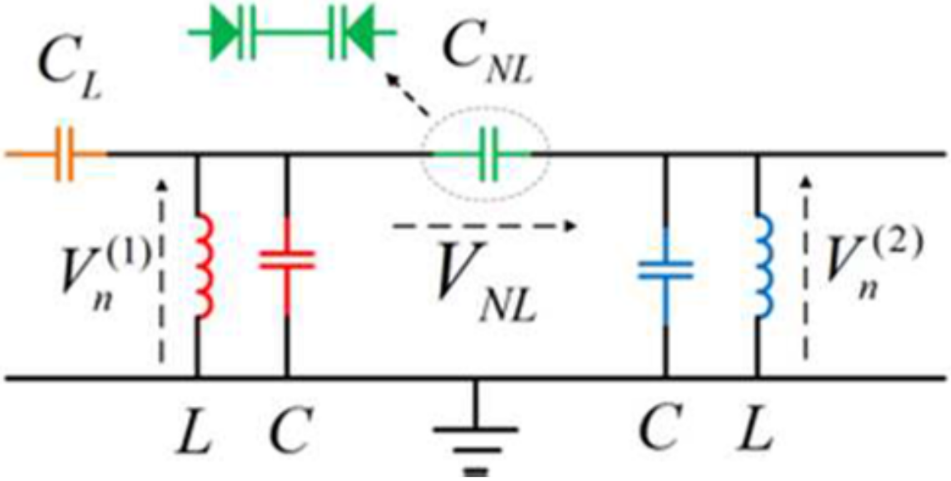

Figure 1.4: A unit cell of electric circuit chain implementing model (1.2.1), FIGURE 1(b) of [1].

linear version of SSH model introduced in [1]. There, the authors remark that (1.2.1) have an "local" intensity-induced topological phase change. In fact, if A_n is small, the intracell coupling is weaker than κ, corresponding to the topological trivial regime of (1.1.2), and if A_n is large, the topological nontrivial regime of (1.1.2). Since the band touch at $k = \pi/\Delta$, one can study the system by looking at slow-changing envelopes of Bloch wave $e^{ink} = (-1)^n$. The envelope profile a_n satisfies $a_n \sim (-1)^n b_n$, for $n \in \mathbb{Z}$.

Proposition 1.1 (Equivalent discrete system). *$\left\{a_n^{(1,2)}(t)\right\}_{n\in\mathbb{Z}}$ is a solution to the dynamical system* (1.2.1)*, if and only if there exists an infinite sequence of $\mathbb{C}^2$ vectors $\left\{b_n^{(1,2)}(t)\right\}_{n\in\mathbb{Z}}$, which is given by*

$$\begin{aligned} a_n^{(1)} &= (-1)^n \mathrm{i} e^{-\mathrm{i}\omega_0 t} B_0 b_n^{(1)}\left((\nu_0-\kappa)t\right) \\ a_n^{(2)} &= (-1)^n e^{-\mathrm{i}\omega_0 t} B_0 b_n^{(2)}\left((\nu_0-\kappa)t\right) \end{aligned} \tag{1.2.2}$$

and solves the DS

$$\begin{aligned} \dot{b}_n^{(1)} - \delta^{-1}\left(b_n^{(2)} - b_{n-1}^{(2)}\right) - \mathcal{N}\left(\left|b_n^{(1)} + \mathrm{i}b_n^{(2)}\right|^2\right) b_n^{(2)} &= 0 \\ \dot{b}_n^{(2)} - \delta^{-1}\left(b_{n+1}^{(1)} - b_n^{(1)}\right) + \mathcal{N}\left(\left|b_n^{(1)} + \mathrm{i}b_n^{(2)}\right|^2\right) b_n^{(1)} &= 0 \end{aligned} \tag{1.2.3}$$

Where the discreteness parameter $\delta = \frac{\nu_0}{\kappa} - 1$, $\nu_0 = \nu(0)$, and "threshold amplitude" B_0 is the *unique real number such that* $\nu(B_0^2) = \kappa$. *The scaled and always decreasing nonlinearity is given by*

$$\mathcal{N}(r^2) = \frac{\nu(B_0^2 r^2) - \kappa}{\nu_0 - \kappa} \tag{1.2.4}$$

Now formally replacing the difference in (1.2.3) by spatial differentiation:

$$\delta^{-1}\left(b_{n+1}^{(1)} - b_n^{(1)}\right) \longrightarrow \partial_y b_1(y = n\delta, t), \quad \delta^{-1}\left(b_n^{(2)} - b_{n-1}^{(2)}\right) \longrightarrow \partial_y b_2(y = n\delta, t)$$

and restrict $b_{1,2}^{(n)} = u, v$ to be real, whence

$$\mathcal{N}\left(\left|b_n^{(1)} + \mathrm{i} b_n^{(2)}\right|^2\right) = \mathcal{N}\left(u^2 + v^2\right)$$

we obtain the PDE system (1.0.1) the current work studies.

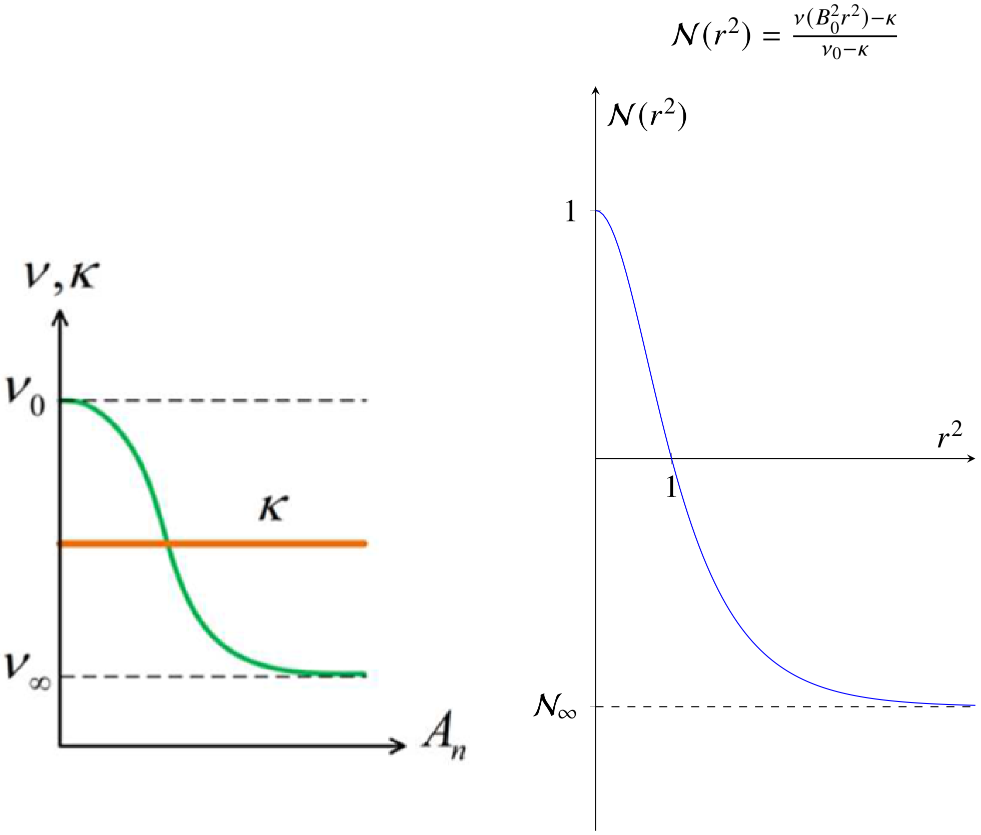

Figure 1.5: Left panel: profile of nonlinearity ν, FIGURE 1(c) of [1]. Right panel: a typical profile of a saturable nonlinearity (see SECTION 1.3) $\mathcal{N}(r^2)$.

1.3 Basic properties

We next set up the problem mathematically, discuss numerics which exhibit the phenomenon of convective stabilization of pulses and solitons, and summarize our analytical results.

Throughout this article, we make the following assumptions on the nonlinearity in (1.0.1):

($\mathcal{N}$1) $s \mapsto \mathcal{N}(s)$ is *monotonically decreasing* and smooth for $0 \leq s < \infty$.

($\mathcal{N}$2) $\lim_{s\to+\infty} \mathcal{N}(s) = \mathcal{N}_\infty \in [-\infty, 0)$

($\mathcal{N}$3) $\mathcal{N}(0) = 1$, $\mathcal{N}(1) = 0$

($\mathcal{N}$4) Let $\mathcal{N}'(s) := \mathrm{d}\mathcal{N}(s)/\,\mathrm{d}s$. We assume

$$K := -\mathcal{N}'(1) > 0. \tag{1.3.1}$$

We say that $\mathcal{N}(s)$ is a **saturable** nonlinearity if $\lim_{s\to+\infty} \mathcal{N}(s) = \mathcal{N}_\infty \in (-\infty, 0)$ exists and $\mathcal{N}(s)$ together with its derivatives converge sufficiently rapidly as $s \to \infty$. Otherwise, we say that $\mathcal{N}(s)$ is a **general** nonlinearity. An example of a saturable nonlinearity is $\mathcal{N}(r^2) = \frac{1-r^2}{1+r^2}$. An example of a general nonlinearity is $\mathcal{N}(r^2) = 1 - r^2$.

The system (1.0.1) is a semilinear hyperbolic system, whose characteristic lines are given by solutions of $dy/dt = \pm 1$. Any C^1 solution satisfies the conservation law

$$\partial_t\big(u^2 + v^2\big) + \partial_y\big(- 2uv\big) = 0. \tag{1.3.2}$$

The conservation law (1.3.2) plays a role in our classification of traveling wave solutions in CHAPTER 2 and in the proof and application of finite propagation speed in SECTION 3.4 and CHAPTER 4. The system (1.0.1) does not appear to be of Hamiltonian type. It has certain discrete symmetries which we summarize below.

Proposition 1.2 (Discrete Symmetries)**.** *System (1.0.1) has the following discrete symmetries. Assuming* $b(y,t) = [u(y,t), v(y,t)]$ *is a solution, then*

$$\begin{aligned}\big[\mathcal{P}b\big](y,t) &:= [-u(y,t), -v(y,t)]\\ \big[\mathcal{T}b\big](y,t) &:= [u(y,-t), -v(y,-t)]\\ \big[\mathcal{C}b\big](x,t) &:= [v(-y,-t), u(-y,-t)]\end{aligned}$$

are also solutions. Moreover,

$$\mathcal{P}^2 = \mathcal{T}^2 = \mathcal{C}^2 = \mathrm{id}$$

$$\mathcal{P}\mathcal{C} = \mathcal{C}\mathcal{P},\ \mathcal{P}\mathcal{T} = \mathcal{T}\mathcal{P},\ \mathcal{T}\mathcal{C} = \mathcal{C}\mathcal{P}\mathcal{T}$$

1.4 Overview of phenomena motivating this work

System (1.0.1) has spatially uniform equilibria: either $b = 0$ or those b for which $|b| = 1$ *viz.* $\mathcal{N}(b) = 0$. We classify the **traveling wave solutions** (TWS) of (1.0.1), $b_*(y,t) = b_*(x := y - ct)$, which tend to asymptotic equilibria at both infinities:

$$\lim_{x\to\pm\infty} b_*(x) = \text{constants}$$

These traveling wave solution profiles, $b_*(x)$, given by heteroclinic orbits in the phase portrait of a 2 dimensional dynamical system obtained from (1.0.1). We interpret numerically observed [9][1] stability of the **cores** of kinks and supersonic pulses with an appropriate notion of **spectral stability**; see DEFINITION 5.1.

1.4.1 Convective stability and weighted spaces

Consider a supersonic ($|c| > 1$) pulse, b_*, whose profile is a heteroclinic orbit connecting distinct equilibria satisfying $|b| = 1$. FIGURE 1.6 displays snapshots of the time-evolution of b_*

with a small and rapidly decaying (Gaussian) perturbation. A small and localized perturbation at $t = 0$ generates perturbations of the pulse which appear to travel to the left and away from the traveling pulse core (fixed in the moving frame of reference) while also growing in amplitude. Note that, in a frame of reference moving with speed $c > 0$, the deviation from an exact traveling wave profile, when measured within the "window" $[R, \infty)$, tends zero as t increases; perturbations exit the window at $x = R$ as t increases. Recall our convention that $x = y - ct$ is the spatial coordinate in the moving frame with speed c, where y is the spatial coordinate in the non-moving frame. We say that the supersonic pulse (or its core) is **convectively stable**. Other examples of convective stability have been considered in, for example, [10, 11, 12].

For saturable nonlinearities ($\mathcal{N}_\infty > -\infty$), the perturbation $B(y,t) = b(y,t) - b_*(y - ct)$ exists globally in time. However, our *a priori* bounds on the perturbation (see THEOREM 3.3) does not preclude $B(y,t)$ from growing without bound, for example in the L^∞ norm. As noted, the core of the traveling wave persists as it "outruns" perturbations that decays faster than some exponential rate dependent only on b_* and the nonlinearity. Such perturbations "lag behind" the supersonic pulse. For kink solutions which are shown to always be subsonic, the situation is more nuanced. However, we do observe in numerical simulations that the perturbation only grows as it moves in the *opposite* direction as is the speed of the underlying kink.

We capture this stabilization of the traveling wave core by working in **weighted** function spaces. In a reference frame *moving* with the traveling wave solution b_*, perturbations are studied as elements of spaces such as $H^1\left(\mathbb{R}; W(x)\,\mathrm{d}x\right)$. The weight $W(x)$ is chosen to be of the **exponential type** which is monotone and given by

$$W(x) = e^{w(x)}, \quad w(x) \in \mathbb{R};$$

see SECTION 5.1.1. If, in the *moving frame* (speed $c > 1$), the perturbation travels in the direction of decrease of $w(x)$ (to the left), then it can be registered in such spaces as decaying if its amplitude growth rate is not too large.

Remark 1.3. We note that numerical simulations of the nonlinear PDEs suggest that the perturbation of traveling wave may be growing without bound. (Note that we have no H^1 a priori bound on the solution; see THEOREM 3.3.) However, as time advances, the perturbation grows in regions which are further and further away from the traveling wave core. This behavior of the perturbation is registered as time-decay with respect to the weighted norm. This convective stability scenario differs from the more typical scenarios in solitary wave stability. For example, in KdV type equations, which are Hamiltonian and come with an *a priori* bound on the H^1 norm, the perturbation remains bounded and is in fact comprised of small amplitude solitary waves and a radiation component which together decay in appropriate weighted or local energy norms; see, for example, [10, 11].

1.5 Summary of results

We summarize the results of the present work:

- THEOREM 4.1: For saturable nonlinearities, with assumptions $(\mathcal{N}1)$-$(\mathcal{N}4)$ satisfied in SECTION 1.3 with $-\infty < \mathcal{N}_\infty < 0$), supersonic pulses (w.l.o.g. $c > 1$) are nonlinearly convectively stable, where the perturbation decays exponentially fast in time, when measured in $H^1([R, \infty))$ in a frame of reference with speed $c > 1$. In particular, we focus on the core of a supersonic pulse b_*.

- THEOREM 7.1: For more general nonlinearities, supersonic pulses are *spectrally stable* in an appropriate weighted L^2 space, denoted L^2_w; these weighted spaces are introduced in SECTION 5.1.1. More specifically, by spectral stability of a traveling wave, we mean that the L^2_w- spectrum of the linearized operator about the traveling wave profile, b_*, in a frame moving with its speed, c, is contained in the closed left half plane.

- *Spectral stability of kinks* ($|c| < 1$):

  (i) THEOREM 8.3: $c = 0$ (static / non-moving kinks).

(ii) THEOREM 8.8: $|c| < 1$ (moving kinks). Spectral stability of moving kinks, provided the nonlinearity, $\mathcal{N}$, satisfies the additional *concavity* assumption:

($\mathcal{N}$5) (Concavity) $\mathcal{N}(s)$ is *concave* on $s \in [0, 1]$; equivalently $\mathcal{N}'(s)$ is negative and monotonically decreasing on $s \in [0, 1]$, and as a result $\mathcal{N}''(s) \leq 0$,

then the kink is spectrally stable.

1.6 Future directions, open questions

We list some possible directions for future investigation and corresponding open questions.

1.6.1 Spectral stability with respect to other, less constrained, norms

Our stability results for pulses (nonlinear and spectral stability) and kinks (spectral stability) are formulated in function spaces, requiring exponential decay of the perturbation in the direction of propagation of the traveling wave. It would be of interest to extend these stability results to spaces with weaker spatial localization requirements; see, for example, [13], [11].

1.6.2 Nonlinear stability with respect to more general perturbations

Our results regarding nonlinear stability of supersonic pulses requires the initial perturbation to decay at a rate above some threshold (cf. THEOREM 4.1). It would be of interest to investigate the dynamics in the case where the perturbation's decay rate is slower. In fact, consider a supersonic pulse with speed $c > 1$. It can be perturbed into another pulse with speed $c' > c$, and such a perturbation indeed does not respect the decay rate bound. It would be interesting to formulate a selection rule for an asymptotically ($t \to +\infty$) emerging pulse. In particular, does decay rate of initial perturbation determine the pulse component of the solution that the perturbed pulse eventually settles down to? A paradigm is the well-known FKPP [14][15][16] equation exhibits such selection rules, where the final speed of the front solution depends on the decay rate of the initial condition.

1.6.3 Nonlinear stability of kinks

Our spectral stability analysis and numerical simulations (see FIGURE 1.7) suggest that the *family of spatial translates of a kink* is nonlinearly convectively stable. We conjecture the following: Let $b_*(x)$ denote a kink and $B_0(x)$ a sufficiently rapidly decaying initial perturbation. Then, there exists $x_0 \in \mathbb{R}$, depending on B_0 (and $b_*(x)$), such that the solution $b(x,t)$ to (2.0.1) with initial data $b_*(x) + B_0(x)$, satisfies

$$\lim_{t\to\infty} \left\| b(x,t) - b_*(x - x_0) \right\|_{H^1([R,\infty),dx)} = 0 \tag{1.6.1}$$

where $x = y - ct$ is the spatial coordinate in the moving frame with speed c, whereas y is the spatial coordinate in the non-moving frame. The phase shift in (1.6.1) is connected with the zero energy translation mode of the linearized operator, see THEOREM 8.8 and REMARK 8.9. In contrast, THEOREM 4.1 on nonlinear and convective (asymptotic) stability of supersonic pulses, requires no asymptotic phase adjustment. This is corroborated by numerical studies showing no phase shift in the emerging stable supersonic pulse, see FIGURE 1.6. Note: although there is a zero energy translation state of the linearized operator in this case as well, this state is not in the appropriate weighted L^2 space; see THEOREM 7.1 the discussion following PROPOSITION 7.4.

Another question is to clarify the scenario described in REMARK 1.3, which is based on numerical simulations. And a further technical question concerning kinks is whether, for example, spectral stability can be established if the concavity assumption ($\mathcal{N}5$) (used in (8.3.2)), on the nonlinearity, is relaxed.

1.6.4 Periodic solutions

System (1.0.1) has a rich family of periodic traveling wave solutions (periodic train waves) which correspond to nontrivial closed orbits of the 2-D dimensional dynamical system. Their stability is an open problem.

1.6.5 Relation between discrete and continuum models

Finally, system (1.0.1) is introduced in [1] as a formal continuum approximation for a nonlinear discrete array of coupled nonlinear circuits, valid for excitations whose spatial scale is slow on the inter-dimer length scale . After scaling and nondimensionalization, the discrete system takes the form (1.2.3). As demonstrated in [1] there is evidence of the pulse-like and kink-like behaviors in the discrete system (1.2.3). It is of interest to understand the relation between such behaviors that we study analytically and numerically in (1.0.1) and those observed, thus far only numerically, in (1.2.3). For example, on what time-scales do the coherent structures observed in the continuum system (1.0.1) persist for (1.2.3)?

1.7 Notation and conventions

1. Weighted spaces. Following the convention in [10], we define the **weighted spaces** with weight $W(x) = e^{w(x)}$ where $w(x)$ is a real-valued function on $\mathbb{R}$ as

$$L^2_w := L^2\big(\mathbb{R}, e^{w(x)}\,\mathrm{d}x\big), \quad H^1_w := \Big\{ f(x) \in L^1_{\mathrm{loc}} : \ e^{w(x)} f(x) \in H^1 \Big\} \tag{1.7.1}$$

   for details of the particular weighted spaces used in this work, see SECTION 5.1.1.

2. Coordinates. The linear stability analysis of this work is always conducted in the frame of references that travel at the same speeds of the underlying traveling wave solutions. For this reason, we denote with y the spatial coordinate in the non-moving (lab) frame of reference, cf. (1.0.1), and with $x = y - ct$ the spatial coordinate in the frame of reference traveling with some speed c, cf. (2.0.1).

3. Default branch of the square root function. We define function $z \mapsto \sqrt{z}$ in such a way that its values have non-negative real parts. In particular, $\sqrt{1} = 1$ and $\sqrt{z}$ is conformal from the cut complex plane, $\mathbb{C} \setminus (-\infty, 0]$, to the open right-half plane $\big\{\mathtt{Re}\, z > 0\big\}$. For $z \le 0$, $\sqrt{z}$ is continued from above the cut and its values always have non-negative imaginary parts, e.g.,

$\sqrt{-1} = \mathrm{i}$.

4. Pauli matrices. We use the standard convention of defining Pauli matrices, $\sigma_0, \sigma_1, \sigma_2$ and σ_3, as a set of basis in the linear space of 2-by-2 complex matrices:

$$\begin{aligned} \sigma_0 &= \begin{bmatrix} 1 & 0 \\ 0 & 1 \end{bmatrix}, \qquad \sigma_1 = \begin{bmatrix} 0 & 1 \\ 1 & 0 \end{bmatrix} \\ \sigma_2 &= \begin{bmatrix} 0 & \mathrm{i} \\ -\mathrm{i} & 0 \end{bmatrix}, \qquad \sigma_3 = \begin{bmatrix} 1 & 0 \\ 0 & -1 \end{bmatrix} \end{aligned} \tag{1.7.2}$$

These matrices have the following commutation and anti-commutation relations:

$$\begin{aligned} &\sigma_i \sigma_j = -\sigma_j \sigma_i \text{ for } i, j = 1, 2, 3 \text{ and } i \neq j \\ &\sigma_i^2 = \sigma_0. \end{aligned} \tag{1.7.3}$$

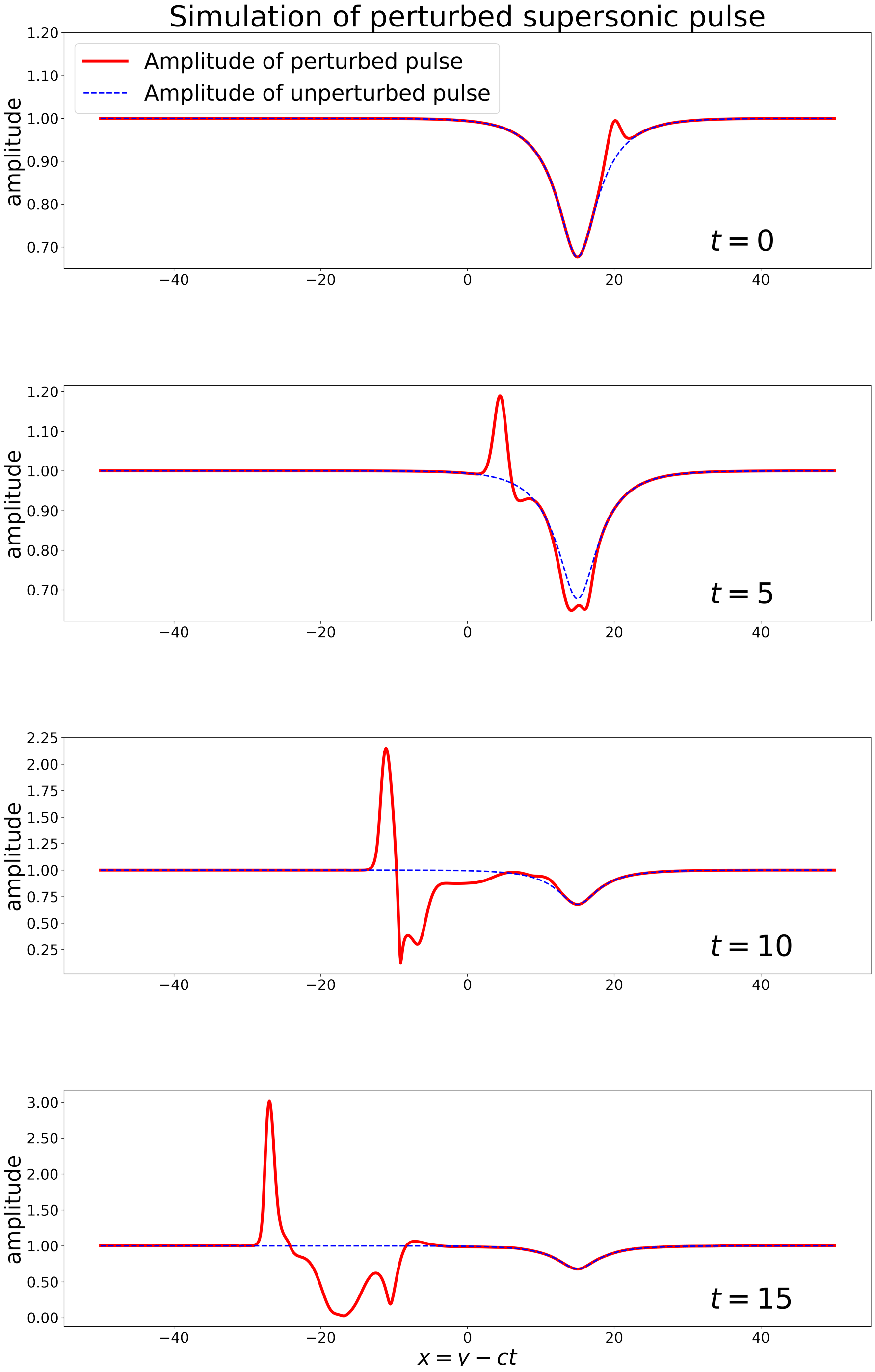

Figure 1.6: Convective stability. Snapshots of perturbed supersonic ($c = 2 > c_0 = 1$) pulse of (1.0.1)) in a reference frame of the same speed. Perturbation at $t = 0$ is concentrated to the right of its core. Red curve indicates the solution amplitude at different times. Blue dashed curves indicate the amplitude profile of the unperturbed TWS. The amplitude scales of the different panels are increasing with t, and perturbations becomes increasingly large as compared to the unperturbed pulse, but lags behind and the core is almost restored without any phase shift at $t = 15$.

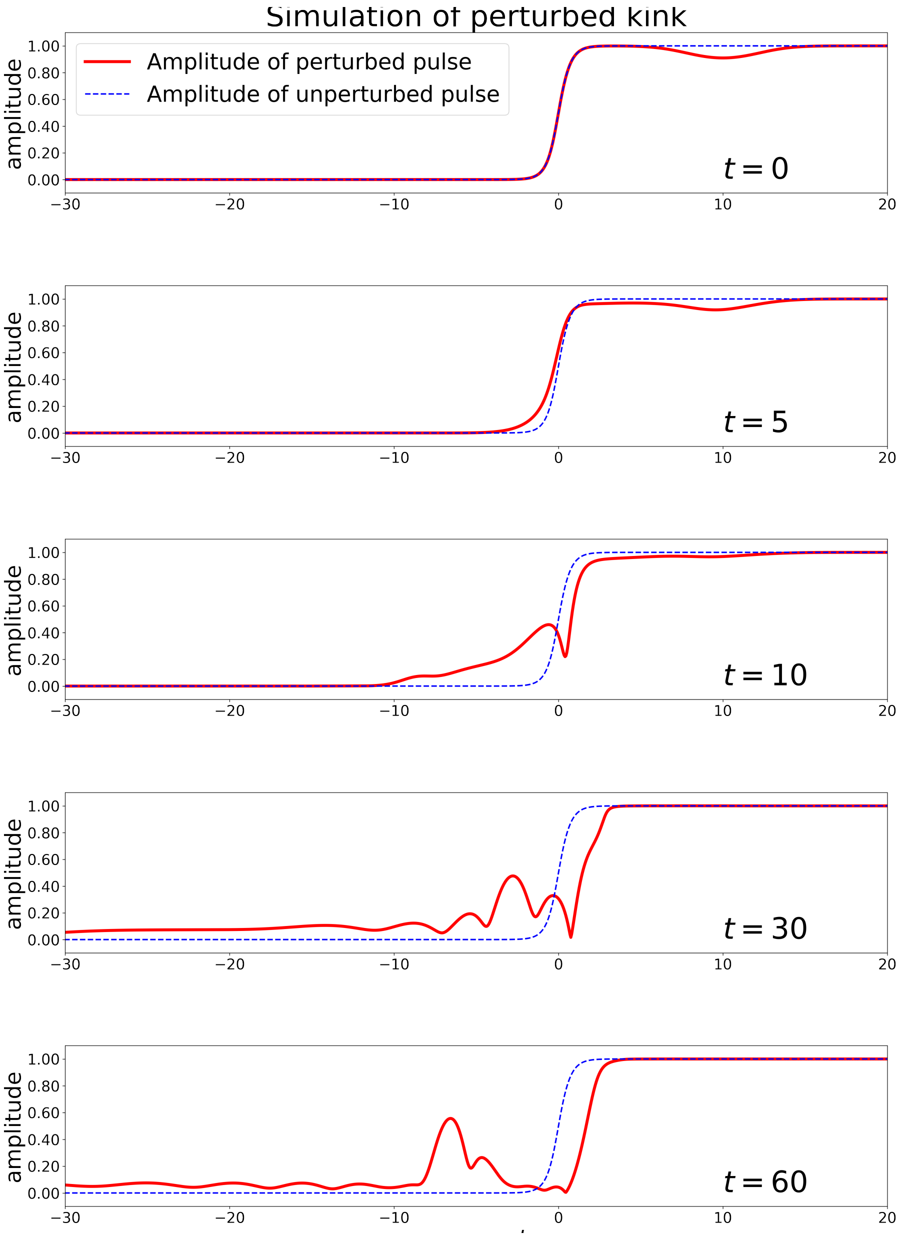

Figure 1.7: Numerical evidence for kink's convective stability. Snapshots of perturbed kink ($c = 0.9$) of (1.0.1)) in a reference frame of the same speed. Perturbation at $t = 0$ is concentrated to the right of its core. Red curve indicates the solution amplitude at different times. Blue dashed curves indicate the amplitude profile of the unperturbed TWS. The perturbation leaves the kink to the left, stabilizing in amplitude and travels to the left. The core is almost restored *with a phase shift* at $t = 60$.

Chapter 2: Traveling wave solutions

In a moving frame of speed $c \neq \pm 1$, (1.0.1) becomes the following, where the spatial coordinate is denoted by $x := y - ct$:

$$\begin{aligned} u_t &= cu_x + v_x + \mathcal{N}(u^2+v^2)v \\ v_t &= u_x + cv_x - \mathcal{N}(u^2+v^2)u \end{aligned} \tag{2.0.1}$$

For $c \neq 1$, the system (2.0.1) has the **equilibria**:

$$b_* = b_O = \begin{bmatrix} 0 \\ 0 \end{bmatrix} \quad \text{and} \quad b_* = b_\theta = \begin{bmatrix} \cos\theta \\ \sin\theta \end{bmatrix} \quad \text{where } \theta \in \mathbb{R}/2\pi\mathbb{Z} \tag{2.0.2}$$

The profile of a **traveling wave solution** (TWS) profile, $b_* = \begin{bmatrix} u(x) & v(x) \end{bmatrix}^\mathsf{T}$, of speed $c \neq \pm 1$ is an orbit of the dynamical system

$$\begin{aligned} u' &= \frac{\mathcal{N}(u^2+v^2)}{1-c^2}\big(u + cv\big) \\ v' &= \frac{\mathcal{N}(u^2+v^2)}{1-c^2}\big(-cu - v\big) \end{aligned} \tag{2.0.3}$$

If $|c| > 1$, we say the TWS is *supersonic* and if $|c| < 1$ say that it is *subsonic*.

2.1 Basic properties of system (2.0.3)

(i) The set of fixed points consists exactly of the origin O, and $\partial B_1(0) = \{(u,v) : u^2 + v^2 = 1\}$, irrespective of speed c; note that $\mathcal{N}(1) = 0$ as required in SECTION 1.3.

(ii) There is a conserved quantity E_c on any orbit $b(x) = \begin{bmatrix} u(x) & v(x) \end{bmatrix}^\mathcal{T}$ of (2.0.3) with speed $|c| \neq 1$.

$$E_c(u,v) = \frac{-1+c}{2}(u-v)^2 + \frac{1+c}{2}(u+v)^2 = c(u^2+v^2) + 2uv \tag{2.1.1}$$

which may be referred to as E_c, $E_c[b]$ etc., when the context is clear.

For a fixed c, the level curves

$$\Gamma_c(E) = \{(u, v) : E_c(u, v) = E\}$$

are families either of hyperbolas , for $|c| < 1$,with a fixed pair of asymptotes depending only on c; or of ellipses, for $|c| > 1$, of fixed eccentricity which again only depend on c.

In particular

(a) For $-1 < c < 1$ and $E \neq 0$, E_c can be expressed as

$$E_c(u, v) = \frac{\left((u + v)/\sqrt{2}\right)^2}{\left(1/\sqrt{1+c}\right)^2} - \frac{\left((-u + v)/\sqrt{2}\right)^2}{\left(1/\sqrt{1-c}\right)^2} = E \tag{2.1.2}$$

stands for the equation of a pair of hyperbolas of which the asymptotes are obtained by setting $E = 0$,

$$u\left(\sqrt{1+c} \pm \sqrt{1-c}\right) = v\left(-\sqrt{1+c} \pm \sqrt{1-c}\right) \tag{2.1.3}$$

(b) For $-1 < c < 1$ and $E = 0$, $\Gamma_c(E) = \Gamma_c(0)$ is a pair of asymptote lines (2.1.3).

(c) $\Gamma_c(E)$ is an ellipse if either both $c > 1$ and $E > 0$, or both $c < -1$ and $E < 0$. WLOG let $c > 1$ and let E_0 be given, the equation

$$E_c(u, v) = \frac{\left((u + v)/\sqrt{2}\right)^2}{\left(1/\sqrt{1+c}\right)^2} + \frac{\left((-u + v)/\sqrt{2}\right)^2}{\left(1/\sqrt{-1+c}\right)^2} = E \tag{2.1.4}$$

is that of an ellipse if and only if $E > 0$, whose long axis is on line $u = -v$, and whose short axis is on line $u = v$. Similarly, let $c < -1$ then if and only if $E < 0$, $\Gamma_c(E)$ is an ellipse given again given by (2.1.4) but whose long axis is on line $u = v$, and whose short axis is on line $u = -v$.

(d) For $|c| > 1$, the image of $\Gamma_c(0)$ is O, the origin; if $c > 1$ and $E < 0$ (or $c < -1$ and $E > 0$) then $\Gamma_c(E) = \varnothing$.

(iii) The images of an orbit is either a fixed point of (2.0.3), or is a subset of a level curve $\Gamma_c(E)$; in the latter case, it is a connected component of $\Gamma_c(E) \setminus (O \cup \partial B_1(0))$ for some $c \neq \pm 1$ and $E \in \mathbb{R}$ provided $\Gamma_c(E)$ is not empty.

(iv) System (2.0.3) has no homoclinic orbit except for fixed points.

In the following proposition, we discuss relations among traveling wave orbits, which are implied by the symmetries of (1.0.1). A TWS with speed c and conserved quantity E given by (2.1.1) will be denoted $b_{c,E}$

Proposition 2.1 (Discrete symmetries of the family of traveling wave solutions)**.** *Let $b(x)$ be the* ***profile*** *of a TWS with speed c. The corresponding solution $b(y-ct)$ of (1.0.1) can be transformed into other TWSs under* ***discrete*** *transformations $\mathcal{P}$, $\mathcal{T}$ and C given in* PROPOSITION *1.2. In particular, the profiles of and corresponding conserved quantity E_c of the transformed traveling wave solution is listed below.*

(i) $\mathcal{P}b(x)$ is a TWS with speed c whose profile is $-b(x)$ and $E_c[\mathcal{P}b] = E_c[b(x)]$.

(ii) $\mathcal{T}b(x)$ is a TWS with speed $-c$ whose profile is $\sigma_3 b(x)$ and $E_{-c}[\mathcal{T}b] = -E_c[b(x)]$.

(iii) $Cb(x)$ is a TWS with speed c whose profile is $\sigma_1 b(-x)$ and $E_c[Cb] = E_c[b(x)]$.

Remark 2.2. **N.B.** In view of PROPOSITION 2.1 we shall focus, particularly in our stability analyses, on the case of right-moving pulses and kinks, $c \geq 0$. The linearized spectra of TWSs indeed observe these symmetries, see THEOREM 6.7. A complete classification of all TWS solutions, and their relation through discrete transformations, is given in APPENDIX 2.4.

2.2 Homoclinic traveling wave solutions; pulses and kinks

System (2.0.3) has fixed points at the origin and on the unit circle, and apart from which there are no homoclinic orbits. There are periodic orbits in the supersonic regime, which we do not study in this work. Of particular interest are so-called **kink/antikink** (moving domain wall) solutions and **pulse** solutions.

A kink solution $b_{c,0}(x)$ with $0 < c < 1$ is an orbit connecting the origin to the unit circle, with $E[b_{c,0}] = 0$, while its amplitude grows to 1 as $x \to \infty$. The kink and antikink solutions are orbits which are parts the asymptotic lines of the family of hyperbolas given by (2.1.2), bounded by the trivial fixed point $b_O = \begin{bmatrix} 0 & 0 \end{bmatrix}^\mathsf{T}$ and some $b_\theta = \begin{bmatrix} \cos\theta & \sin\theta \end{bmatrix}^\mathsf{T}$. Since the asymptotic lines go through the origin, for a fixed c, there is constant θ such that $u(x) = r(x)\cos\theta$ and $v(x) = r(x)\sin\theta$, where $r(x)$ is the amplitude of such solutions. In FIGURE 2.1 are plotted some representative kinks and antikinks, along with their discrete transformations. We define kinks to be solutions among those depicted in FIGURE 2.1 whose amplitudes grow in the same direction as the direction of its speed c, and antikinks to be those whose amplitudes decays in the direction of c.

Now plug $u(x) = r(x)\cos\theta$ and $v(x) = r(x)\sin\theta$ in (2.1.2) and set $E = 0$:

$$
\begin{aligned}
0 &= r^2 \frac{\left((\cos\theta + \sin\theta)/\sqrt{2}\right)^2}{\left(1/\sqrt{1+c}\right)^2} - r^2 \frac{\left((-\cos\theta + \sin\theta)/\sqrt{2}\right)^2}{\left(1/\sqrt{1-c}\right)^2} \\
\implies (1+c)\bigl(1+\sin 2\theta\bigr) &= (1-c)\bigl(1-\sin 2\theta\bigr)
\end{aligned}
$$

since $r(x) \neq 0$, and immediately we have

$$\sin 2\theta = -c \tag{2.2.1}$$

There are four $\theta \in \mathbb{R}/2\pi\mathbb{Z}$ that satisfy (2.2.1). Owing to PROPOSITION 2.1, we only need to work with $\theta_{c,0} = -\frac{1}{2}\arcsin c$ with $c \geq 0$. Namely, the eight orbits in FIGURE 2.1 are given by that of b_c which corresponds to the solid blue line in FIGURE 2.1a or its discrete transformations. Now from the first equation of (2.0.3):

$$
\begin{aligned}
r'(x)\cos\theta_{c,0} &= r \cdot \frac{\mathcal{N}\left(u^2+v^2\right)}{1-c^2}\bigl(\cos\theta_{c,0} - \sin\theta_{c,0}\sin 2\theta_{c,0} \\
&= \frac{r\mathcal{N}\left(r^2\right)}{1-c^2}\cos\theta_{c,0}\left(1 - 2\sin^2\theta_{c,0}\right) \\
&= \frac{r\mathcal{N}\left(r^2\right)}{1-c^2}\cos\theta_{c,0}\cos 2\theta_{c,0}
\end{aligned}
$$

since $\cos 2\theta_{c,0} = \sqrt{1-c^2}$ we have the following equation for the kink profile $b_c = b_{c,0}$

$$\begin{aligned} r'(x) &= \frac{r(x)\mathcal{N}(r(x)^2)}{\sqrt{1-c^2}}, \ r(0) = \frac{1}{2} \\ u(x) &= r(x)\cos\theta_{c,0} \\ v(x) &= r(x)\sin\theta_{c,0} \end{aligned} \tag{2.2.2}$$

where $r(x) > 0$ and $\theta_{c,0} = -\frac{1}{2}\arcsin c$. An antikink with $0 \leq c < 1$ is similar to a kink, except that its amplitude decays to 0 as $x \to \infty$.

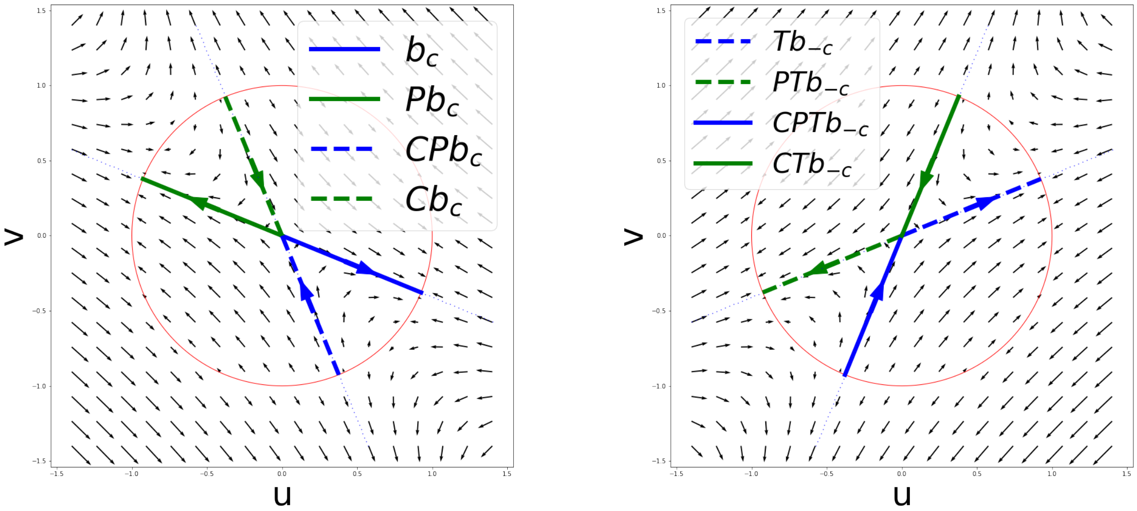

(a)

(b)

Figure 2.1: Kinks, antikinks and their relation through discrete symmetries. (a) $c \in [0,1)$ (b) $c \in (-1,0]$. In both of the plots, solid lines stand for kinks whose amplitudes $|b|$ increase in the same direction of their speed c; dashed lines are antikinks, whose amplitudes decrease *against* the direction of their speed c.

A pulse solution $b_{c,E}$ is a heteroclinic orbit connecting fixed points on the unit circle with speed c and $E_c[b_{c,E}] = E$ where E is bounded by

$$-1 + c < E < 1 + c$$

Depending on whether $|c| > 1$ or $|c| < 1$ they are called supersonic or subsonic pulses. For supersonic pulses which we will study extensively, we require $u(0) = v(0) = \sqrt{\frac{E}{2(c+1)}}$, corresponding to the solid blue line in FIGURE 2.2a and the solid green line in FIGURE 2.2b. Subsonic pulses are plotted in FIGURE 2.3.

2.3 Convergence rate of heteroclinic orbits to asymptotic equilibria

We next give formulas for the endpoints of the heteroclinic orbits, i.e., the equilibrium asymptotic states of traveling wave solutions, and then study the rates at which these equilibria are approached.

Assume that TWS, $b_*(x)$, with speed c and phase portrait energy $E_c[b_*] = E$ converges to an equilibrium (fixed point) $\begin{bmatrix}\cos\theta & \sin\theta\end{bmatrix}^\mathsf{T}$ as $x \to \infty$ or as $x \to -\infty$. Then, by (2.1.1), θ satisfies

$$E_c[b_*] = c + 2\cos\theta\sin\theta = E \quad \text{or} \quad \sin 2\theta = E - c. \tag{2.3.1}$$

There are four different solutions of (2.3.1):

$$\theta = \theta_{c,E} = -\frac{1}{2}\arcsin(E-c) \text{ or } \theta = \frac{\pi}{2} - \theta_{c,E}, -\frac{\pi}{2} - \theta_{c,E}, \pi + \theta_{c,E} \tag{2.3.2}$$

Along a trajectory in the phase portrait, as $(u(x), v(x))$ approaches its asymptotic state $\begin{bmatrix}u_0 & v_0\end{bmatrix}^\mathsf{T} = \begin{bmatrix}\cos\theta & \sin\theta\end{bmatrix}^\mathsf{T}$ on the circle, along the stable manifold of its asymptotic equilibria. The behavior, near an equilibrium (u_0, v_0), is characterized by the constant coefficient linearization of (2.0.3):

$$\frac{\mathrm{d}}{\mathrm{d}x}\begin{bmatrix}\delta u \\ \delta v\end{bmatrix} = -\frac{2K}{1-c^2}\begin{bmatrix}u_0 + cv_0 \\ -cu_0 - v_0\end{bmatrix}\begin{bmatrix}u_0 & v_0\end{bmatrix}\begin{bmatrix}\delta u \\ \delta v\end{bmatrix}. \tag{2.3.3}$$

The matrix in (2.3.3) has eigenpairs:

$$\mu = 0, \quad \vec{v}_0 = \begin{bmatrix} -v_0 \\ u_0 \end{bmatrix}, \tag{2.3.4}$$

$$\mu_\theta = -\frac{2K}{1-c^2}\cos 2\theta, \quad \vec{v}_\theta = \begin{bmatrix} u_0 + cv_0 \\ -cu_0 - v_0 \end{bmatrix} \tag{2.3.5}$$

Now we have the asymptotic behavior of kink $b_{c,0}$ as $x \longrightarrow \infty$:

$$\begin{bmatrix} \delta u(x) \\ \delta v(x) \end{bmatrix} \sim \begin{bmatrix} \cos\theta_{c,0} \\ \sin\theta_{c,0} \end{bmatrix} \exp\left(-\frac{2K}{\sqrt{1-c^2}}x\right) \tag{2.3.6}$$

and as $|x| \longrightarrow \infty$, for kinks

$$\begin{bmatrix} \delta u(x) \\ \delta v(x) \end{bmatrix} \sim \begin{bmatrix} u_{\pm\infty} + cv_{\pm\infty} \\ -cu_{\pm\infty} - v_{\pm\infty} \end{bmatrix} \exp\left(-\frac{2K}{c^2-1}\sqrt{1-(E-c)^2}|x|\right) \tag{2.3.7}$$

The translation modes $\partial_x b_*(x)$ has the same exponential decaying behavior, *viz.*, for kinks, as $x \longrightarrow \infty$,

$$\partial_x \begin{bmatrix} u(x) \\ v(x) \end{bmatrix} \sim \exp\left(-\frac{2K}{\sqrt{1-c^2}}x\right) \tag{2.3.8}$$

and as $|x| \longrightarrow \infty$, for supersonic pulses

$$\partial_x \begin{bmatrix} u(x) \\ v(x) \end{bmatrix} \sim \exp\left(-\frac{2K}{c^2-1}\sqrt{1-(E-c)^2}|x|\right) \tag{2.3.9}$$

2.4 A complete list of the bounded traveling wave solutions

The following list of *bounded* TWS types is exhaustive.

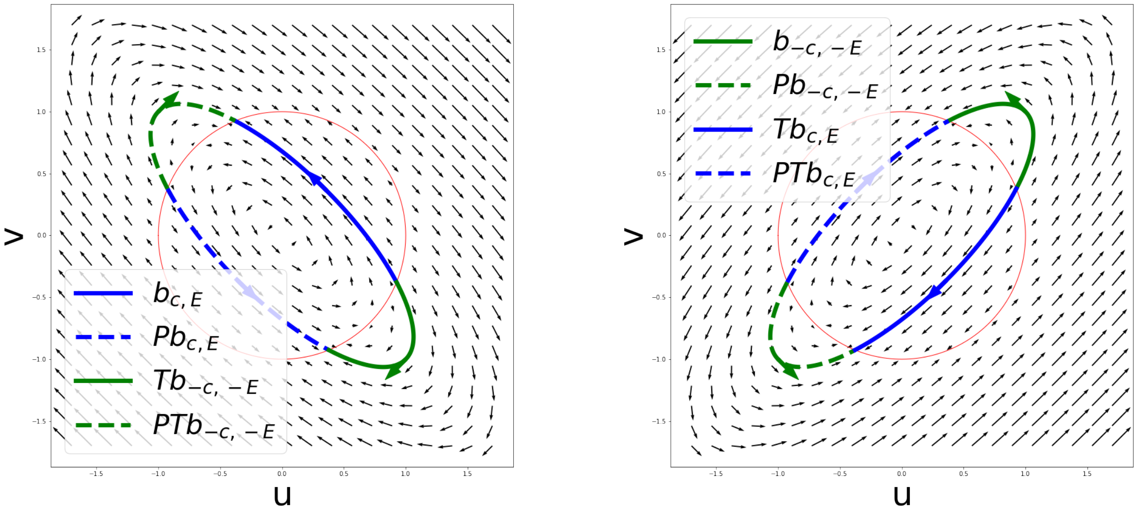

(a)

(b)

Figure 2.2: Supersonic pulses and their relation through discrete symmetries. (a) $c > 1$ (b) $c < -1$.

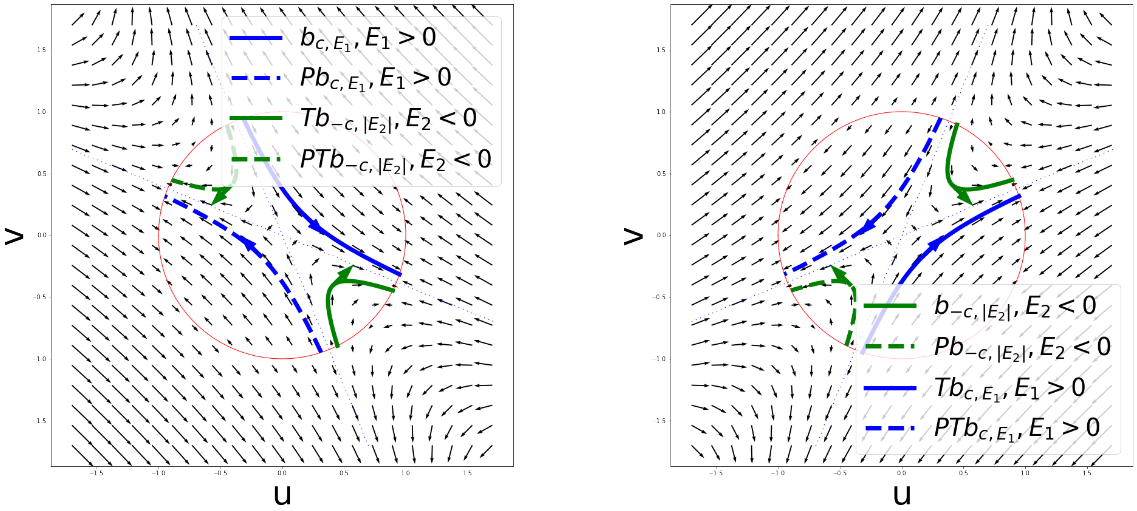

(a)

(b)

Figure 2.3: Subsonic pulses and their relation through discrete symmetries. (a) $c \geq 0$ (b) $c \leq 0$.

1. Equilibria. These corresponds to spatially constant time-independent solutions of (1.0.1):

$$\left\{[0,0]\right\} \cup \left\{\left[\cos\theta, \sin\theta\right] : \theta \in (-\pi, \pi]\right\}$$

which are TWSs of arbitrary speeds $c \in \mathbb{R}$.

2. Kinks and antikinks. For each $0 \le c < 1$, there are four kink-like solutions; in particular, they are $b_{c,0}, \mathcal{P}b_{c,0}$ which are kinks, and $\mathcal{C}\mathcal{P}b_{c,0}, \mathcal{C}b_{c,0}$ which are antikinks; for each $-1 < c \le 0$, there are four kink-like solutions. In particular, they are $\mathcal{C}\mathcal{P}\mathcal{T}b_{|c|,0} = \mathcal{T}\mathcal{C}b_{|c|,0}$, $\mathcal{C}\mathcal{T}b_{|c|,0}$ which are kinks, and $\mathcal{T}b_{|c|,0}, \mathcal{P}\mathcal{T}b_{|c|,0}$ which are antikinks. See FIGURE 2.1.

   TWSs of all the following types are invariant under $\mathcal{C}$.

3. Subsonic pulses. In each of the four following cases there are two subsonic pulse solutions. For each $0 \le c < 1$ and each $0 < E < 1 + c$ they are $b_{c,E}$ and $\mathcal{P}b_{c,E}$; for each $0 \le c < 1$ and each $-1 + c < E < 0$ they are $\mathcal{T}b_{-c,|E|}$ and $\mathcal{P}\mathcal{T}b_{-c,|E|}$; for each $-1 < c < 0$ and each $0 < E < 1 + c$ they are $\mathcal{T}b_{|c|,E}$ and $\mathcal{P}\mathcal{T}b_{|c|,E}$; for each $-1 < c < 0$ and each $-1 + c < E < 0$ they are $b_{c,|E|}$ and $\mathcal{P}b_{c,|E|}$. For each of the following cases there are four supersonic pulse solutions, except for the marginal cases which will be indicated. For each $c > 1$ and each $0 < -1 + c \le E \le 1 + c$, these are $b_{c,E}, \mathcal{P}b_{c,E}$ which respectively degenerates to $\pm[1,1]/\sqrt{2}$ at $E = 1 + c$, and $\mathcal{T}b_{-c,-E}$ and $\mathcal{P}\mathcal{T}b_{-c,-E}$ which respectively degenerates to $\pm[-1,1]/\sqrt{2}$ at $E = -1 + c$. For each $c < -1$ and each $-1 + c \le E \le 1 + c < 0$, they are $\mathcal{T}b_{|c|,|E|}$ and $\mathcal{P}\mathcal{T}b_{|c|,|E|}$ which respectively degenerates to $\pm[-1,1]/\sqrt{2}$ at $E = -1 - c$, and $b_{c,E}$ and $\mathcal{P}b_{c,E}$ which respectively degenerates to $\pm[1,1]/\sqrt{2}$ at $E = -1 + c$. See FIGURE 2.2.

4. Periodic wave trains. For each of the following cases there is one periodic wave train solution. In particular, for each $c > 1$ and $0 < E < 1 - c$, it is counterclockwise and "small"; for each $c > 1$ and each $E > 1 + c$, it is clockwise and "large"; for each $c < -1$ and $-1 + c < E < 0$ it is clockwise and "small"; for each $c < -1$ and each $E < -1 - c$ it is counterclockwise and "large".

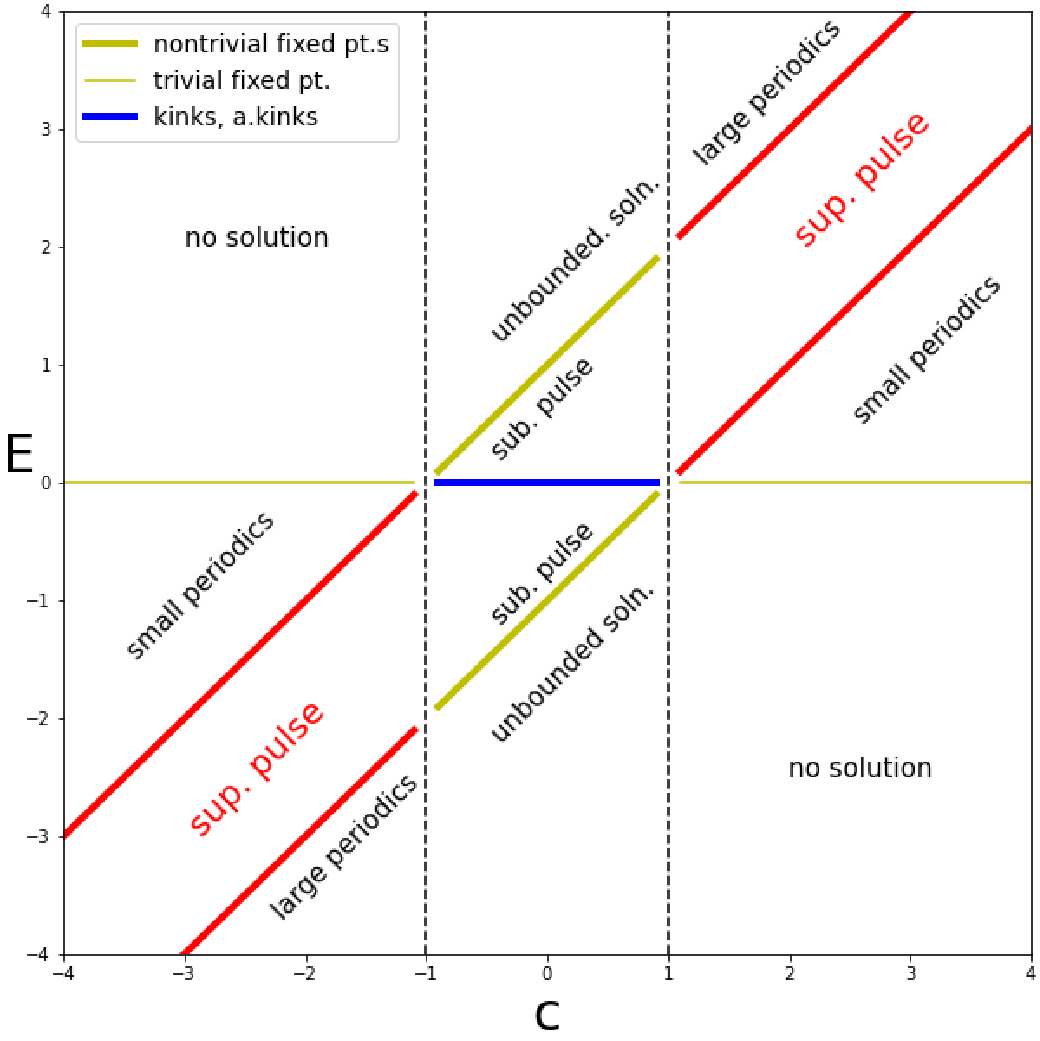

Figure 2.4: A phase diagram of traveling wave solutions of system (1.0.1), equivalently the orbits of (2.0.3)

Chapter 3: Nonlinear dynamics around traveling wave solutions

Only in this section, we require the nonlinearity to be **saturable**, see SECTION 1.3. We write down the PDE satisfied by a perturbation

$$B(x,t) = \begin{bmatrix} U(x,t) \\ V(x,t) \end{bmatrix}$$

on top of some TWS b_*, as (3.1.1). We then prove some well-posedness results with the help of standard fixed-point techniques and Grönwall integral inequalities. We also prove the finite propagation of data as a result of the hyperbolicity of (3.1.1), with energy-type arguments. With such result, we will provide a growth bound on arbitrary perturbations, as well as the convective stability of supersonic pulses, if the rate of decay of the initial perturbation $B_0(x)$ is fast enough as $x \longrightarrow \infty$.

3.1 Local and global well-posedness

Consider (2.0.1) with a perturbed TWS at $t = 0$. Let $b_0(x) = b_*(x) + B_0(x)$ where $B_0(x)$ is a perturbation on a TWS $b_*(x)$. Plug $b(x,t) = b_*(x) + B(x,t)$ in (2.0.1) then $B(x,t) = \begin{bmatrix} U(x,t) & V(x,t) \end{bmatrix}$ solves the IVP given by:

$$\begin{aligned} \begin{bmatrix} U \\ V \end{bmatrix}_t &= \Sigma \begin{bmatrix} U \\ V \end{bmatrix}_x + N_*\big(x; U(x,t), V(x,t)\big) \\ &:= \begin{bmatrix} c & 1 \\ 1 & c \end{bmatrix} \begin{bmatrix} U \\ V \end{bmatrix}_x + \begin{bmatrix} \mathcal{N}\big(r_*(x)^2\big)V \\ -\mathcal{N}\big(r_*(x)^2\big)U \end{bmatrix} + \begin{bmatrix} \delta\mathcal{N}_*(x; U, V)v_*(x) \\ -\delta\mathcal{N}_*(x; U, V)u_*(x) \end{bmatrix} \end{aligned} \tag{3.1.1}$$

where $r_*(x) \equiv |b_*(x)| = \sqrt{u_*^2(x) + v_*^2(x)}$ and

$$\delta\mathcal{N}_*(x; U, V) := \mathcal{N}\Big(\big(u_*(x) + U\big)^2 + \big(v_*(x) + V\big)^2\Big) - \mathcal{N}\big(u_*(x)^2 + v_*(x)^2\big) \tag{3.1.2}$$

with initial data $B(x,0) = B_0(x)$. By Duhamel's principle given initial data $B_0(x)$, we have another integral version of

$$B(x,t) = T_c(t)B_0(x) + \int_0^t T_c(t-t')N_*\big(x; B(x,t')\big)\,\mathrm{d}t' \tag{3.1.3}$$

with

$$T_c(t) = \exp\left(t\begin{bmatrix} c & 1 \\ 1 & c \end{bmatrix}\partial_x\right)$$

stands for a semigroup generated in spaces in which solutions are required to live. A solution $B(x,t)$ of (3.1.3) is called a **mild solution** of 3.1.1. Note that H^s can be defined (see CHAPTER 6 of [17]) to be those $f(x) \in \mathcal{D}'\big(\mathbb{R}\big)$ of which the Fourier transform satisfies:

$$\|f\|_{H^s}^2 := \int_{\mathbb{R}} (1 + |k|^2)^s \big|\hat{f}(k)\big|^2\,\mathrm{d}k < \infty$$

For $f \in H^s$, Fourier transform with respect to x of $T_c(t)f(x)$ gives

$$\big(T_c(t)f\big)^\wedge(k) = \exp\left(\mathrm{i}\begin{bmatrix} c & 1 \\ 1 & c \end{bmatrix}kt\right)\hat{f}(k)$$

Therefore $T_c(t)$ is a unitary group on H^s for all $s \in \mathbb{R}$ by Plancherel's identity. In particular, it is a unitary group on L^2 and H^1, which suffice for our application.

To prove the following well-posedness results, we will need some properties of the nonliearity N_* in (3.1.1) summarized in the following proposition and proved in APPENDIX 3.2:

Proposition 3.1. *Consider the nonlinear mapping $N_*(B) = N_*\big(x; U(x), V(x)\big)$ given implicitly in (3.1.1). N_* as a mapping only depends on the nonlinearity profile $\mathcal{N}_*(r^2)$ and the TWS b_*.*

For N_*, the following hold:

1. *N_* is* *globally* *Lipschitz on L^2. Namely, for any $B, \tilde{B} \in L^2$, there is a constant independent $B, \tilde{B}$, such that*

$$\left\|N_*(B) - N_*(\tilde{B})\right\|_{L^2} \leq C\left\|B - \tilde{B}\right\|_{L^2} \tag{3.1.4}$$

2. *N_* is* *locally* *Lipschitz on H^1. In particular, for any $B, \tilde{B} \in H^1$, there is a constant C independent of $B, \tilde{B}$ such that*

$$\left\|N_*(B) - N_*(\tilde{B})\right\|_{H^1} \leq C\Big(1 + \min\left\{\|B\|_{H^1}, \|\tilde{B}\|_{H^1}\right\}\Big)\left\|B - \tilde{B}\right\|_{H^1} \tag{3.1.5}$$

   As a special case, for any $B \in H^1$,

$$\left\|N_*(B)\right\|_{H^1} \leq C\|B\|_{H^1} \tag{3.1.6}$$

3.2 Proof of PROPOSITION 3.1

Recall

$$N_*\big(x; B\big) = \begin{bmatrix} \mathcal{N}\big(r_*^2\big)V + \delta\mathcal{N}_*\big(x; B\big)v_* \\ -\mathcal{N}\big(r_*^2\big)U - \delta\mathcal{N}_*\big(x; B\big)u_* \end{bmatrix} = \begin{bmatrix} \mathtt{I}_1 + \mathtt{II}_1 \\ \mathtt{I}_2 + \mathtt{II}_2 \end{bmatrix} \tag{3.2.1}$$

where $\mathcal{N}\big(r^2\big)$ is bounded, real-valued and sufficiently smooth, satisfying $\mathcal{N}(0) = 1$, $\mathcal{N}(1) = 0$ and $r^2 = 1$ is the only zero of $\mathcal{N}\big(r^2\big)$. Moreover, there is $\mathcal{N}_\infty < 0$ such that $\left|\mathcal{N}\big(r^2\big) - \mathcal{N}_\infty\right| = O\big(r^{-\alpha}\big)$ as $r \to \infty$, and for each $k = 1, 2, \cdots$ there is $C > 0$ such that $\left|\mathcal{N}^{(k)}\big(r^2\big)\right| = O\big(r^{-\alpha-k}\big)$ as $r \to \infty$. Moreover, b_*, the TWS we work with, as well as its components and all their derivatives with respect to x, asymptotes to their respective limits exponentially as $x \to \pm\infty$, and are all bounded, in particular. WLOG we only need to work out the estimate details for terms $\mathtt{I}_1$ and $\mathtt{II}_1$ in (3.2.1), since those for $\mathtt{I}_2$ and $\mathtt{II}_2$ are almost identical.

3.2.1 Self-mapping properties

Estimates for $\mathtt{I}_1$ on H^1

If $V \in H^1$ we have $\left\|N\left(r_*^2\right)V\right\|_{L^2} \leq C\left\|V\right\|_{L^2}$, also (V being weakly differentiable), for each x:

$$\left|\left[\mathcal{N}\left(r_*(x)^2\right)V(x)\right]_x\right| \leq \left|\mathcal{N}(r_*^2)V' + 2\mathcal{N}'(r_*^2)r_*r_*'V\right| \leq C\left[\left|V'(x)\right| + \left|V(x)\right|\right]$$

Thus

$$N\left(r_*(x)^2\right)V(x) \in H^1\left(\mathbb{R}_x\right)$$

$$\left\|N\left(r_*(x)^2\right)V(x)\right\|_{H^1\left(\mathbb{R}_x\right)} \leq C\left\|V\right\|_{H^1}$$

Where C only depends on b_* and the profile of $\mathcal{N}_*$.

Estimates for $\mathtt{II}_1$ in L^2

The following calculus lemma will be repeatedly used in the sequel.

Lemma 3.2. *Let $\eta \in \mathbb{R}^\ell$, and define*

$$F\left(x, \eta\right) \in C^1\left(\mathbb{R}_x \times \mathbb{R}^\ell_\eta, \mathbb{R}^k\right) \tag{3.2.2}$$

with ℓ, k being positive integers. Assume

(i) $F(x, 0) = 0$ for all $x \in \mathbb{R}$, and F is bounded.

(ii) There is a nonnegative continuous function $f \geq 0$ on $[0, \infty)$ such that

$$\left\|\frac{\partial F\left(x, \eta\right)}{\partial \eta}\right\|_{M^{\ell \times k}\left(\mathbb{R}\right)} \leq f\left(|\eta|\right)$$

uniformly for all $x \in \mathbb{R}$

Then there is a constant $C > 0$ such that, uniformly in $x \in \mathbb{R}$, there is

$$\left|F(x,\eta)\right| \le C|\eta|$$

Proof of LEMMA 3.2. For any $M > 0$ and for all $|\eta| \ge M$,

$$\left|F(x,\eta)\right| \le \|F\|_{L^\infty} \le \frac{\|F\|_{L^\infty}}{M}|\eta|$$

For $|\eta| \le M$, uniformly in x there is

$$\left|F(x,\eta)\right| \le \int_0^{|\eta|} f(r)\,\mathrm{d}r \le |\eta| \max_{r\in[0,M]} f(r)$$

Then uniformly in x and for all $\eta \in \mathbb{R}^\ell$, there is

$$\left|F(x,\eta)\right| \le \max\left\{\frac{\|F\|_{L^\infty}}{M}, \max_{r\in[0,M]} f(r)\right\}|\eta|$$

and we are done. □

Recall

$$\delta\mathcal{N}_*(x;U,V) = \mathcal{N}\Big(\big(u_*(x)+U\big)^2 + \big(v_*(x)+V\big)^2\Big) - \mathcal{N}\big(r_*(x)^2\big)$$

Now we apply LEMMA 3.2 to $B \mapsto \delta\mathcal{N}_*\big(x;B\big)v_*(x)$ which is continuously differentiable, bounded, and vanishes for $B = 0$. Moreover

$$\begin{aligned}
\left|\frac{\partial\delta\mathcal{N}_*\big(x;B\big)v_*(x)}{\partial B}\right| &= \left|2v_*\mathcal{N}'\Big(\big(u_*+U\big)^2 + \big(v_*+V\big)^2\Big)\begin{bmatrix} u_*+U \\ v_*+V \end{bmatrix}\right| \\
\le& C\sqrt{\Big[u_*(x)+U\Big]^2 + \Big[v_*(x)+V\Big]^2} \le C\sqrt{\|b_*\|_{L^\infty}^2 + 2\|b_*\|_{L^\infty}|B| + |B|^2} \\
\le& C\sqrt{1+|B|^2}
\end{aligned}$$

is uniformly bounded by an increasing and continuous function of $|B|$. Therefore LEMMA 3.2 can be applied to $F\big(x,B\big) = \delta\mathcal{N}_*\big(x;B\big)v_*(x)$, thus pointwise

$$\Big|\delta\mathcal{N}_*\big(x;B\big)v_*(x)\Big| \le C\Big|B(x)\Big|$$

For $B \in L^2$:

$$\delta\mathcal{N}_*\big(x;B\big)v_*(x) \in L^2$$

$$\big\|\delta\mathcal{N}_*\big(x;B\big)v_*(x)\big\|_{L^2} \le C\big\|B\big\|_{L^2}$$

for C only depending on b_* and $\mathcal{N}$ and we have:

$$\Big\|N_*\big(x;B\big)\Big\|_{L^2} \le C\big\|B\big\|_{L^2}$$

Estimates for $\mathtt{II}_1$ on H^1

We only need to prove the derivative in x of $\delta\mathcal{N}_*\big(x;B\big)v_*(x)$ namely the following function is in L^2:

$$\Big[\delta\mathcal{N}_*\big(x;B(x)\big)v_*(x)\Big]_x = \big(\delta\mathcal{N}_*\big(x;B(x)\big)\big)_x\, v_*(x) + \delta\mathcal{N}_*\big(x;B(x)\big)v_*'(x)$$

Apply LEMMA 3.2 to $\delta\mathcal{N}_*(x;B)v_*'(x)$ there is

$$\Big|\delta\mathcal{N}_*(x;U,V)v_*'(x)\Big| \le C\Big|B(x)\Big|$$

thus

$$\delta\mathcal{N}_*(x;U,V)v_*'(x) \in L^2$$

$$\big\|\delta\mathcal{N}_*(x;U,V)v_*'(x)\big\|_{L^2} \le C\big\|B\big\|_{L^2}$$

For a fixed $x \in \mathbb{R}$,

$$\begin{aligned}
&\left(\frac{\mathrm{d}}{\mathrm{d}x}\delta\mathcal{N}_*(x;B)\right)v_*(x)\\
=&2\bigg[\mathcal{N}'\left(\left(u_*+U\right)^2+\left(v_*+V\right)^2\right)\left[\left(u_*+U\right)\left(u_*'+U'\right)+\left(v_*+V\right)\left(v_*'+V'\right)\right]\\
&-\mathcal{N}'\left(u_*^2+v_*^2\right)\left(u_*u_*'+v_*v_*'\right)\bigg]v_*\\
=&2\left[\mathcal{N}'\left(\left|b_*(x)+B(x)\right|^2\right)\left(b_*(x)+B(x)\right)\cdot\left(b_*'(x)+B'(x)\right)-\mathcal{N}'\left(\left|b_*(x)\right|^2\right)b_*(x)\cdot b_*'(x)\right]v_*(x)
\end{aligned}$$

We only need to estimate the expression inside $\left[\cdots\right]$, since $|v_*|$ is bounded:

$$\begin{aligned}
&\left|\mathcal{N}'\left(\left|b_*(x)+B(x)\right|^2\right)\left(b_*(x)+B(x)\right)\cdot\left(b_*'(x)+B'(x)\right)-\mathcal{N}'\left(\left|b_*(x)\right|^2\right)b_*(x)\cdot b_*'(x)\right|\\
\le&\left|\mathcal{N}'\left(\left|b_*(x)+B(x)\right|^2\right)\left(b_*(x)+B(x)\right)\cdot B'(x)\right|\\
&+\left|\left[\mathcal{N}'\left(\left|b_*(x)+B(x)\right|^2\right)\left(b_*(x)+B(x)\right)-\mathcal{N}'\left(\left|b_*(x)\right|^2\right)b_*(x)\right]\cdot b_*'(x)\right|\\
\le&C\left|B'(x)\right|+C\left|B(x)\right|
\end{aligned}$$

the first term can be bounded because $\mathcal{N}'(r^2)$ decays fast enough as $r \to \infty$ so $\mathcal{N}'\left(r^2\right)r$ is bounded since it is also continuous. Then we apply to the second term LEMMA 3.2 and note that $b_*'(x)$ is bounded. Therefore

$$\left|\left(\frac{\mathrm{d}}{\mathrm{d}x}\delta\mathcal{N}_*(x;B)\right)v_*(x)\right|\le C\left(\left|B(x)\right|+\left|B'(x)\right|\right)$$

$$\left\|\left(\frac{\mathrm{d}}{\mathrm{d}x}\delta\mathcal{N}_*(x;B)\right)v_*(x)\right\|_{L^2\left(\mathbb{R}_x\right)}\le C\left\|B\right\|_{H^1}$$

Thus we have:

$$\left\|\mathcal{N}_*\left(x;B(x)\right)\right\|_{H^1\left(\mathbb{R}_x\right)}\le C\left\|B\right\|_{H^1}$$

for a constant $C > 0$ depending only on b_* and $\mathcal{N}$.

3.2.2 Lipschitz properties on L^2

$\mathtt{I}_1$ is trivially globally Lipschitz

$\mathtt{I}_1 = \mathcal{N}\big(r_*(x)^2\big)V(x)$ is trivially globally Lipschitz in $B(x)$ since it is linear in V.

Lipschitz property of $\mathtt{II}_1$

Let $\tilde{B} = \big[\tilde{U}, \tilde{V}\big] \in \mathcal{X} = L^2$. Note that

$$\Big|\nabla\mathcal{N}\big(|B|^2\big)\Big| = 2\Big|\mathcal{N}'\big(|B|^2\big)\Big|\big|B\big|$$

is bounded:

$$\begin{aligned}
&\Big|\delta\mathcal{N}_*\big(x; B(x)\big)v_*(x) - \delta\mathcal{N}_*\big(x; \tilde{B}(x)\big)v_*(x)\Big|\\
\le&\left|\mathcal{N}\Big(\big|b_*(x) + B(x)\big|^2\Big) - \mathcal{N}\Big(\big|b_*(x) + \tilde{B}(x)\big|^2\Big)\right|\big\|v_*\big\|_{L^\infty}\\
\le&\big|B(x) - \tilde{B}(x)\big| \sup_{s\in[0,1]} \left|\nabla\mathcal{N}\Big(|b_*(x) + (1-s)B(x) + s\tilde{B}(x)|^2\Big)\right|\\
\le&C\big|B(x) - \tilde{B}(x)\big|
\end{aligned}$$

Integrating both sides we have

$$\big\|\delta\mathcal{N}_*\big(x; B(x)\big)v_*(x) - \delta\mathcal{N}_*\big(x; \tilde{B}(x)\big)v_*(x)\big\|_{L^2\left(\mathbb{R}_x\right)} \le C\big\|B - \tilde{B}\big\|_{L^2}$$

Doing the same estimate for $\mathtt{I}_2$ and for $\mathtt{II}_2$ and we have obtained the global Lipschitz property:

$$\Big\|N_*\big(x; B(x)\big) - N_*\big(x; \tilde{B}(x)\big)\Big\|_{L^2\left(\mathbb{R}_x\right)} \le C\big\|B - \tilde{B}\big\|_{L^2}$$

3.2.3 Lipschitz properties on H^1

$\mathtt{I}_1$ is trivially globally Lipschitz on H^1

$\mathtt{I}_1 = \mathcal{N}\big(r_*(x)^2\big)V(x)$ is trivially globally Lipschitz since it is linear in V for $B \in H^1$ and $\mathcal{N}\big(r_*(x)^2\big)$ is smooth in x.

Lipschitz property of $\mathtt{II}_1$

Now we estimate

$$\begin{aligned}
&\left\| \left[\Big(\delta\mathcal{N}_*\big(x; B(x)\big) - \delta\mathcal{N}_*\big(x; \tilde{B}(x)\big) \Big) v_*(x) \right]_x \right\|_{L^2(\mathbb{R}_x)} \\
\leq &\left\| \big(\delta\mathcal{N}_*\big(x; B(x)\big) - \delta\mathcal{N}_*\big(x; \tilde{B}(x)\big) \big)_x \, v_*(x) \right\|_{L^2(\mathbb{R}_x)} \\
&+ \left\| \big(\delta\mathcal{N}_*\big(x; B(x)\big) - \delta\mathcal{N}_*\big(x; \tilde{B}(x)\big) \big) \, v_*'(x) \right\|_{L^2(\mathbb{R}_x)}
\end{aligned}$$

the second term can be estimated similarly as in is the L^2 Lipschitz estimate above:

$$\left\| \big(\delta\mathcal{N}_*\big(x; B(x)\big) - \delta\mathcal{N}_*\big(x; \tilde{B}(x)\big) \big) \, v_*'(x) \right\|_{L^2(\mathbb{R}_x)} \leq C \left\| B - \tilde{B} \right\|_{L^2}$$

To estimate the first term, note that

$$\begin{aligned}
&\left| \frac{1}{2} \left(\delta\mathcal{N}_*\big(x; B(x)\big) - \delta\mathcal{N}_*\big(x; \tilde{B}(x)\big) \right)_x \right| = \left| \frac{1}{2} \left[\mathcal{N}\Big(\big| b_*(x) + B(x) \big|^2 \Big) - \mathcal{N}\Big(\big| b_*(x) + \tilde{B}(x) \big|^2 \Big) \right]_x \right| \\
= &\left| \mathcal{N}'\Big(\big| b_*(x) + B(x) \big|^2 \Big) \big(b_*(x) + B(x) \big) \cdot \Big(b_*'(x) + B'(x) \Big) - \mathcal{N}'\Big(\big| b_*(x) + \tilde{B}(x) \big|^2 \Big) \big(b_*(x) + \tilde{B}(x) \big) \cdot \Big(b_*'(x) + \tilde{B}'(x) \Big) \right| \\
\leq &\left| \mathcal{N}'\Big(\big| b_*(x) + B(x) \big|^2 \Big) \big(b_*(x) + B(x) \big) \right| \left| B'(x) - \tilde{B}'(x) \right| \\
&\left| \mathcal{N}'\Big(\big| b_*(x) + B(x) \big|^2 \Big) \big(b_*(x) + B(x) \big) - \mathcal{N}'\Big(\big| b_*(x) + \tilde{B}(x) \big|^2 \Big) \big(b_*(x) + \tilde{B}(x) \big) \right| \left| b_*'(x) + \tilde{B}'(x) \right| \\
=: &\,\mathtt{III} + \mathtt{IV}
\end{aligned} \tag{3.2.3}$$

Term $\mathtt{III}$ is bounded pointwise by

$$C \left| B'(x) - \tilde{B}'(x) \right|$$

since $\mathcal{N}'\big(r^2\big) r$ is bounded. For term $\mathtt{IV}$, set $\eta = B - \tilde{B}$ and define

$$F(x, \eta) := \mathcal{N}'\Big(\big| b_*(x) + \tilde{B}(x) + \eta \big|^2 \Big) \big(b_*(x) + \tilde{B}(x) + \eta \big) - \mathcal{N}'\Big(\big| b_*(x) + \tilde{B}(x) \big|^2 \Big) \big(b_*(x) + \tilde{B}(x) \big)$$

Then F is a bounded function of η, and continuously differentiable, vanishes for $\eta = 0$. Consider the gradient of $F(x,\eta)$ with respect to η for a fixed $x \in \mathbb{R}$ (suppressing explicit dependence on x):

$$\begin{aligned}\frac{\partial F}{\partial \eta} =& 2\mathcal{N}''\Big(\big|b_* + \tilde{B} + \eta\big|\Big)\big(b_* + \tilde{B} + \eta\big)\big(b_* + \tilde{B} + \eta\big)^{\mathsf{T}} + \\ &+ \mathcal{N}'\Big(\big(b_* + \tilde{B} + \eta\big)\Big)\sigma_0\end{aligned}$$

Both of the terms are bounded uniformly for all η. Therefore applying LEMMA 3.2 on $F\big(x,\eta\big)$, and note that

$$\mathtt{IV} = \Big|F\big(x, B(x) - \tilde{B}(x)\big)\Big|\Big|b_*'(x) + \tilde{B}'(x)\Big|$$

there is

$$\begin{aligned}\mathtt{IV} \leq& C\Big|B(x) - \tilde{B}(x)\Big|\Big|b_*'(x) + \tilde{B}'(x)\Big| \\ \leq& C\Big(\Big|B(x) - \tilde{B}(x)\Big|\Big|b_*'(x)\Big| + \Big|B(x) - \tilde{B}(x)\Big|\Big|\tilde{B}'(x)\Big|\Big)\end{aligned}$$

Where C here is a constant only depending on the profile of $\mathcal{N}$.

Thus integrating $\mathtt{III}$ and $\mathtt{IV}$,

$$\begin{aligned}&\Big\|\Big(\delta\mathcal{N}_*\big(x; B(x)\big) - \delta\mathcal{N}_*\big(x; \tilde{B}(x)\big)\Big)v_*(x)\Big\|_{H^1} \\ \leq& C\Big\|B - \tilde{B}\Big\|_{L^2} + C\Big\|B' - \tilde{B}'\Big\|_{L^2} + C\|\tilde{B}'\|_{L^2}\Big\|B - \tilde{B}\Big\|_{L^\infty} \\ \leq& C\Big(1 + \|\tilde{B}\|_{H^1}\Big)\Big\|B - \tilde{B}\Big\|_{H^1}\end{aligned}$$

The last inequality is due to Sobolev embedding.

3.3 Well-posedness results

The following global well-posedness results in H^1 hold:

Theorem 3.3 (Global well-posedness of the mild solution of (3.1.1))**.** *For $B_0 \in H^1$, there exists a unique global mild solution $B(x,t) \in C^0\Big([0,\infty)_t, H^1\big(\mathbb{R}_x\big)\Big)$ of (3.1.1), and the H^1 norm of the* *perturbation grows at most exponentially:*

$$\left\|B\right\|_{H^1} \leq Ce^{Ct}\left\|B_0\right\|_{H^1} \tag{3.3.1}$$

where C does not depend on B_0, but only on $\mathcal{N}$ and b_*. Moreover, $B(\cdot,t)$ is a strong solution to (3.1.1) in L^2 with $B_0 \in H^1 \subset L^2$, namely $B(x,t) \in C^1L^2$.

The proof for local well-posedness is standard with the application of Banach's fixed point theorem, see for example THEOREM 1 of [18]; the hypotheses on the nonlinearity term N_* are given and checked in PROPOSITION 3.1 The global existence follows readily:

Proof of THEOREM *3.3*. First we prove the local well-posedness with standard Banach fixed-point approach.

Recall the mild solution is defined to be $B(\cdot,t) \in H^1$ satisfying, for all $t \in [0,T]$,

$$B(x,t) = T_c(t)B_0(x) + \int_0^t T_c(t-s)N_*\big(x; B(x,s)\big)\,\mathrm{d}s$$

where the C_0-semigroup is well-defined and is generated by $\Sigma\partial_x$. We now define

$$\eta(x,t) := B(x,t) - T_c(t)B_0(x) \tag{3.3.2}$$

The proof is standard with the application of Banach's fixed point theorem, see for example THEOREM 1 of [18], of which the hypothesis are satisfied by 3.1.3 by virtue of PROPOSITION 3.1. We present the proof here for completeness.

Now 3.1.3 becomes the following fixed-point problem:

$$\eta(t,x) = \mathcal{F}\big(\eta(t,x)\big) := \int_0^t T_c(t-s)N_*\big(x; \mathtt{T}_c(s)B_0(x) + \eta(x,s)\big)\,\mathrm{d}s \tag{3.3.3}$$

Note that $\mathtt{T}_c(t)$ is a unitary group.

Now fix $R > 0$. For $\|B_0\|_{H^1} \leq R$ we have, for $\eta \in X_T$ satisfying $\left\|\eta\right\|_{X_T} \leq R$ there is

$$\begin{aligned}
&\left\|\mathcal{F}(\eta)\right\|_{X_T} \\
=&\sup_{t\in[0,T)} \left\|\int_0^t T_c(t-s) N_*\big(x; T_c(s)B_0(x) + \eta(x,s)\big)\,\mathrm{d}s\right\|_{H^1\left(\mathbb{R}_x\right)} \\
\leq& T \sup_{t\in[0,T)} \left\|N_*\big(x; T(t)B_0(x) + \eta(x,t)\big)\right\|_{H^1\left(\mathbb{R}_x\right)} \\
\leq& R
\end{aligned} \tag{3.3.4}$$

The last inequality holds if we choose T to be small enough, and this choice depends on $\|B_0\|$. The last line holds since we have the local Lipschitz estimate of N_*. Therefore for a ball $B_R^{X_T}(0)$ in X_T, centering at $\eta(t,x) \equiv 0$ of radius R, we conclude on $B_R^{X_T}(0)$ the nonlinear map $\mathcal{F}$ of $\eta \in B_R^{X_T}(0)$ is a self-map.

Now we prove that on $B_R^{X_T}(0)$ the map $\mathcal{F}$ is a strict contraction. If this is proved then by Banach's fixed point theorem we can conclude the local existence and uniqueness of the mild solution.

In fact, for a given B_0, we choose $R > 0$ satisfying

$$\|B_0\|_{H^1} \leq R, \ \sup_{t\in[0,T)} \sup_{x\in\mathbb{R}} \|\eta(x,t)\| \leq R, \ \sup_{t\in[0,T)} \sup_{x\in\mathbb{R}} \|\zeta(x,t)\| \leq R \tag{3.3.5}$$

Then with the help of the local Lipschitz constant $C(1+2R)$ there is

$$\begin{aligned}
&\|\mathcal{F}(\eta) - \mathcal{F}(\zeta)\|_{X_T} \\
=& \sup_{t\in[0,T]} \left\|\int_0^t T_c(t-s)\Big[N_*\big(x; T_c(t)B_0(x) + \eta(x,s)\big)\,\mathrm{d}s \right. \\
&\left. -N_*\big(x; T_c(t)B_0(x) + \zeta(x,s)\big)\,\mathrm{d}s\Big]\right\|_{H^1\left(\mathbb{R}_x\right)} \\
\leq& \sup_{t\in[0,T]} \int_0^t C(1+2R) \sup_{x\in\mathbb{R}} \left\|\eta(x,s) - \zeta(x,s)\right\|_{H^1\left(\mathbb{R}_x\right)} \mathrm{d}s \\
\leq& TC(1+2R)\left\|\eta - \zeta\right\|_{X_T}
\end{aligned} \tag{3.3.6}$$

Thus, since T is small enough, we have shown $\mathscr{F}$ is a contraction map on $B_R^{X_T}(0)$ and we have concluded the proof of the local well-posedness.

The global existence then is a direct consequence of THEOREM 2 of [18]. However the following calculation, similar to that in [19], provides more clarity. From (3.1.3) and estimate (3.1.6),

$$\begin{aligned} \left\|B\right\|_{H^1} \leq \left\|B_0\right\|_{H^1} + \int_0^t \left\|N_*(x; B(x,t'))\right\|_{H^1} \mathrm{d}t' \\ \leq \left\|B_0\right\|_{H^1} + \int_0^t C\left\|B(x,t')\right\|_{H^1} \mathrm{d}t' \end{aligned}$$

Therefore Grönwall's integral inequality[20] yields:

$$\left\|B\right\|_{H^1} \leq Ce^{Ct}\left\|B_0\right\|_{H^1}$$

which is exactly (3.3.1). Therefore following standard arguments, for example that used in THEOREM 2 of [18], we conclude the global existence of mild solutions to (3.1.3) in H^1.

The regularity $B(x,t) \in C^1L^2$ is a direct consequence of the original form of the equation (3.1.1), since both sides are in L^2, and is continuous in time, with initial data $B_0 \in H^1$. □

3.4 Finite propagation speed

In the *non-moving* frame, substitute $u(y,t) = u_*(y,t) + U(y,t)$ and $v(y,t) = v_*(y,t) + V(y,t)$ in (1.0.1), we have

$$\begin{aligned} U_t =& V_y + \mathcal{N}_*(U,V)V + \Big[\mathcal{N}_*(U,V) - \mathcal{N}_*(0,0)\Big]v_* \\ V_t =& U_y - \mathcal{N}_*(U,V)U - \Big[\mathcal{N}_*(U,V) - \mathcal{N}_*(0,0)\Big]u_* \end{aligned} \tag{3.4.1}$$

is the equation for perturbation $B(y,t) = \begin{bmatrix} U(y,t) & V(y,t) \end{bmatrix}^{\mathsf{T}}$ in the non-moving reference frame, where for simplicity, we define

$$\mathcal{N}_*(U,V) := \mathcal{N}\Big(r_*^2 + 2u_*U + 2v_*V + U^2 + V^2\Big) \tag{3.4.2}$$

with $u_* = u_*(y - ct)$ etc.

The following result says the speed of propagation of data for the system (3.1.1) is at most $|c_0| = 1$:

Proposition 3.4. *Consider the initial value problem given by (3.4.1)*

1. *Let the initial data be $B_0 \in H^1$. For any $y \in \mathbb{R}, t > 0$, $B(y', t') = 0$ on the domain of dependence of (y, t):*

$$\Delta(y,t) := \left\{(y',t') \in \mathbb{R}^2 |\, 0 \leq t' \leq t - |y - y'|\right\} \tag{3.4.3}$$

   if $B_0(y') = 0$ on $[y - t, y + t]$.

2. *Assume there are two initial perturbations $A_0 = (W_0, Z_0), B_0 = (U_0, V_0) \in H^1$ such that $B_0(y') = A_0(y')$ for $y' \in [y - t, y + t]$, $t > 0$. Then, for any $y \in \mathbb{R}$, $B(y', t') = A(y', t')$ on $\Delta(y, t)$.*

3. *If $B_0(y) = A_0(y)$ on $y \in [\ell, \infty)$ for some $\ell \in \mathbb{R}$, then for all (y, t) satisfying $y \geq \ell + t$ we have $B(y, t) = A(y, t)$. In the moving frame with speed c where the spatial coordinate is $x = y - ct$, we have $B(x, t) = A(x, t)$ for all $x \geq \ell - (c - 1)t$.*

It suffices to prove only Part 2 and Part 3 of this proposition, since Part 1 follows from the case $A_0 = 0$.

Proof. Define characteristic variables

$$\tilde{U} = \frac{U + V}{\sqrt{2}}, \tilde{V} = \frac{-U + V}{\sqrt{2}} \tag{3.4.4}$$

and

$$\tilde{u}_* = \frac{u_* + v_*}{\sqrt{2}}, \tilde{v}_* = \frac{-u_* + v_*}{\sqrt{2}}$$

As a result:

$$
\begin{aligned}
(\partial_t - \partial_y)\tilde{U} &= \mathcal{N}_*(U,V)\tilde{V} + \Big[\mathcal{N}_*(U,V) - \mathcal{N}_*(0,0)\Big]\tilde{v}_* \\
(\partial_t + \partial_y)\tilde{V} &= -\mathcal{N}_*(U,V)\tilde{U} - \Big[\mathcal{N}_*(U,V) - \mathcal{N}_*(0,0)\Big]\tilde{u}_*
\end{aligned}
\tag{3.4.5}
$$

Denote $A = \begin{bmatrix} W & Z \end{bmatrix}^{\mathsf{T}}$ a second solution which satisfies (3.4.1). Analogously we define, via (3.4.4), $\tilde{A} = \begin{bmatrix} \tilde{W} & \tilde{Z} \end{bmatrix}^{\mathsf{T}}$. Therefore

$$
\begin{aligned}
(\partial_t - \partial_y)(\tilde{U} - \tilde{W}) &= \mathcal{N}_*(U,V)\tilde{V} - \mathcal{N}_*(W,Z)\tilde{Z} + \Big[\mathcal{N}_*(U,V) - \mathcal{N}_*(W,Z)\Big]\tilde{v}_* \\
(\partial_t + \partial_y)(\tilde{V} - \tilde{Z}) &= -\mathcal{N}_*(U,V)\tilde{U} + \mathcal{N}_*(W,Z)\tilde{W} - \Big[\mathcal{N}_*(U,V) - \mathcal{N}_*(W,Z)\Big]\tilde{u}_*
\end{aligned}
\tag{3.4.6}
$$

Multiply both sides of the first equation of (3.4.6) with $2(\tilde{U}-\tilde{W})$, and similarly the second equation in (3.4.6) with $2(\tilde{V} - \tilde{Z})$. Adding the results gives

$$
\begin{aligned}
&(\partial_t - \partial_y)(\tilde{U} - \tilde{W})^2 + (\partial_t + \partial_y)(\tilde{V} - \tilde{Z})^2 \\
=&2\Big[\mathcal{N}_*(U,V) - \mathcal{N}_*(W,Z)\Big]\Big[(\tilde{U} - \tilde{W})\tilde{v}_* - (\tilde{V} - \tilde{Z})\tilde{u}_* + \tilde{U}\tilde{Z} - \tilde{V}\tilde{W}\Big]
\end{aligned}
\tag{3.4.7}
$$

Now WLOG, we consider the point $(0, \ell)$ on the t-axis. The following argument makes no use of the particular value of y in the pair (y, t) in the statement of Part 2 of this proposition.

Assume H^1 initial data $B_0(y) = A_0(y)$ on $y \in [-\ell, \ell]$ where $\ell > 0$, and consider the closed trapezoidal region on the (y, t)-plane:

$$
\Omega_t = \bigcup_{0 \le s \le t} \big\{(y, s) \ : \ -\ell + s \le y \le \ell - s\big\},
\tag{3.4.8}
$$

where $0 < t < \ell$. The region Ω_t is bounded by the four line segments $\Gamma_{1,2,3,4}$ and is shown in figure 3.1. It is easy to check

$$
\Omega_\ell = \Delta(0, \ell) = [-\ell, +\ell]
$$

where $\Delta(0, \ell)$ is the domain of dependence of spacetime point $(0, \ell)$; see (3.4.3).

The energy identity (3.4.7) can be expressed in terms of the $(y, t)-$ divergence of the vector

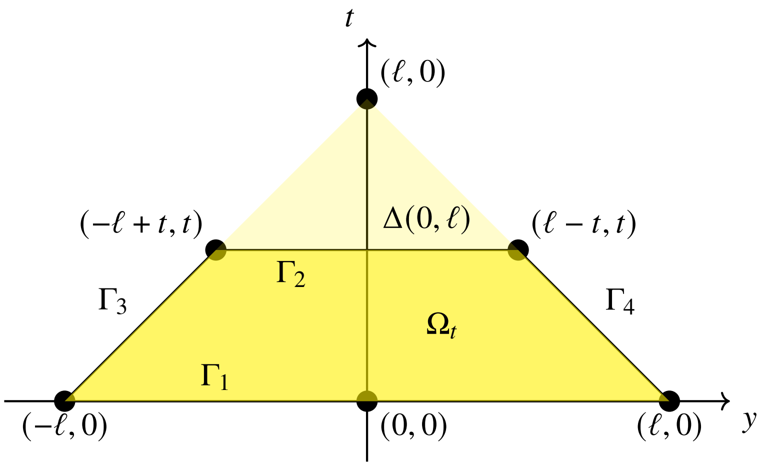

Figure 3.1: The closed trapezoidal region Ω_t used in the proof of PROPOSITION 3.4, shaded with darker yellow; the domain of dependence of point $(0,\ell)$ is Ω_t along with the top region shaded with lighter yellow.

field:

$$\Phi = \left[-\left(\tilde{U}-\tilde{W}\right)^2 + \left(\tilde{V}-\tilde{Z}\right)^2, \left(\tilde{U}-\tilde{W}\right)^2 + \left(\tilde{V}-\tilde{Z}\right)^2 \right]; \tag{3.4.9}$$

equation (3.4.7) is equivalent to

$$\operatorname{div}\Phi = \text{RHS of (3.4.7)} \tag{3.4.10}$$

Integrating (3.4.10) over Ω_t and applying Gauss's divergence theorem we obtain:

$$\begin{aligned}
&\int_{\Omega_t} \operatorname{div}\Phi \, \mathrm{d}y \, \mathrm{d}t = \int_{\Gamma_1} \Phi\hat{n}\cdot \mathrm{d}l + \int_{\Gamma_2} \Phi\hat{n}\cdot \mathrm{d}l + \int_{\Gamma_3} \Phi\hat{n}\cdot \mathrm{d}l + \int_{\Gamma_4} \Phi\hat{n}\cdot \mathrm{d}l \\
&= -\int_{-\ell}^{\ell} \left(\tilde{U}_0(y)-\tilde{W}_0(y)\right)^2 + \left(\tilde{V}_0(y)-\tilde{Z}_0(y)\right)^2 \mathrm{d}y \text{ (this term vanishes)} \\
&\quad + \int_{-\ell+t}^{\ell-t} \left(\tilde{U}(y,t)-\tilde{W}(y,t)\right)^2 + \left(\tilde{V}(y,t)-\tilde{Z}(y,t)\right)^2 \mathrm{d}y \\
&\quad + \int_0^t 2\left(\tilde{U}(-\ell+y,y)-\tilde{W}(-\ell+y,y)\right)^2 \mathrm{d}y \text{ (this term} \geq 0\text{)} \\
&\quad + \int_0^t 2\left(\tilde{V}(\ell-y,y)-\tilde{Z}(\ell-y,y)\right)^2 \mathrm{d}y \text{ (this term} \geq 0\text{)} \\
&= \int_{\Omega_t} 2\left[\mathcal{N}_*(U,V)-\mathcal{N}_*(W,Z)\right]\left[\left(\tilde{U}-\tilde{W}\right)\tilde{v}_* - \left(\tilde{V}-\tilde{Z}\right)\tilde{u}_* + \tilde{U}\tilde{Z} - \tilde{V}\tilde{W}\right] \mathrm{d}y \, \mathrm{d}t
\end{aligned} \tag{3.4.11}$$

Now we bound pointwise the absolute value of the integrand on the last line. Note that u_*, v_* are bounded since the TWSs we work with in this paper are all bounded. The derivative of the nonlinearity, $\mathcal{N}'$, is also bounded since it is continuous, and its arguments are all bounded. By the growth rate bound (3.3.1) of THEOREM 3.3 we have that for $0 \leq t \leq \ell$, the H^1 thus the L^∞ norm of the perturbation is bounded. Moreover,

$$\begin{aligned}
\left|\mathcal{N}_*(U,V) - \mathcal{N}_*(W,Z)\right| &\leq C\left[|\tilde{U} - \tilde{W}| + |\tilde{V} - \tilde{Z}|\right] \\
\left|(\tilde{U} - \tilde{W})\tilde{v}_* - (\tilde{V} - \tilde{Z})\tilde{u}_*\right| &\leq C\left[\left|\tilde{U} - \tilde{W}\right| + \left|\tilde{V} - \tilde{Z}\right|\right] \\
\left|\tilde{U}\tilde{Z} - \tilde{V}\tilde{W}\right| \leq \left|\tilde{U}\right|\left|\tilde{W} - \tilde{Z}\right| + \left|\tilde{U} - \tilde{V}\right|\left|\tilde{W}\right| &\leq C\left[\left|\tilde{U} - \tilde{W}\right| + \left|\tilde{V} - \tilde{Z}\right|\right],
\end{aligned}$$

where the constants C depends on the nonlinearity, TWS profile b_* as well as ℓ. These estimates imply that the absolute value of the expression on the last line of (3.4.11) is has the upper bound:

$$\begin{aligned}
&\int_{\Omega_t} 2\left|\mathcal{N}_*(\tilde{U},\tilde{V}) - \mathcal{N}_*(W,Z)\right|\left|(\tilde{U} - \tilde{W})\tilde{v}_* - (\tilde{V} - \tilde{Z})\tilde{u}_* + \tilde{U}\tilde{Z} - \tilde{V}\tilde{W}\right| \mathrm{d}y\, \mathrm{d}t' \\
\leq &C \int_0^t \int_{-\ell+t'}^{\ell-t'} \left[\left|\tilde{U}(y,t') - \tilde{W}(y,t')\right|^2 + \left|\tilde{V}(y,t') - \tilde{Z}(y,t')\right|^2\right] \mathrm{d}y\, \mathrm{d}t'
\end{aligned}$$

Let $I(t)$ be the nonnegative function of t defined by the third line of (3.4.11):

$$I(t) := \int_{-\ell+t}^{\ell-t} \left|\tilde{U}(y,t) - \tilde{W}(y,t)\right|^2 + \left|\tilde{V}(y,t) - \tilde{Z}(y,t)\right|^2 \mathrm{d}y \geq 0$$

Then,

$$I(t) \leq C \int_0^t I(t')\, \mathrm{d}t'$$

where we used that $I(0) = 0$ by the assumption $B_0(y) = A_0(y)$ on $[-\ell, \ell]$. By Grönwall's inequality $I(t) = 0$ for $0 \leq t \leq \ell$. This proves Part 2 of PROPOSITION 3.4.

Part 3 of PROPOSITION 3.4 is an immediate consequence of Part 2. To see this, suppose $B_0(y) = A_0(y)$ on (ℓ, ∞) for some ℓ. Now if $y > \ell + t$, then $[y - t, y + t] \cap (-\infty, \ell] = \emptyset$. Hence, for all such (y,t), we have $B(y',t') = A(y',t')$ for $(y',t') \in \Delta(y,t)$. Thus, $B(y,t) = A(y,t)$ for all (y,t) such that $y > \ell + t$. Equivalently, in a frame of reference moving with speed c: $x = y - ct > \ell - ct + t$. See FIGURE 3.2 for illustration of this part of the proof. Part 3 is thus proved, and the proof of PROPOSITION 3.4 is now complete. □

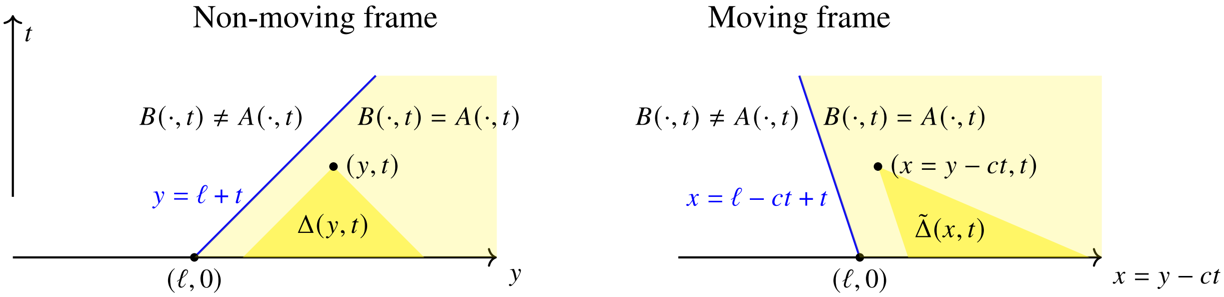
Non-moving frame
Moving frame
t
$B(\cdot,t) \neq A(\cdot,t)$
$B(\cdot,t) = A(\cdot,t)$
(y,t)
$y = \ell + t$
$\Delta(y,t)$
$(\ell,0)$
y
$B(\cdot,t) \neq A(\cdot,t)$
$B(\cdot,t) = A(\cdot,t)$
$(x = y - ct, t)$
$x = \ell - ct + t$
$\tilde{\Delta}(x,t)$
$(\ell,0)$
$x = y - ct$

Figure 3.2: Illustration of the proof of Part 3 of PROPOSITION 3.4. Here, at time $t = 0$, in the lab frame, $B_0(y) = A_0(y)$ and in the moving frame where $x = y - ct$, $B_0(x) = A_0(x)$. The yellow regions in both frames are the spacetime region on on (y,t) and $(x = y - ct, t)$ planes respectively, where $B(\cdot,t) = A(\cdot,t)$. The darker yellow triangles in the left panel stands for $\Delta(y,t)$, the domain of dependence of (y,t); whereas in the right panel the *same* domain of dependence of $(x = y - ct, t)$, observed in the moving frame. The blue lines are borders of the regions $B(\cdot,t) \neq A(\cdot,t)$ and $B(\cdot,t) = A(\cdot,t)$, in either reference frame respectively.

Chapter 4: Nonlinear convective stability of supersonic pulses

The following theorem is stated in the comoving frame of a supersonic pulse, i.e., for an "observer" that travels with the pulse at the same speed c as does the latter travels. For this result, we still assume the nonlinearity to be saturable as we do for the last section; see SECTION 1.3.

Theorem 4.1 (Supersonic pulses are nonlinearly convectively stable)**.** *Let b_* be a supersonic pulse with speed $c > 1$.*

1. *Consider equation (3.4.1) for the perturbation in a non-moving frame of reference, with initial data $B(y,0) = B_0(y)$. There exist $\gamma_0 > 0$ so that if $\gamma > \frac{\gamma_0}{c-1}$, then*

$$\left\|B_0\right\|_{H^1\left([\ell,\infty)\right)} = o\left(e^{-\gamma\ell}\right), \quad as \quad \ell \to \infty. \tag{4.0.1}$$

   Then, for any $R \in \mathbb{R}$, we have exponential time-decay:

$$\left\|B(y,t)\right\|_{H^1\left([R+ct,\infty)_y\right)} = \mathcal{O}\left(e^{-\left(\gamma(c-1)-\gamma_0\right)t}\right). \tag{4.0.2}$$

2. *Equivalently, consider equation (3.1.1) for the perturbation of b_* in the comoving frame of reference ($x = y - ct$), traveling with the same speed c, with initial data $B(x,0) = B_0(x)$ satisfying (4.0.1). Then, for any $R \in \mathbb{R}$,*

$$\left\|B(x,t)\right\|_{H^1\left([R,\infty)_x\right)} = \mathcal{O}\left(e^{-\left(\gamma(c-1)-\gamma_0\right)t}\right). \tag{4.0.3}$$

In particular, if B_0 is any Gaussian perturbation, not necessarily centered at 0, B_0 satisfies (4.0.1), consistent with the simulated phenomena shown in figure 1.6. THEOREM 4.1 can be interpreted this way: as long as the initial perturbation decays fast enough as $x \to \infty$, if we look the

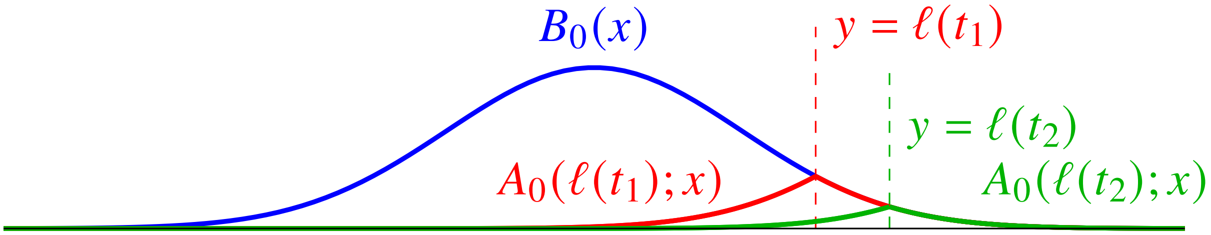

Figure 4.1: Illustration of the construction of the family of initial data $A_0(\ell; y) \equiv A_0(\ell; x)$ used in the proof of THEOREM 4.1. This is only a *schematic* plot, since B_0 and A_0 are vector-valued.

pulse in any finite window *in the comoving frame with speed* c, the perturbed profile will eventually be almost identical to the unperturbed profile. The profile of the perturbation itself outside this window may, and usually does become intractable with our current approach.

Proof of THEOREM *4.1.* We only prove Part 2; its equivalency to Part 1 is immediate. From THEOREM 3.3, there is a constant γ_0, depending only on the nonlinearity and the traveling wave solution b_* whose perturbations we study, such that for all $B_0 \in H^1(\mathbb{R})$:

$$\|B(\cdot, t)\|_{H^1(\mathbb{R})} \leq \gamma_0 e^{\gamma_0 t} \|B_0\|_{H^1(\mathbb{R})} \tag{4.0.4}$$

Now we fix $B_0 \in H^1$, and require that it satisfies (4.0.1), and $B(x, t)$ will denote the solution to (3.1.1) with initial data B_0 for the rest of this proof.

Next, we define a family of initial data given this *fixed* B_0. Let $\ell \in \mathbb{R}$. Let $A_0(\ell; y)$ be defined on all $\mathbb{R}$ as the function obtained by symmetrize the tail of B_0 to the right of $y = \ell$ about $y = \ell$:

$$A_0(\ell; y) = \begin{cases} B_0(y) & \text{for } y \geq \ell \\ B_0(2\ell - y) & \text{for } y < \ell. \end{cases} \tag{4.0.5}$$

A schematic illustration of the construction of $\mathcal{A}(\ell; y)$ is given in FIGURE 4.1. Further, we introduce $A(\ell; x, t)$, the solution of the IVP (3.1.1) (posed in the moving frame) with initial data

$A(\ell; x, t = 0) = A_0(\ell; x)$. Therefore, by (4.0.4) we have

$$\left\|A(\ell; \cdot, t)\right\|_{H^1} \leq \gamma_0 e^{\gamma_0 t} \left\|A_0(\ell; \cdot)\right\|_{H^1}, \quad \text{for all } t \geq 0 \text{ and } \ell \in \mathbb{R}. \tag{4.0.6}$$

Now $B(x, t)$ and $A(\ell; x, t)$ are defined for each $x, \ell \in \mathbb{R}$ and $t \geq 0$. Note that $B_0(y) = A_0(\ell; y)$ for $y \geq \ell$, since for $t = 0$, $x = y - ct = y$. Then by Part 3 of PROPOSITION 3.4, for any $x, \ell \in \mathbb{R}$ and any $t \geq 0$:

$$B(x, t) = A(\ell; x, t), \quad \text{if } x + (c - 1)t \geq \ell \tag{4.0.7}$$

In the following, we shall use as a family of functions $A(\ell; x, t)$*, which depends on* ℓ, x, t*, and which satisfies the* $\ell-$ *parameterized family of identities* (4.0.7) *to bound the solution* $B(x, t)$. Fix any $R \in \mathbb{R}$. Then, for any $t \geq 0$ and $x \geq R$, we have

$$x + (c - 1)t \geq R + (c - 1)t = \ell(t).$$

Therefore, by (4.0.7), let $\ell = R + (c - 1)t$, we have,

$$B(x, t) = A(R + (c - 1)t; x, t), \quad \text{for all } x \geq R \text{ and } t \geq 0. \tag{4.0.8}$$

See FIGURE 4.2 for illustration as well as the idea of competing growth/decay rates used in the current proof below.

We note that as a function of t, the RHS of (4.0.8) is not a solution to (3.1.1), in general. It follows that for for all $R \in \mathbb{R}$, all $t \geq 0$, we have

$$\begin{aligned} &\left\|B(\cdot, t)\right\|_{H^1\left([R,\infty)\right)} = \left\|A(R + (c - 1)t; \cdot, t)\right\|_{H^1\left([R,\infty)\right)} \\ \leq &\left\|A(R + (c - 1)t; \cdot, t)\right\|_{H^1} \end{aligned} \tag{4.0.9}$$

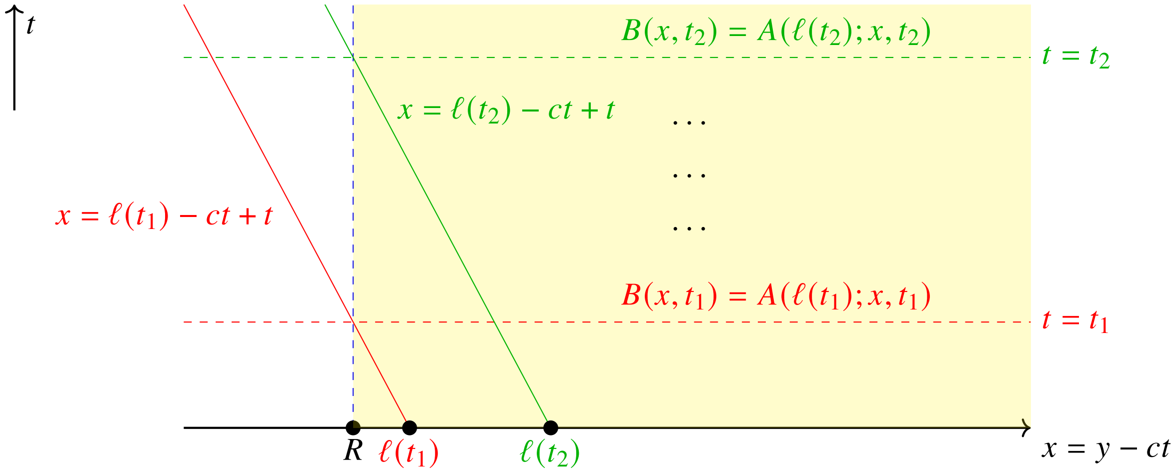

Figure 4.2: Illustration of (4.0.8) used in the proof of THEOREM 4.1. For all $t \geq 0$, here illustrated by $t = t_1$ and $t = t_2$, the identity (4.0.8) holds for all $x \geq R$, colored yellow. Compare with the right panel with FIGURE 3.2. Moreover, the arrows on the right schematically shows the two effects on the tail norm of the perturbation $B_(x,t)$ on $[R,\infty)$.

By bound (4.0.6):

$$\left\|A(R+(c-1)t;\cdot,t)\right\|_{H^1} \leq \gamma_0 e^{\gamma_0 t}\left\|A_0(R+(c-1)t;\cdot)\right\|_{H^1} \tag{4.0.10}$$

Combining (4.0.9) and (4.0.10),

$$\left\|B(\cdot,t)\right\|_{H^1\left([R,\infty)\right)} \leq \gamma_0 e^{\gamma_0 t}\left\|A_0(R+(c-1)t;\cdot)\right\|_{H^1} \tag{4.0.11}$$

where the RHS depends only on data B_0 through A_0 defined by (4.0.5). Now we proceed to bound the RHS of (4.0.11).

By assumption (4.0.1), we can choose $M \in \mathbb{R}$ large enough, such that

$$\left\|B_0\right\|^2_{H^1\left([z,\infty)\right)} \leq \frac{1}{2}\left(Me^{-\gamma z}\right)^2, \quad z \in \mathbb{R}.$$

By the definition (4.0.5) of A_0 we have

$$\left\|A_0(z;\cdot)\right\|^2_{H^1} = 2\left\|B_0\right\|^2_{H^1\left([z,\infty)\right)} \leq M^2 e^{-2\gamma z} \tag{4.0.12}$$

Now we apply (4.0.12) and set $z = R + (c-1)t$,

$$\left\|A_0(R + (c-1)t; \cdot)\right\|_{H^1} \leq Me^{-\gamma R}e^{-\gamma(c-1)t} \tag{4.0.13}$$

So by (4.0.11) and (4.0.13),

$$\left\|B(\cdot, t)\right\|_{H^1\left([R,\infty)\right)} \leq M\gamma e^{-\gamma R}e^{-\left(\gamma(c-1)-\gamma_0\right)t}. \tag{4.0.14}$$

Finally, since by hypothesis $\gamma > \frac{\gamma_0}{c-1}$, where $c > 1$, we have $\gamma(c-1) - \gamma_0 > 0$, and hence (4.0.14) implies exponential decay in time as asserted in (4.0.3). □

Chapter 5: Linearized stability analysis

The nonlinear stability analysis of supersonic pulses of the previous section relies on the assumption that nonlinearity is saturable and, in particular, both $\mathcal{N}(r^2)$ and its derivative $\mathcal{N}'(r^2)$ are bounded.

If the Lipschitz constant of the nonlinearity grows with growing amplitude, then it appears to be a possibility that some solutions may blow up (become singular) in H^1 in finite time. Without global-in-time existence of solutions with *a priori* upper bound on the rate of growth, the above strategy cannot be implemented.

Thus, we are motivated to pursue a linearized stability analysis of traveling wave solutions, including supersonic pulses.

Our stability analysis of supersonic pulses does *not* apply to kink-type traveling wave solutions; see Figure 2.1. Recall that kink solutions are *always* subsonic ($|c| < 1$); hence a kink does not "outrun" small perturbations which moves with the linearized wave speeds $= \pm 1$. In contrast, supersonic ($|c| > 1$) pulses do outrun disturbances of speed ± 1; this observation underlies THEOREM 4.1. This motivates our linearized stability analysis for the case of kinks.

We next give a general discussion of the linear spectral analysis for pulses and kinks and then present results on the spectral stability properties of equilibria, which arise as the $x \to \pm\infty$ limits of traveling wave solutions. In SECTION 7 we turn to the spectral stability of supersonic pulses, and then in SECTION 8 to the spectral stability of kink traveling wave solutions.

5.1 Linearized spectral stability analysis of pulses and kinks; qualitative discussion

Traveling wave solutions $b_*(x)$ have non-zero constant limits as $x \to \pm\infty$. These constants correspond to fixed points of the system (2.0.3). A study of the linearized operator about these equilibria indicates that they are, in general, exponentially unstable. In fact under the evolution of the linearized perturbation equations, a system of constant coefficient wave equations, an initial perturbation of such equilibria splits into left-moving and right-moving parts, one of which grows with time.

By REMARK *2.2, on symmetries relating traveling wave solutions, we expect that it suffices to focus our study on traveling waves (pulses and kinks) with speeds $c \geq 0$.* As demonstrated in CHAPTER 4 for supersonic pulses, and numerically for both supersonic pulses and kinks, if we appropriately localize the perturbation to the region of space into which the traveling wave is propagating, we may expect the perturbation to decay. This observation of *convective stabilization* is consistent with the previous analyses of traveling wave systems. The biased localization to one side is achieved through L^2 exponentially weighted spaces [10][21] L^2 algebraically weighted spaces algebraic weights [21] and H^1_{loc} spaces[11]. Here, we study the linearized dynamics of perturbations in **exponentially weighted spaces**, which we next introduce.

5.1.1 Exponentially weighted spaces

We introduce a class of weights $W(x)$ which asymptotes to different exponential functions as x tend to plus or minus infinity:

$$W(x) \equiv e^{w(x)} = \begin{cases} e^{a_- x} \text{ for } x \leq -1 \\ e^{a_+ x} \text{ for } x \geq 1 \end{cases} \tag{5.1.1}$$

where $a_\pm \in \mathbb{R}$, and $W(x)$, which interpolates between $e^{a_- x}$ and $e^{a_+ x}$, is chosen to be monotone and smooth. The corresponding weighted Lebesgue and Sobolev spaces are introduced analogous to those used in [10]:

$$L^2_w := L^2\left(\mathbb{R}, e^{w(x)}\, \mathrm{d}x\right), \quad H^1_w := \left\{ f(x) \in L^1_{\text{loc}} : \ e^{w(x)} f(x) \in H^1 \right\}$$

In the present work, we encounter the cases:

1. $a_- = a_+ = a$. In this case we take $W(x) = e^{ax}$, and for simplicity we will write

$$L_a^2 := L^2\big(\mathbb{R}, e^{ax}\,\mathrm{d}x\big), \quad H_a^1 := \left\{f(x) \in L^1_{\mathrm{loc}} \,:\, e^{ax} f(x) \in H^1\right\}$$

2. $a_- = 0$, $a_+ = a \neq 0$. Thus, $W(x) = 1$ for $x < -1$ and $W(x) = e^{ax}$ for $x > 1$.

3. $a_+ = 0$, $a_- = a \neq 0$.

5.1.2 Linearized perturbation equation in a moving frame with speed $c \geq 0$

The equation for the perturbation, $B = \begin{bmatrix} U & V \end{bmatrix}^{\mathsf{T}}$, about the traveling wave solution $b_*(x) = (u_*(x), v_*(x))$ in the traveling frame of reference with the same speed c is displayed in (3.1.1). Formal first-order Taylor expansion of (3.1.1) yields the following *linearized* evolution equation for the perturbations:

$$B_t = L_* B, \quad L_* = \Sigma\partial_x + A_* \tag{5.1.2}$$

with

$$A_*(x) = \begin{bmatrix} 2\mathcal{N}'\big(r_*^2\big)u_* v_* & \mathcal{N}_*\big(r_*^2\big) + 2\mathcal{N}'\big(r_*^2\big)v_*^2 \\ -\mathcal{N}\big(r_*^2\big) - 2\mathcal{N}'\big(r_*^2\big)u_*^2 & -2\mathcal{N}'\big(r_*^2\big)u_* v_* \end{bmatrix} \tag{5.1.3}$$

and

$$\Sigma := \begin{bmatrix} c & 1 \\ 1 & c \end{bmatrix} \tag{5.1.4}$$

We shall refer to L_* as the *linearized operator about* b_*.

Suppose $\lambda \in \mathbb{C}$ with $\mathrm{Re}\lambda > 0$, and $0 \neq B_0(x) \in L^2$ are such that $L_* B_0 = \lambda B_0$. Then, $B(x,t) = e^{\lambda t} B_0(x)$ is a solution of (5.1.2), such that $\|B(\cdot,t)\|_2$ grows exponentially as $t \to \infty$. However, in appropriately weighted spaces $B(x,t)$ needs not always grow. Indeed, the weighted perturbation $e^{w(x)}B(x,t)$ satisfies

$$\partial_t\left(e^{w(x)}B(x,t)\right) = L_{*,w}\left(e^{w(x)}B(x,t)\right),$$

where $L_{*,w}$ is related to L_* by conjugation:

$$L_{*,w} := e^{w(x)} L_* \big(e^{-w(x)} \cdot \big) = \Sigma\big(\partial_x - w'(x)\big) + A_*(x) \tag{5.1.5}$$

The study of the weighted perturbation $e^{w(x)}B(x,t)$ in L^2 or H^1 is equivalent to the study of $B(x,t)$ in the corresponding weighted spaces L^2_w or H^1_w.

Definition 5.1 (Spectral stability)**.** *Let $b_*(x)$ denote a TWS with speed c whose profile satisfies (2.0.3). Let L_* denote the linearized operator of b_*. We say that b_* is spectrally stable if*

$$L^2_w(\mathbb{R})-\textit{ spectrum of } L_* \ \subset \{z : \mathtt{Re} z \leq 0\},$$

or equivalently

$$L^2(\mathbb{R})-\textit{ spectrum of } L_{*,w} \ \subset \{z : \mathtt{Re} z \leq 0\}.$$

Suppose that for a choice of weight $W(x) = e^{w(x)}$ of the exponential type (5.1.1) the traveling wave solution b_* is spectrally stable in the sense of Definition 5.1. Then, if the context is clear, then we shall refer to b_* as being spectrally stable without explicit reference to the particular weight $W(x) = e^{w(x)}$.

5.2 Spectral stability of equilibria

We study the spectral stability of equilibria

$$b_* = \begin{bmatrix} 0 & 0 \end{bmatrix} \text{ and } b_* = \begin{bmatrix} \cos\theta & \sin\theta \end{bmatrix}$$

in $L^2_a = L^2_w$, where $W(x) = e^{ax}$.

5.2.1 The trivial equilibrium

Consider the trivial equilibrium, $b_* = b_O := [0, 0]$, viewed in a frame of reference moving with speed c. Let $a \in \mathbb{R}$ be fixed. The L^2_a-spectral stability properties are determined by the L^2-spectrum of the operator:

$$L_{O,a} = \begin{bmatrix} c & 1 \\ 1 & c \end{bmatrix} \left(\partial_x - a\right) + \begin{bmatrix} 0 & 1 \\ -1 & 0 \end{bmatrix} = \Sigma(\partial_x - a) + A_O \tag{5.2.1}$$

The spectrum of $L_{O,a}$ is determined [22] by the frequency of non-trivial plane wave solutions of wave numbers $k \in \mathbb{R}$: $B = e^{ikx}B_0$, $B_0 \in \mathbb{C}^2$ and $L_O B_0 = \lambda B_0$, where $\lambda = \lambda(k)$ satisfies:

$$\det\left(\left(\mathrm{i}k - a\right) \begin{bmatrix} c & 1 \\ 1 & c \end{bmatrix} + \begin{bmatrix} 0 & 1 \\ -1 & 0 \end{bmatrix} - \begin{bmatrix} \lambda & 0 \\ 0 & \lambda \end{bmatrix} \right) = 0,$$

yielding two branches (dispersion relations), depending on a, the union of whose images is exactly the L^2-spectrum of $L_{O,a}$, equivalently the L^2_a-spectrum of L_O. It can be seen that the essential spectrum is stable (does not intersect the open right half plane) if and only if $a = 0$. The two branches of $L^2 = L^2_0$ essential spectrum are swept out by the dispersion relations:

$$\lambda(k) = \lambda^{\pm}_O(k) = \mathrm{i}\left(kc \pm \sqrt{1 + k^2}\right), \quad k \in \mathbb{R}. \tag{5.2.2}$$

Proposition 5.2. *The trivial equilibrium, (*$b_* = (0, 0)$*), is spectral stable in* $L^2(\mathbb{R})$.

There are two qualitatively distinct cases:

- $|c| < 1$ (subsonic frame of reference),

$$\sigma(L_O) = \mathrm{i}\mathbb{R} \setminus \mathrm{i}(-\sqrt{1 - c^2}, \sqrt{1 - c^2})$$

i.e. the spectrum is a subset of the imaginary axis and has a gap, which is symmetric about the origin, and

- $|c| > 1$ (supersonic frame of reference)

$$\sigma(L_O) = \mathrm{i}\mathbb{R}$$

Remark 5.3. The relevance of considering the stability of equilbria in different reference frames relates to our requiring this information for the study of supersonic ($|c| > 1$) pulses and kinks, for which $|c| < 1$.

5.2.2 Nontrivial equilibria

Nontrivial equilibria are of the form $b_* = b_\theta := \begin{bmatrix}\cos\theta & \sin\theta\end{bmatrix}$; see (2.0.2). In a frame of reference with speed c, the linearized operator $L_\theta = L_*$ is given by (5.1.2). The weight-conjugated operator (see (5.1.5)) is:

$$L_{\theta,a} = \begin{bmatrix} c & 1 \\ 1 & c \end{bmatrix} \left(\partial_x - a\right) - K \begin{bmatrix} \sin 2\theta & 1 - \cos 2\theta \\ -1 - \cos 2\theta & -\sin 2\theta \end{bmatrix}; \tag{5.2.3}$$

recall that $K = -\mathcal{N}'(1) > 0$ by assumption 1.3.1. The essential spectrum of $L_{\theta,a}$ is characterized by its (bounded) plane wave solutions $e^{\mathrm{i}kx+\lambda t}\xi_0$, with $\xi_0 \in \mathbb{C}^2 \neq 0$. Thus, we obtain dispersion curves

$$\lambda^{\pm}_{\theta,a}(k) = \left(\mathrm{i}k - a\right)c \pm \sqrt{\left(\mathrm{i}k - a\right)\left(\mathrm{i}k - a + 2K\cos 2\theta\right)} \tag{5.2.4}$$

and

$$\sigma(L_{\theta,a}) = \bigcup_{\beta=\pm} \{\lambda^{\beta}_{\theta,a}(k) : k \in \mathbb{R}\}. \tag{5.2.5}$$

We seek conditions on a guaranteeing that $\mathtt{Re}\,\sigma(L_{\theta,a}) \leq 0$. Note from (5.2.4) that for $k \in \mathbb{R}$

$$\mathtt{Re}\,\lambda^{\pm}_{\theta,a}(k) = -ac \pm \mathtt{Re}\sqrt{\left(\mathrm{i}k - a\right)\left(\mathrm{i}k - a + 2K\cos 2\theta\right)} \tag{5.2.6}$$

Using (5.2.6) we obtain the following bounds on $\mathtt{Re}\sigma(L_{\theta,a})$:

Proposition 5.4.

$$\inf \mathtt{Re}\sigma(L_{\theta,a}) = -ac - \left|a - K\cos 2\theta\right| \tag{5.2.7}$$

$$\sup \mathtt{Re}\sigma(L_{\theta,a}) = -ac + \left|a - K\cos 2\theta\right| \tag{5.2.8}$$

Moreover, these extrema are not achieved if and only if $a - K\cos 2\theta \neq 0$; otherwise, if and only if $a - K\cos 2\theta = 0$, $\sigma\left(L_{\theta,a}\right) \subset \mathrm{i}R$.

We shall use the following technical lemma:

Lemma 5.5. *Let $\alpha, \beta \in \mathbb{R}$ be fixed, and consider the mapping $f : k \in \mathbb{R} \mapsto \mathbb{C}$ given by:*

$$f(k) = \sqrt{(\mathrm{i}k - \alpha)(\mathrm{i}k - \beta)}, \quad k \in \mathbb{R}.$$

where the square-root function is defined on the cut complex plane $\mathbb{C} \setminus (-\infty, 0]$ to have a positive real part; on the cut it is taken to have nonnegative real part. Then, for all $k \in \mathbb{R}$, we have

$$\mathtt{Re} f(k) \leq \left|\frac{\alpha + \beta}{2}\right|$$

In particular, if $\alpha + \beta = 0$, then $\mathtt{Re} f(k) = 0$ for all $k \in \mathbb{R}$. And if $\alpha + \beta \neq 0$, then $\sup \mathtt{Re} f(k)$ is attained only in the limit $k \longrightarrow \pm\infty$.

Proof. If $\alpha + \beta = 0$, $\alpha\beta \leq 0$ and $f(k) = \sqrt{\alpha\beta - k^2}$ and is purely imaginary. Therefore $\mathtt{Re} f(k) = 0$ and we are done. Moreover, $f(0) = \sqrt{\alpha\beta}$, $\mathtt{Re} f(0) = 0$ for $\alpha\beta \leq 0$ or $|\alpha\beta| \leq \left|\frac{\alpha+\beta}{2}\right|$ for $\alpha\beta > 0$. So we can study the case when $\alpha + \beta \neq 0$ and $k \neq 0$.

Consider the *conformal* mapping $g(z) = z \mapsto z^2$ from half plane $\mathtt{Re} z > 0$ to $\mathbb{C} \setminus \mathbb{R}_{\leq 0}$. Now the line $\mathtt{Re} z = \left|\frac{\alpha+\beta}{2}\right|$ cuts $\mathtt{Re} z > 0$ into two path-connected components:

$$\Omega_1 = \left\{0 < \mathtt{Re} z \leq \left|\frac{\alpha + \beta}{2}\right|\right\}, \quad \Omega_2 = \left\{\mathtt{Re} z \geq \left|\frac{\alpha + \beta}{2}\right|\right\}$$

and $\Omega_1 \cap \Omega_2 = \left\{ \mathtt{Re}z = \left|\frac{\alpha+\beta}{2}\right| \right\}$. Under $g(z)$, $\mathtt{Re}z = \left|\frac{\alpha+\beta}{2}\right|$ transforms to the parabola Π given by

$$x = p(y) = -\frac{y^2}{(\alpha+\beta)^2} + \left(\frac{\alpha+\beta}{2}\right)^2$$

where $x, y = \mathtt{Re}(z^2), \mathtt{Im}(z^2)$. The set Ω_1 is transformed into $g\big(\Omega_1\big)$ by $g(z)$, which is the "left" path-connected component of the cut complex plane $\mathbb{C} \setminus \mathbb{R}_{\leq 0}$ of which 0 is an element. Now the image of $f(k)$ is a subset of the open right-half plane since $h(z) = z \mapsto \sqrt{z}$ on $\mathbb{C} \setminus \mathbb{R}_{\leq 0}$ is the inverse of $g(z)$. $\mathtt{Re}f(k) \leq \left|\frac{\alpha+\beta}{2}\right|$ is equivalent to that the image of $f(k)$, $k \neq 0$, is in Ω_1; this is further equivalent to the image of $f(k)^2$, $k \neq 0$, is in $g\big(\Omega_1\big)$. In fact,

$$f(k)^2 = \alpha\beta - k^2 - \mathrm{i}(\alpha+\beta)k + \alpha\beta$$

whose image is

$$x = q(y) = -\frac{y^2}{(\alpha+\beta)^2} + \alpha\beta, \quad (y \neq 0)$$

and since $q(y) \leq p(y)$, the image of $f(k)^2$ sits to the left (inclusive) of Π, namely $\mathrm{ran} f(k)^2 \in g(\omega_1)$ and equivalently $\mathrm{ran} f(k) \in \Omega_1$, and this is further equivalent to

$$\mathtt{Re}f(k) \leq \left|\frac{\alpha+\beta}{2}\right|$$

Now we prove that $\sup \mathtt{Re}f(k) = \left|\frac{\alpha+\beta}{2}\right|$. In fact, WLOG assume $\alpha + \beta < 0$ and

$$\mathtt{Re}f(k) = \mathtt{Re}\mathrm{i}k\sqrt{-\alpha\beta/k^2 - (\alpha+\beta)/\mathrm{i}k + 1} = -(\alpha+\beta)/2 = \left|\frac{\alpha+\beta}{2}\right| + o(1)$$

which is exactly what needs to be proved. □

Proof of PROPOSITION *5.4*. Applying LEMMA 5.5 with $\alpha = a$ and $\beta = a - 2K\cos 2\theta$. Therefore

$$-ac - |a - K\cos 2\theta| \leq \mathtt{Re}\lambda^{\pm}_{\theta,a}(k) \leq -ac + |a - K\cos 2\theta|$$

Moreover, the lower and upper bounds above are optimal; if $a \neq K\cos 2\theta$, then the sup in 5.2.8 and inf in 5.2.7 are only attained in the limit $k \longrightarrow \infty$. Otherwise $\mathtt{Re}\lambda^{\pm}_{\theta,a}(k) = -ac$ for all $k \in \mathbb{R}$. $\square$

By definition, b_θ is L^2_a-spectrally stable if and only if $\sup \mathtt{Re}\sigma(L_{\theta,a}) \leq 0$, which by (5.2.8) is the condition

$$\left|a - K\cos 2\theta\right| \leq ac \quad \text{or} \quad -a(c+1) \leq -K\cos 2\theta \leq a(c-1). \tag{5.2.9}$$

For $c > 1$, condition (5.2.9) is equivalent to:

$$a \geq \max\left\{-\frac{K\cos 2\theta}{c-1}, \frac{K\cos 2\theta}{c+1}\right\} \equiv a_{c>1}(\theta, c) \tag{5.2.10}$$

For $c < -1$,

$$a \leq \min\left\{-\frac{K\cos 2\theta}{c-1}, \frac{K\cos 2\theta}{c+1}\right\} \tag{5.2.11}$$

For $-1 < c < 1$,

$$\frac{K\cos 2\theta}{1+c} \leq a \leq \frac{K\cos 2\theta}{1-c}. \tag{5.2.12}$$

For parameters a which satisfy (5.2.12) to exist, it is necessary that the indicated $a-$interval be non-empty. Thus we require:

$$c\cos 2\theta \geq 0. \tag{5.2.13}$$

We summarize the preceding discussion in:

Proposition 5.6. *For a fixed equilibrium solution (see (2.0.2)), consider the linearized operator, L_O or $L_{\theta,a}$, corresponding to a frame of reference moving with speed $c \neq \pm 1$.*

1. *Trivial equilibrium: The trivial equilibrium is spectrally stable if and only if $a = 0$. In this case, L_O is a subset of the imaginary axis.*

2. *Non-trivial equilibria, $\begin{bmatrix}\cos\theta & \sin\theta\end{bmatrix}$: The spectrum $L_{\theta,a}$ is contained in the closed left-half plane if and only if (5.2.9) holds. The condition (5.2.9) is equivalent to (5.2.10) if $c > 1$, or*

(5.2.11) *if* $c < -1$ *and* (5.2.12) *if* $-1 < c < 1$.

Chapter 6: Strategy for studying TWS stability

The spectrum of a closed operator L on a Banach space can be uniquely decomposed into two disjoint subsets of $\mathbb{C}$[22]: the **essential spectrum** $\sigma_{\mathrm{e}}(L)$ and the **discrete spectrum** $\sigma_{\mathrm{d}}(L)$: $\sigma(L) = \sigma_{\mathrm{e}}(L) \cup \sigma_{\mathrm{d}}(L)$ In particular, for $L_{w,*}$, the linearization about a traveling wave solution, $b_*(x)$, we have

$$\sigma(L_{w,*}) = \sigma_{\mathrm{e}}(L_{w,*}) \cup \sigma_{\mathrm{d}}(L_{w,*}).$$

So $\sigma(L_{w,*})$ is contained in the left-half plane (and hence $b_*(x)$ is spectrally stable) if and only if both $\sigma_{\mathrm{e}}(L_{w,*})$ and $\sigma_{\mathrm{d}}(L_{w,*})$ are both contained in the closed left-half plane.

We consider traveling wave solutions $b_*(x)$ which, as $x \longrightarrow \pm\infty$, approach equilibria of (1.0.1); see SECTION 5.2. The corresponding constant-coefficient linear differential operators, **right-** and **left-asymptotic operators**, are operators at $\pm\infty$; formally:

$$L_{\pm} = \lim_{x \longrightarrow \pm\infty} L_{*,w} \tag{6.0.1}$$

$L_{\pm}$ are obtained from $L_{*,w}$ by setting the coefficients equal to their values at $\pm\infty$.

Due to the heteroclinic nature of traveling wave solutions, $L_+ \neq L_-$ in general, and so we introduce the piecewise constant-coefficient **asymptotic operator** which transitions between L_- and L_+ across $x = 0$:

$$L_\infty = \mathbb{1}_{x \leq 0} L_- + \mathbb{1}_{x > 0} L_+. \tag{6.0.2}$$

Since $L_{*,w} - L_\infty$ is spatially well-localized, by Weyl's theorem on the invariance of essential spectrum under relatively compact perturbations, we have

$$\sigma_{\mathrm{e}}\left(L_{*,w}\right) = \sigma_{\mathrm{e}}\left(L_\infty\right);$$

see PROPOSITION 6.4. Therefore

$$\sigma\left(L_{*,w}\right) = \sigma_{\mathrm{e}}\left(L_{\infty}\right) \cup \sigma_{\mathrm{d}}\left(L_{*,w}\right) \tag{6.0.3}$$

In order to determine conditions on the weight, $W(x) = e^{w(x)}$, such that $\sigma_{\mathrm{e}}\left(L_{\infty}\right)$ for all TWSs asymptotic to equilibria of the system (2.0.1), in particular, both supersonic pulses and kinks, we use the following:

Proposition 6.1. *Let $b_*(x)$ denote any TWS with speed c, which is asymptotic to spatially equilibria as $x \to \pm\infty$. Denote by $L_{*,w}$, the operator obtained by conjugating the linearized operator with the weight $W(x) = e^{w(x)}$ of the exponential type; see* SECTION *5.1.1 and* (5.1.5)*. Finally, denote by $L_{\pm}$ (where we suppress the dependence on $w(x)$), the constant coefficient asymptotic operators; see* (6.0.1)*. Then we have*

$$\sigma\left(L_{+}\right) \cup \sigma\left(L_{-}\right) \in \sigma_{\mathrm{e}}(L_{*,w}) \tag{6.0.4}$$

and

$$\sup \mathtt{Re}\sigma_{\mathrm{e}}(L_{*,w}) = \max\left\{\sup \mathtt{Re}\sigma(L_{+}), \sup \mathtt{Re}\sigma(L_{-})\right\} \tag{6.0.5}$$

PROPOSITION 6.1 is a direct application of the theory on the essential spectra of asymptotically constant differential operators, nicely presented in CHAPTER 3 of [22].

6.1 Sketch of proof of PROPOSITION 6.1

Now the asymptotic operator $L_{\infty} = \Sigma\left(\partial_x - a\right) + A(x)$ by (6.0.2). L_{∞} is constant-coefficient for both $x < 0$ and $x > 0$. We can characterize its essential spectrum. We adapt THEOREM 3.1.11 and REMARK 3.1.14 of Kapitula and Promislow (2013) [22].

Theorem 6.2 (Essential spectrum of L_{∞})**.** *$\lambda \in \sigma_{\mathrm{e}}(L_{\infty})$ if and only if either of the following two statements is true:*

(i) $\lambda \in \sigma\left(L_{+}\right) \cup \sigma\left(L_{-}\right)$

(ii) The index of $\lambda - L_\infty$, defined by

$$\operatorname{ind}\left(\lambda I - L_\infty\right) := \dim \mathbb{E}^{\mathrm{u}}\left(\lambda I - L_-\right) - \dim \mathbb{E}^{\mathrm{u}}\left(\lambda I - L_+\right) \tag{6.1.1}$$

is not equal to zero.

In the theorem above, $\dim\mathbb{E}^{\mathrm{u}}\left(\lambda I - L_-\right)$ is the number of independent vectors η such that the following generalized eigenvalue problem is solved with some $\mathtt{Re}k > 0$:

$$L_-\eta e^{\mathrm{i}kx} = \lambda\eta e^{\mathrm{i}kx}$$

similarly for $\mathbb{E}^{\mathrm{u}}\left(\lambda I - L_+\right)$. The following theorem adapted from the THEOREM 3.1.13 of [22] characterizes the border of $\sigma_{\mathrm{e}}\left(L_\infty\right)$:

Theorem 6.3 (Characterization of $\partial\sigma_{\mathrm{e}}\left(L_\infty\right)$)**.** *(i) The border of the essential spectrum of L_∞ is contained in the union of the essential spectra of $L_\pm$. Namely*

$$\partial\sigma_{\mathrm{e}}\left(L_\infty\right) \subset \sigma\left(L_+\right) \cup \sigma\left(L_-\right)$$

(ii) The set

$$\mathbb{C} \setminus \left[\sigma\left(L_+\right) \cup \sigma\left(L_-\right)\right]$$

consists of connected components that are either entirely contained in $\sigma_{\mathrm{e}}\left(L_\infty\right)$ or does not intersect with it.

We are interested in the essential spectrum of $L_{*,w}$. In fact,

Theorem 6.4. *The essential spectra of an $L_{*,w}$ and L_∞ are identical.*

THEOREM 6.4 follows as an immediate corollary of the following THEOREM 6.5 of Weyl on the invariance of the essential spectrum of a linear operator under *relatively compact perturbations* [23], and PROPOSITION 6.6:

Theorem 6.5 (Weyl)**.** *Let $L : \mathcal{D}(\mathcal{L}) \subset X \to Y$ be a closed operator between Banach spaces X and Y, and P relatively compact to L then*

$$\sigma_{\mathrm{e}}(L) = \sigma_{\mathrm{e}}(L + P)$$

We say P is **relatively compact** with respect to L, if it is a compact operator on $\mathcal{D}(L)$ equipped with the **graph norm** to Y. For our case, the domain of $L_{*,w}$ is H^1, and the graph norm of $L_{*,w}$ is equivalent to H^1 norm since $L_{*,w} = \Sigma\partial_x +$some bounded matrix function, with Σ being a invertible constant matrix. To apply THEOREM 6.5 we need the following proposition:

Proposition 6.6. *$L_{*,w}$ is a relatively compact perturbation of L_∞.*

Proof. Note that $L_{*,w} - L_\infty = A_*(x) - A_\infty(x)$ where

$$A_\infty(z) = \big(A_- + w'(-\infty)\big)\mathbb{1}_{(-\infty,0]}(x) + \big(A_+ + w'(\infty)\big)\mathbb{1}_{(-,\infty)}(x)$$

So it can be identified with a piecewise smooth matrix function, with a jump discontinuity at $x = 0$. The proof has two steps. First we prove that for any $N > 0$, the operator defined by

$$\begin{aligned}\delta L_N(x) &= \left(A_*(x) - A_\infty(x)\right)\mathbb{1}_{[-N,N]}(x)\\ &= \left(A_*(x) - A_\infty(x)\right)\mathbb{1}_{[-N,0]}(x) + \left(A_*(x) - A_\infty(x)\right)\mathbb{1}_{(0,N]}(x)\\ &=\delta L_N^-(x) + \delta L_N^+(x)\end{aligned}$$

is compact relative to L_∞. Let $(f_n)_n$ be an arbitrary sequence bounded in H^1 and as a result of the equivalence of $\|\cdot\|_{H^1}$ and the graph norm, it is also bounded in the graph norm. Note that

$$(\delta L_N f_n)_n = \left(\delta L_N^- f_n\right)_n + \left(\delta L_N^+ f_n\right)_n$$

and $\delta L_N^\pm$ can be identified with a bounded smooth matrix function on $[0,\infty)$ and $(-\infty,0]$, respectively. So both sequences $\delta L_N^\pm f_n$ are bounded in H^1, therefore both admit convergent subsequences in L^2, as a result of the Rellich-Kondrachev compactness theorem[24]; so is their sum $\delta L_N f_n$. As a result δL_N compact from H^1 to L^2.

Then we prove $(L_N)_N$ is convergent in norm as bounded operators from H^1 to L^2. Let N be a positive integer and we have

$$\|f\|_{L^\infty} \leq C$$

from Sobolev embedding with C independent of f as long as we fix $\|f\|_{H^1} = 1$. Since $A_*(x) - A^\infty(x) \longrightarrow 0$ exponentially fast as $x \longrightarrow \pm\infty$, we have

$$\begin{aligned} & \|(\delta L_N - L_{*,w} + L_\infty)f\|_{L^2} \\ \leq & \left\|(A_*(x) - A_\infty(x))f(x)\mathbb{1}_{|x|>N}(x)\right\|_{L^2} \\ \leq & C\left\|(A_*(x) - A_\infty(x))\mathbb{1}_{|x|>N}(x)\right\|_{L^2} \|f\|_{L^\infty} \\ \leq & C\left\|(A_*(x) - A_\infty(x))\mathbb{1}_{|x|>N}(x)\right\|_{L^2} \\ \leq & Ce^{-\mu N} \end{aligned}$$

for some $C, \mu > 0$ independent of N, b and vanishes as $N \longrightarrow \infty$. Thus $(\delta L_N)_N$ converges to $L_{*,w} - L_\infty$ in operator norm of $\mathcal{B}\left(H^1, L^2\right)$, the space of bounded linear operators from H^1 to L^2. Since $L_{*,w} - L_\infty$ is compact in this space, it is compact relative to L_∞ and the proof is complete. □

Before proceeding with a detailed discussion of spectra, we note that the linearized spectra of pairs of TWSs related by discrete symmetries, in PROPOSITIONS 1.2 and 2.1, also have simple relations.

Theorem 6.7 (Discrete symmetry of linearized spectra)**.** *Let b_* be a TWS of speed c and conserved quantity $E_c[b] = E$, see (2.1.1). Let $L_{*,w}$ be the weight-conjugated linearized operator of b_* with weight $W(x) = e^{w(x)}$.*

(i) Let $b_\bullet = \mathcal{P}b_*$. Then, $b_\bullet$ is the profile of a TWS of the same speed c and conserved quantity $E_c = E$. Moreover, $L_{\bullet,w} = L_{*,w}$ and therefore $\sigma(L_{\bullet,w}) = \sigma(L_{*,w})$

(ii) Let $b_\bullet = \mathcal{T}\mathcal{C}b_* = \begin{bmatrix} v_*(-x) & -u_*(-x) \end{bmatrix}$. Then, $b_\bullet$ is the profile of a TWS of speed $-c$

with conserved quantity $E_c = -E$*. Let* $\tilde{w}(x) = w(-x)$*. Then,* $L_{\bullet,\tilde{w}} = L_{*,w}$*, and therefore* $\sigma(L_{\bullet,\tilde{w}}) = \sigma(L_{*,w})$*.*

Remark 6.8. THEOREM 6.7 is convenient since it reduces checking the spectral stability of TWSs to checking that of representative ones. In particular, for supersonic pulses with speed $\pm c$ we only need to work with $b_{c,E}$ and $\mathcal{T} b_{-c,-E}$, corresponding to the solid blue line and the solid green line in FIGURE 2.2a. Other supersonic pulses with speed $\pm c$ schematically shown in FIGURE 2.2 can be obtained by acting $\mathcal{P}$ and $\mathcal{TC}$ on these two representative solutions. Note that pulse solutions are all invariant under $\mathcal{C}$. On the other hand, for kinks, we only need to work with $b_{c,0}$ kink with $c \geq 0$, represented by the solid blue line in FIGURE 2.1a. For details of how TWSs transform under discrete symmetries, see SECTION 2.4.

Proof of THEOREM *6.7*. The first case is straightforward, since in this case $b_\bullet = -b_*$ by definition of

$$\mathcal{P}\begin{bmatrix} u(y,t) & v(y,t)\end{bmatrix}^{\mathsf{T}} = -\begin{bmatrix} u(y,t) & v(y,t)\end{bmatrix}^{\mathsf{T}}$$

and the linear dynamics of disturbance on $b_\bullet$ given by $-B$ is identical to the B disturbance on b_*. Therefore in the linear regime,

$$\partial_t B = L_{*,w} B$$

for perturbation on b_* and

$$\partial_t(-B) = L_{\bullet,w}(-B)$$

on $b_\bullet$, and as a result

$$L_{*,w} = L_{\bullet,w}$$

We prove the $\mathcal{TC} = \mathcal{CPT}$ case in detail. The traveling wave solution generated by acting $\mathcal{TC}$ on $b_*(y-ct) = \left[u_*(y-ct), v_*(y-ct)\right]$, according to PROPOSITION 1.2, is

$$\mathcal{TC}\left[u_*, v_*\right](y,t) = \left[v_*(-y,t), -u_*(-y,t)\right] = \Big[v_*\big(-(y+ct)\big), -u_*\big(-(y+ct)\big)\Big] \tag{6.1.2}$$

therefore the resulting traveling wave solution

$$\left[u_\bullet(y,t), v_\bullet(y,t)\right] = \left[u_\bullet(y+ct), v_\bullet(y+ct)\right]$$

is one that travels with speed $-c$ with

$$\begin{bmatrix} u_\bullet(x) \\ v_\bullet(x) \end{bmatrix} = \begin{bmatrix} v_*(-x) \\ -u_*(-x) \end{bmatrix} = \left[\mathrm{i}\sigma_2 \mathcal{R} b_*\right](x) \tag{6.1.3}$$

where $\mathcal{R}f(z) := f(-z)$, note that $\mathcal{R}$ commutes with $\mathrm{i}\sigma_2$ and $\mathcal{R}^2 = \mathrm{id}$ and $\sigma_2^2 = \sigma_0$.

Therefore the linearized dynamics of a disturbance $\tilde{B}(x,t)$ in the frame moving with speed $-c$ given by (5.1.2) is

$$\Big(\Sigma_{-c}\big(\partial_x - \tilde{w}'(z)\big) + A\left[u_\bullet, v_\bullet\right](x)\Big)\tilde{B}(x,t) = \partial_t \tilde{B}(x,t) \tag{6.1.4}$$

So the transformed linearized operator is given by

$$L_{\bullet,\tilde{w}}\left(x, \partial_x\right) = \Sigma(-c)\big(\partial_x - \tilde{w}'(x)\big) + A\left[u_\bullet, v_\bullet\right](x) \tag{6.1.5}$$

Now $\lambda \in \rho\big(L_\bullet\big)$ is equivalent to that the equation $\big(L_{\bullet,\tilde{w}} - \lambda\big)\tilde{B} = \tilde{f}$ is solvable for any $\tilde{f} \in L^2$, which is equivalent to

$$\mathrm{i}\sigma_2 \mathcal{R}\big(L_{\bullet,\tilde{w}} - \lambda\big)\mathcal{R}^{-1}\big(- \mathrm{i}\sigma_2^{-1}\big)B = \mathrm{i}\sigma_2 \mathcal{R} f \tag{6.1.6}$$

is solvable for any $f \in L^2$, So the conjugated operator is

$$\begin{aligned}
&\mathrm{i}\sigma_2\mathcal{R}\big(L_{\bullet,\tilde{w}} - \lambda\big)\mathcal{R}^{-1}\big(-\mathrm{i}\sigma_2^{-1}\big)\\
&= \begin{bmatrix} 0 & 1 \\ -1 & 0 \end{bmatrix} \mathcal{R} \begin{bmatrix} -c & 1 \\ 1 & -c \end{bmatrix} \big(\partial_x - \tilde{w}'(x)\big)\mathcal{R} \begin{bmatrix} 0 & -1 \\ 1 & 0 \end{bmatrix}\\
&\quad + \begin{bmatrix} 0 & 1 \\ -1 & 0 \end{bmatrix} \mathcal{R} \begin{bmatrix} -2\mathcal{N}\big(r_*(-x)^2\big)v_*(-x)u_*(-x) & \mathcal{N}_*\big(r_*(-x)^2\big) + 2\mathcal{N}'\big(r_*(-x)^2\big)u_*(-x)^2 \\ -\mathcal{N}_*\big(r_*(-x)^2\big) - 2\mathcal{N}'\big(r_*(-x)^2\big)v_*(-x)^2 & 2\mathcal{N}\big(r_*(-x)^2\big)v_*(-x)u_*(-x) \end{bmatrix} \mathcal{R} \begin{bmatrix} 0 & -1 \\ 1 & 0 \end{bmatrix}\\
&= \begin{bmatrix} c & 1 \\ 1 & c \end{bmatrix} \Big[\partial_x - \big(-\tilde{w}'(-x)\big)\Big] + \begin{bmatrix} 2\mathcal{N}\big(r_*(x)^2\big)u_*(x)v_*(x) & \mathcal{N}\big(r_*(x)^2\big) + 2\mathcal{N}'\big(r_*(x)^2\big)v_*(x)^2 \\ -\mathcal{N}\big(r_*(x)^2\big) - 2\mathcal{N}'\big(r_*(x)^2\big)u_*(x)^2 & -2\mathcal{N}\big(r_*(x)^2\big)u_*(x)v_*(x) \end{bmatrix}
\end{aligned} \tag{6.1.7}$$

Note that $\mathcal{R}\partial_x\mathcal{R}^{-1}g(x) = -\partial_x g(x)$ for any $g \in H^1$, and $RA(x)\mathcal{R}^{-1}g(x) = A(-x)g(x)$ for any matrix-valued function $A(x)$ and any $g \in L^2$. Therefore, choose $\tilde{w}(x) = w(-x) = \mathcal{R}w(x)$ then there is

$$L_{\bullet,\mathcal{R}w} = L_{*,w} \tag{6.1.8}$$

since

$$\mathcal{P}\mathrm{i}\sigma_2\mathcal{R}\tilde{b} = b_*, \mathcal{R}\tilde{w} = w \tag{6.1.9}$$

we can conclude the equivalence. □

Chapter 7: Supersonic pulses

By REMARK 6.8, we need only study the two supersonic pulses corresponding to the solid blue and green trajectories in FIGURE 2.2a. Recall $K = -\mathcal{N}'(1) > 0$; see (1.3.1).

Theorem 7.1 (Spectral stability for supersonic pulses)**.** *Let $b_*(x)$ be a supersonic pulse of speed $c > 1$ and corresponding to a trajectory of* (2.0.3) *with phase portrait energy $E_c = E$ for $c > 1$, marked with* *solid* *blue or* *solid* *green lines in figure* 2.2*. Then,*

1. *b_* is spectrally stable in L^2_a, i.e.* $\sup \mathtt{Re}\sigma(L_{*,a}) \leq 0$, *if and only if*

$$a \geq \frac{K}{c-1}\sqrt{1-(E-c)^2} \tag{7.0.1}$$

   In fact,

$$\sup \mathtt{Re}\sigma\left(L_{*,a}\right) = -a\left(c-1\right) + K\sqrt{1-\left(E-c\right)^2} \leq 0$$

   Hence, if strict inequality holds in (7.0.1)*, then* $\sup \mathtt{Re}\sigma(L_{*,a}) < 0$.

2. *Assume $E \neq c \pm 1$, or $E = c \pm 1$ and $a \neq 0$, then, $\sigma(L_{*,a})$ is always in the* *open* *left-half plane; the supremum is not attained. If $E = c \pm 1$ and $a = 0$, $\sigma(L_{*,a})$ is in the closed left-half plane and not in the open left-half plane.*

3. $0 \notin \sigma(L_{*,a})$*. In particular, the translation mode: $e^{ax}\,\partial_x b_*$, which satisfies $L_{*,a}\left(e^{ax}\,\partial_x b_*\right) = 0$, is not an $L^2(\mathbb{R})$ solution of $L_{*,a}Y = 0$.*

4. *For supersonic pulses with $c < -1$ we have similar results by* THEOREM *6.7 and* REMARK *6.8.*

We now proceed with the proof of THEOREM 7.1. We have the decomposition $\sigma(L_{*,a}) = \sigma_{\mathrm{e}}(L_{*,a}) \cup \sigma_{\mathrm{d}}(L_{*,a})$. We will prove, for an appropriate choice of weight e^{ax}, that both the *essential* *spectrum* and the *discrete spectrum* of operator $L_{*,a}$ are contained in the *open* left-half plane, *for most cases*.

Remark 7.2. The *only cases* when $\sigma(L_{*,a})$ is contained in the **closed** left-half plane, but not the open left-half plane, are when $E = c \pm 1$ and $a = 0$.

7.1 Essential spectrum for supersonic pulses

The essential spectrum is determined by the operator $L_{*,a}$ evaluated on its asymptotic equilibria; in particular, we have the expression on the supremum of its essential spectrum; see PROPOSITION 6.1. For pulses, $b_*(x) = \big[u_*(x), v_*(x)\big] = b_{c,E}$ or $\mathcal{T}b_{-c,-E}$, are the representative profiles, see REMARK 6.8. $b_* = b_{c,E}$ asymptotics to

$$\begin{aligned} \big[u_*(-\infty), v_*(-\infty)\big] &= \big[\cos\theta \quad \sin\theta\big] \\ \big[u_*(\infty) \quad v_*(\infty)\big] &= \big[\sin\theta \quad \cos\theta\big] = \Big[\cos\Big(\tfrac{\pi}{2}-\theta\Big) \quad \sin\Big(\tfrac{\pi}{2}-\theta\Big)\Big] \end{aligned} \tag{7.1.1}$$

while $b_* = \mathcal{T}b_{-c,-E}$ asymptotics to

$$\begin{aligned} \big[u_*(-\infty), v_*(-\infty)\big] &= \big[\cos\theta \quad \sin\theta\big] \\ \big[u_*(\infty) \quad v_*(\infty)\big] &= \big[-\sin\theta \quad -\cos\theta\big] = \Big[\cos\Big(-\tfrac{\pi}{2}-\theta\Big) \quad \sin\Big(-\tfrac{\pi}{2}-\theta\Big)\Big] \end{aligned} \tag{7.1.2}$$

where $\theta = \theta_{c,E} = \frac{1}{2}\arcsin(E-c)$, see (2.3.2).

By PROPOSITION 6.1 we have

$$\sup \mathtt{Re}\,\sigma_{\mathrm{e}}(L_{*,a}) = \max\big\{\sup \mathtt{Re}\,\sigma(L_-), \sup \mathtt{Re}\,\sigma(L_+)\big\},$$

where $L_- = L_{\theta,a}$ and $L_+ = L_{\pm\frac{\pi}{2}-\theta,a}$ whose expressions are given in (5.2.3), which we shall prove to be non-positive for a satisfying (7.0.1). Note that the two choices of $L_+ = L_{\pm\frac{\pi}{2}-\theta,a}$ are identical operators, since by their definition (5.2.3), $L_{\pm\frac{\pi}{2}-\theta,a}$ only depend on $\pm\frac{\pi}{2}-\theta$ through cosine or sine of $2\Big(\pm\frac{\pi}{2}-\theta\Big)$, which give the same values.

Now we apply PROPOSITION 6.1 to the weighted operator $L_{*,a}$ of supersonic pulse $b_*(x)$ to find the range of a for both the spectra of $L_\pm$ to be contained in the *open* left-half plane, or to be on the imaginary axis. By PROPOSITION 5.6, $\sigma(L_-)$ is in the closed left-half plane if (5.2.10) is satisfied:

$$a \geq \max\left\{-\frac{K\cos 2\theta}{c-1}, \frac{K\cos 2\theta}{c+1}\right\} = \frac{K\cos 2\theta}{c+1}$$

Note that $\cos 2\theta > 0$. Similarly for $\sigma(L_+) = \sigma(L_{\pm\frac{\pi}{2}-\theta,a})$, since $\cos 2(\pm\pi/2-\theta) = -\cos 2\theta \leq 0$, $\sup \mathtt{Re}\sigma(L_+) \leq 0$ if and only if

$$a \geq \max\left\{-\frac{-K\cos 2\theta}{c-1}, \frac{-K\cos 2\theta}{c+1}\right\} = \frac{K\cos 2\theta}{c-1}$$

again as a result of (5.2.10). So

$$\sup \mathtt{Re}\sigma_{\mathrm{e}}(L_{*,a}) = \max\left\{\sup \mathtt{Re}\sigma(L_-), \sup \mathtt{Re}\sigma(L_+)\right\} \leq 0$$

is equivalent to

$$a \geq \max\left\{\frac{K\cos 2\theta}{c-1}, \frac{K\cos 2\theta}{c+1}\right\} = \frac{K\cos 2\theta}{c-1} = \frac{K}{c-1}\sqrt{1-(E-c)^2}$$

since $\theta = \theta_{c,E} = \frac{1}{2}\arcsin(E-c)$ and $\cos 2\theta = \sqrt{1-(E-c)^2}$. This is exactly (7.0.1). Moreover, the suprema of $\mathtt{Re}\sigma(L_-) \equiv \mathtt{Re}\sigma(L_{\theta,a})$ and $\mathtt{Re}\sigma(L_+) \equiv \mathtt{Re}\sigma(L_{\pm\frac{\pi}{2}+\theta,a})$ satisfy the following inequality

$$\sup \mathtt{Re}\sigma(L_{\theta,a}) = -ac - \left|a - K\cos 2\theta\right| \leq -ac + \left|a + K\cos 2\theta\right| \leq \sup \mathtt{Re}\sigma(L_{\pm\frac{\pi}{2}+\theta,a})$$

since $\cos 2\theta = \sqrt{1-(E-c)^2} \geq 0$, and there is

$$\sup \mathtt{Re}\sigma_{\mathrm{e}}(L_{*,a}) = \mathtt{Re}\sigma(L_+). \tag{7.1.3}$$

If $E \neq c \pm 1$, the supremum is never achieved is a consequence of PROPOSITION 5.4, *i.e.* $\sup \sigma_{\mathrm{e}}(L_{*,a}) \subset \{\mathtt{Re}\, x < 0\}$. If $E = c \pm 1$, then (7.0.1) becomes $a \geq 0$. If $a = 0$, then from (5.2.3), both $\sigma_{\mathrm{e}}(L_{\pm})$ are both subsets the imaginary axis. So we have proved

Proposition 7.3. 1. *The essential spectrum of $L_{*,a}$, $\sigma_{\mathrm{e}}(L_{*,a})$, is contained in the closed left half plane, if and only if condition* (7.0.1) *on the weight parameter a is satisfied.*

2. *Assume* (7.0.1). *$\sigma_{\mathrm{e}}(L_{*,a})$ is in the open left-half plane, if and only if additionally we have that either $E \neq c \pm 1$ or $a \neq 0$.*

3. *Assume* (7.0.1). *Then, $\sigma_{\mathrm{e}}(L_{*,a})$ is on the imaginary axis if and only if $E = c \pm 1$ and $a = 0$.*

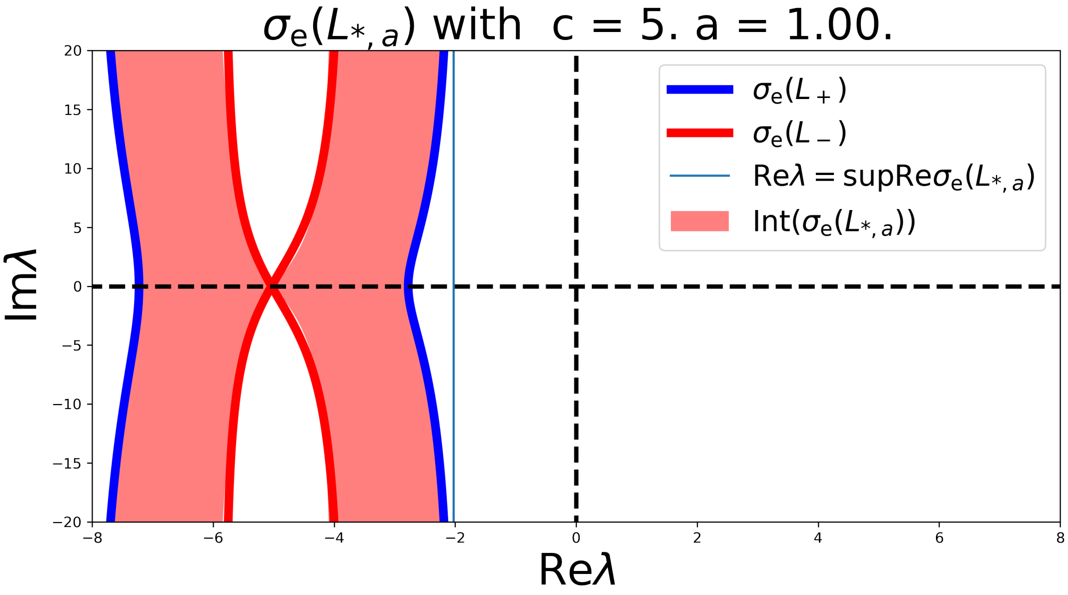

Figure 7.1: *Spectral stability of supersonic pulses via* THEOREM *7.1:* Essential spectrum, $\sigma_{\mathrm{e}}(L_{*,a})$ of weight-conjugated linearized operator $L_{*,a}$ for a supersonic pulse $b_* = b_{c,E}$. Parameters: $K = -\mathcal{N}'(1) = 2$, speed $c = 5$ and phase portrait energy $E_c = 4.84$. Weight parameter $a = 1$ ($W(x) = e^x$) satisfies $a \geq 0.494$, the lower bound in (7.0.1). Shown are spectra of $L_{\pm}$ (dark blue and red curves) which enclose $\sigma_{\mathrm{e}}(L_{*,a})$ (shaded light red). Vertical light blue line: $\mathtt{Re}\lambda = \sup \mathtt{Re}\sigma_{\mathrm{e}}(L_{*,a}) < 0$. There is no discrete spectrum

We have plotted the essential spectrum of a supersonic pulse in an appropriate weighted space L^2_a, to illustrate PROPOSITION 7.3, in FIGURE 7.1.

7.2 Discrete spectrum for supersonic pulses

In this section we prove that for *any* $a \in \mathbb{R}$, $L_{*,a}$ does not have any discrete spectrum to the right of its essential spectrum. That is,

$$\mathtt{Re}\sigma_{\mathrm{d}}(L_{*,a}) \leq \sup \mathtt{Re}\sigma_{\mathrm{e}}(L_{*,a}). \tag{7.2.1}$$

PROPOSITION 7.3 ensures that if that if (7.0.1) holds, then $\sup \mathtt{Re}\sigma_{\mathrm{e}}(L_{*,a}) \leq 0$ which implies spectral stability, $\sup \mathtt{Re}\sigma(L_{*,a}) \leq 0$ along with (7.2.1).

We now prove (7.2.1). By definition, $\lambda \in \sigma_{\mathrm{d}}(L_{*,a})$ if and only if there is an L^2 function $f(x)$ such that $(\lambda I - L_{*,a})f = 0$. We rewrite this spectral problem as an equivalent system of ODEs:

$$\partial_x f(x) = \Big[a + \Sigma^{-1}\big(\lambda - A_*(x)\big)\Big] f(x) \equiv \mathcal{A}(x,\lambda) f(x) \tag{7.2.2}$$

where $A_*(x)$ is given by (5.1.3) and Σ is given by (5.1.4). We show that for all $\lambda \in \mathbb{C}$ such that $\mathtt{Re}\lambda > \mathtt{Re}\sigma_{\mathrm{e}}(L_{*,a})$, that $\lambda \notin \sigma_{\mathrm{d}}(L_{*,a})$; this is the case if for such λ, all nontrivial solutions of (7.2.2) are unbounded as $x \to +\infty$. We claim that the matrix $\mathcal{A}(x,\lambda)$ has the following properties:

($\mathcal{A}$1) $x \mapsto \mathcal{A}(x,\lambda) \in C^1[0,\infty)$ is a C^1 mapping into the space of complex square matrices which, for each x, varies analytically for all $\lambda \in \mathbb{C}$.

($\mathcal{A}$2)

$$\sup_{\lambda \in \mathbb{C}} \|\mathcal{A}(x,\lambda) - \mathcal{A}_+(\lambda)\|_{\mathbb{C}^{n\times n}} \to 0$$

exponentially fast as $x \to +\infty$, where $\mathcal{A}_+(\lambda) = \lim_{x\to+\infty} \mathcal{A}(x,\lambda)$ is analytic for all $\lambda \in \mathbb{C}$.

($\mathcal{A}$3) For all $\lambda \in \mathbb{C}$, such that $\mathtt{Re}\lambda > \sup \mathtt{Re}\sigma_{\mathrm{e}}(L_{*,a})$, $\mathcal{A}_+(\lambda)$ has two eigenvalues with strictly positive real parts.

Assuming ($\mathcal{A}$3) holds, the set of all solutions of ODE are expressible as a linear combinations of (a) either two linearly independent solutions with exponential growth rates equal to the (positive) real parts of eigenvalues of $\mathscr{A}_+(\lambda)$ or (b) in the case of a non-diagonal Jordan normal form (due to a degenerate eigenvalue $\tilde{\mu}$) a solution with growth $\sim e^{\tilde{\mu}x}$ and a solution with growth $\sim x\ e^{\tilde{\mu}x}$. Hence, all solutions grow exponentially as $x \to +\infty$.

It suffices to verify ($\mathscr{A}$1)-($\mathscr{A}$3) for any given $a \in \mathbb{R}$, in particular for a that satisfies (7.0.1). Properties ($\mathscr{A}$1) and ($\mathscr{A}$2) are trivial. We next show ($\mathscr{A}$3). Due to the equivalence of the equation $(\lambda I - L_+)f = 0$ to (7.2.2), the eigenvalues, μ, of $\mathscr{A}_+(\lambda)$ are roots of the characteristic polynomial, arising by seeking solutions of $(\lambda I - L_+)f = 0$, with ansatz $f = f_0 e^{\mu x}$ where $f_0 \in \mathbb{C}^2$ is a nonzero vector. Recall that L_+, is the weight-conjugated linearized operator $L_{*,a}$ evaluated at $x = +\infty$ using the nontrivial equilibrium $\begin{bmatrix} \cos\vartheta & \sin\vartheta \end{bmatrix}^{\mathsf{T}}$, where $\vartheta = \pm\frac{\pi}{2} - \theta$, see (5.2.3).

Therefore, $\mu = \mu(\lambda)$ satisfies

$$\begin{aligned} 0 =& \det\left(\begin{bmatrix} c & 1 \\ 1 & c \end{bmatrix}(\mu - a) - K\begin{bmatrix} \sin 2\vartheta & 1 - \cos 2\vartheta \\ -1 - \cos 2\vartheta & -\sin 2\vartheta \end{bmatrix} - \begin{bmatrix} \lambda & 0 \\ 0 & \lambda \end{bmatrix}\right). \\ =& \left(c^2 - 1\right)(\mu - a)^2 - 2\left(\lambda c + K\cos 2\theta\right)(\mu - a) + \lambda^2 \end{aligned}$$

These roots given given by

$$\mu_\pm(\lambda) = a + \frac{\lambda c + K\cos 2\vartheta \pm \sqrt{\lambda^2 + 2\lambda c K \cos 2\vartheta + K^2 \sin^2 2\vartheta}}{c^2 - 1}. \tag{7.2.3}$$

Recall that $K > 0$ and $c > 1$. Define $\mu_1(\lambda) = \min \mathtt{Re}\mu_\pm(\lambda)$.

As λ varies over $\mathbb{C}$ the *set* of roots μ is always equal to $\{\mu_-(\lambda), \mu_+(\lambda)\}$. In a neighborhood which is small enough of any point where these roots vary analytically. To be precise, there is a pair of analytic functions in some small neighborhood of λ, μ_1 and μ_2, such that $\mu_1(\lambda) = \mu_-(\lambda)$ and $\mu_2(\lambda) = \mu_+(\lambda)$. This is true even if $\lambda \neq \lambda_{1,2}$ but on the cut of the square root appearing in (7.2.3). If λ is not on the cut, we can simply choose $\mu_1 = \mu_-$ and $\mu_2 = \mu_+$. These roots coincide at those values of λ for which

$$q(\lambda) \equiv \sqrt{\lambda^2 + 2\lambda c K \cos 2\vartheta + K^2 \sin^2 2\vartheta} = 0.$$

This occurs at the two values $\lambda_1(\theta)$ and $\lambda_2(\theta)$ given by:

$$K^{-1}\lambda_1(\theta) = c\cos 2\theta + \sqrt{c^2\cos^2 2\theta - \sin^2 2\theta}$$
$$K^{-1}\lambda_2(\theta) = c\cos 2\theta - \sqrt{c^2\cos^2 2\theta - \sin^2 2\theta}$$

where we used identities $\cos 2\vartheta = -\cos 2\theta$, $\sin 2\vartheta = -\sin 2\theta$. Note that $\mathtt{Re}\mu_+(\lambda_j) = \mathtt{Re}\mu_-(\lambda_j)$ for $j = 1, 2$, and $\mathtt{Re}\mu_\pm(\lambda) \longrightarrow \mathtt{Re}\mu_\pm(\lambda_j)$ as $\lambda \longrightarrow \lambda_j$. Hence

$$m(\lambda) = \min\{\mathtt{Re}\mu_+(\lambda), \mathtt{Re}\mu_-(\lambda)\}$$

varies continuously on $\mathbb{C}$.

We claim next that for all λ satisfying $\mathtt{Re}\lambda > \sup \mathtt{Re}\sigma_{\mathrm{e}}(L_{*,a})$, we have that $m(\lambda) > 0$. Indeed, for $\lambda = M \in \mathbb{R}$ such that $M \gg 1$:

$$\mu_+(M) = \frac{M}{c+1} + O(1), \quad \mu_-(M) = \frac{M}{c-1} + O(1), \tag{7.2.4}$$

implying, since $c > 1$. Hence, $m(M) > 0$ for all large M.

Now consider λ varying over the region $\mathtt{Re}\lambda > \sup \mathtt{Re}\sigma_{\mathrm{e}}(L_{*,a})$. Suppose $\mu_1(\lambda)$ is not always positive in this region. Since $m(\lambda)$ is continuous, there must be a $\hat{\lambda}$ for which

$$\mathtt{Re}\hat{\lambda} > \sup \mathtt{Re}\sigma_{\mathrm{e}}(L_{*,a}) \tag{7.2.5}$$

such that $m(\hat{\lambda}) = 0$. Therefore either $\mu_+(\hat{\lambda})$ or $\mu_-(\hat{\lambda})$ is purely imaginary. Without loss of generality we may assume that $\mu_+(\hat{\lambda}) = \mathrm{i}\hat{\xi}$ for $\xi \in \mathbb{R}$. It follows there is a function $Y \sim e^{i\hat{\xi}x}$, such that $(\hat{\lambda}I - L_+)Y = 0$. Since $\sigma_{\mathrm{e}}(L_+) \subset \sigma_{\mathrm{e}}(L_{*,a})$, it follows that $\hat{\lambda} \in \sigma_{\mathrm{e}}(L_{*,a})$. However, this contradicts (7.2.5). This contradiction implies that for all λ such that (7.2.5) holds, we have $\mathtt{Re}\mu_\pm(\lambda) > 0$.

Summarizing the result in this section, we have:

Proposition 7.4. *Let $L_{*,a}$ denote the linearization about a supersonic pulse, with a satisfying*

(7.0.1). *Then,*

1. *If* $\mathtt{Re}\lambda > 0$*, then* λ *is not in* $\sigma_{\mathrm{d}}(L_{*,a})$*.*
2. $0 \notin \sigma(L_{*,a})$*. In particular, the translation mode:* $e^{ax}\,\partial_x b_*$*, which satisfies* $L_{*,a}\,(e^{ax}\,\partial_x b_*) = 0$*, is not an* $L^2(\mathbb{R})$ *solution of* $L_{*,a}Y = 0$*.*

We need only verify Part 2. Note that if $b_*(x)$ satisfies (2.0.1), then $L_*\partial_x b_* = 0$ and hence $L_{*,a}\,(e^{ax}\,\partial_x b_*) = 0$. We claim that $\partial_x b_* \notin L^2_a$ for a satisfying (7.0.1). Note that

$$\partial_x b_*(x) \sim \exp\left(-\frac{2K\sqrt{1-(E-c)^2}}{c^2-1}\right),$$

from (2.3.9). Further, by (7.0.1), we have

$$a \geq \frac{K\sqrt{1-(E-c)^2}}{c-1} > \frac{2K\sqrt{1-(E-c)^2}}{(c-1)(c+1)} = \frac{2K\sqrt{1-(E-c)^2}}{c^2-1}.$$

Therefore $e^{ax}\partial_x b_*(x) \longrightarrow \infty$ as $x \longrightarrow \infty$, and $e^{ax}\partial_x b_*(x)$ is not in L^2.

7.3 Remarks on instability of subsonic pulses and antikinks

PROPOSITION 6.1 implies, for a TWS to be spectrally stable in some exponential weighted space L^2_w, it is necessary that both the spectra of asymptotic operators $L_\pm$ of $L_{*,w}$ is in the closed left-half plane. Since we have restricted the weight $W(x) = e^{w(x)}$ to be of exponential type defined in (5.1.1), both of the asymptotic equilibria $b(\pm\infty)$ of b_* need to be spectrally stable in some $L^2_{a_\pm}$ space, when observed in the reference frame moving with the same speed c of b_*. Conversely, if it is impossible to find, WLOG, a_+, such either $b(\infty)$ is stable in $L^2_{a_+}$, as a result, for any $W(x) = e^{w(x)}$ of the exponential type, $\sup \mathtt{Re}\sigma_{\mathrm{e}}(L_{*,w}) \geq \sup \mathtt{Re}\sigma(L_+) > 0$ and b_* is not stable in any L^2_w with exponential type weight. This is precisely what happens for the subsonic pulses, as well as antikinks.

In fact, since the subsonic pulses and antikinks are all subsonic, it is straightforward to verify that one of the asymptotic equilibria of a subsonic pulse, as well as the $b(-\infty)$ equilibrium of an antikink, are impossible to be rendered spectrally stable in any L^2_a space since for these equilibria (5.2.13) is violated.

Chapter 8: Spectral stability of kinks

Consider a kink profile $b_*(x)$ satisfying (2.2.2). As noted in REMARK 6.8, we may restrict our attention to kinks with speed $0 \leq c < 1$, $b_* = b_{c,0}$, where $b_{c,0}$ is the solution to (2.2.2), represented by the solid blue line in FIGURE 2.1a. The profile $b_*(x)$ tends to the equilibrium $\begin{bmatrix} 0 & 0 \end{bmatrix}^{\mathsf{T}}$ as $x \to -\infty$ and to a non-trivial equilibrium at $x \to +\infty$. We have shown in SECTION 5.2.1 that the trivial equilibrium is spectrally stable in the $\underline{\text{unweighted}}$ ($a = 0$) space, $L^2(\mathbb{R})$. We will first characterize the essential spectrum of kinks by applying PROPOSITION 6.1 again, before tackling the problem of locating the discrete spectrum.

8.1 Essential spectrum for kinks

Let L_* denote the linearized operator about b_*. Introduce a smooth spatial exponential weight $W(x) = e^{w(x)}$, where

$$w(x) = \begin{cases} 0 & x \leq -1 \\ ax & x \geq 1 \end{cases} \tag{8.1.1}$$

The linearized operator whose $L^2(\mathbb{R}; dx)$ spectrum determines the spectrum of L_* in $L^2(\mathbb{R}; W(x)dx)$ is given by $L_{*,w} = \Sigma\big(\partial_x - w'(x)\big) + A_*(x)$; see (5.1.5).

Proposition 8.1. *Assume that the weight $W(x) = e^{w(x)}$ is given by (8.1.1), where*

$$K\sqrt{\frac{1-c}{1+c}} \leq a \leq K\sqrt{\frac{1+c}{1-c}}. \tag{8.1.2}$$

Here, recall $K = -\mathcal{N}'(1) > 0$; see (1.3.1). Then, the essential spectrum of $L_{*,w}$ is contained in the closed left-half plane, i.e. $\mathtt{Re}\sigma_{\mathrm{e}}(L_{*,w}) \leq 0$.

For illustration of the essential spectrum of a typical kink where (8.1.2) is satisfied, see

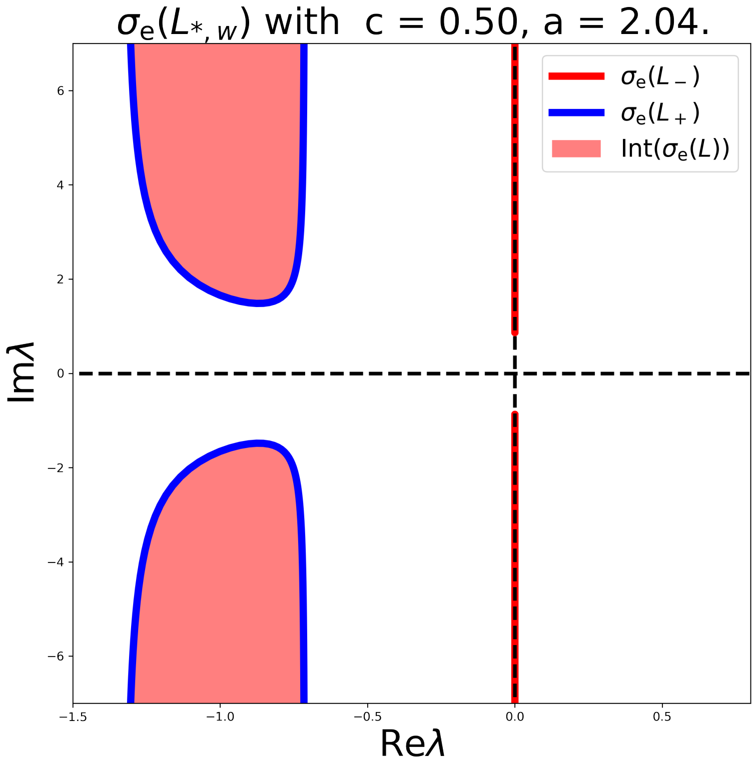

Figure 8.1: The essential spectrum of a kink with speed $c = 1/2$ with $a = 2.04$. Here the nonlinearity satisfies $K = -\mathcal{N}'(1) = 2$.

Proof. The ODE for a kink profile is given in (2.2.2). The kink is a heteroclinic connection between the trivial equilibrium at $x = -\infty$ and the nontrivial equilibrium $\begin{bmatrix}\cos\theta & \sin\theta\end{bmatrix}^{\mathsf{T}}$ at $x = \infty$, with $\theta = \theta_{c,0} = -\frac{1}{2}\arcsin c$; see (2.3.2). By PROPOSITION 6.1, the supremum of essential spectrum $\sigma_e(L_{*,w})$ is determined by the spectra of the asymptotic operators $L_- = L_O$ and $L_+ = L_{\theta,a}$; specifically,

$$\sup \mathtt{Re}\sigma_e(L_{*,w}) = \max\left\{\sup \mathtt{Re}\sigma(L_O), \sup \mathtt{Re}\sigma(L_{\theta,a})\right\}$$

The spectrum of L_O is on the imaginary axis, by PROPOSITION 5.2, so $\sup \mathtt{Re}\sigma(L_O) = 0$. Therefore $\sup \mathtt{Re}\sigma_e(L_{*,w}) \leq 0$ if and only if $\sup \mathtt{Re}\sigma_e(L_{\theta,a}) = 0$. By PROPOSITION 5.6, the spectrum of $L_{\theta,a}$ is in the closed left-half plane if and only if a satisfies (5.2.12). Hence, $\sup \mathtt{Re}\sigma_e(L_{*,w}) = 0$ if and only if (5.2.12) is satisfied. Since $\cos 2\theta = \sqrt{1 - c^2}$, condition (5.2.12) is equivalent to (8.1.2).

□

8.2 Neutral spectral stability of Non-moving ($c = 0$) kinks

Remark 8.2. The fact that non-moving kinks are spectrally stable in some weighted L^2 space is a special case of THEOREM 8.8 in SECTION 8.3 later. However, the current SECTION 8.2 provides a stronger result and simpler treatment for the $c = 0$ special case. Therefore we advise that the readers start with this section first, for pedagogical purposes. In particular, in the current section we do not assume that the nonlinearity $\mathcal{N}(r^2)$ satisfies the concavity condition (8.3.2). Moreover, the transformation (8.2.8) in the current section is a special case of the one provided in PROPOSITION 8.11 in SECTION 8.3, and is less complicated.

For non-moving kinks with speed $c = 0$ the only possible asymptotic weight as $x \to \infty$ is e^{Kx} if it were to be spectrally stable in L^2_w, as a result of PROPOSITION 8.1 where the only possible a is $a = K$. There are four non-moving kinks, each connecting the trivial equilibrium to different nontrivial equilibria, but WLOG we study the one that asymptotes to $[1, 0]$ as $x \to \infty$, by virtue of THEOREM 6.7. The polar angle of this equilibrium on the phase plane of (2.0.3) is $\theta = 0$, setting $c = 0$ and $E = 0$ in (2.3.2). Now we note that, for this particular kink, $u_*(x) = r_0(x) \geq 0$ in (2.2.2), which now implies

$$r_0'(x) = r_0(x)\mathcal{N}\big(r_0(x)^2\big), \quad r_0(0) = \frac{1}{2} \tag{8.2.1}$$

So $r_0(x) \to 0$ exponentially as $x \to -\infty$, and $r_0(x) \to 1$ exponentially as $x \to \infty$.

As declared by the theorem below, a non-moving kink is neutrally spectrally stable since its spectrum is a subset of the imaginary axis.

Theorem 8.3. *Consider the non-moving kink ($c = 0$) namely $b_* = b_{0,0}$ satisfying (2.2.2) with $c = 0$, connecting the trivial fixed point and the fixed point $[1, 0]$ on the phase plane. Let $W(x) = e^{w(x)} \in C^1$ such that*

$$W(x) = e^{w(x)} = \begin{cases} 1 & \text{for } x \leq -1 \\ e^{Kx} & \text{for } x \geq 1 \end{cases}$$

Then, b_* is neutrally spectrally stable in L^2_w, i.e. $\sigma\big(L_{*,w}\big) \subset \mathrm{i}\mathbb{R}$. In particular,

(i) The essential spectrum of $L_{*,w}$ is a subset of the imaginary axis:

$$\sigma_{\mathrm{e}}\big(L_*\big) = \mathrm{i}\mathbb{R} \setminus \mathrm{i}\big(-\kappa, \kappa\big)$$

where $\kappa = \min\big\{1, K\big\} > 0$.

(ii) The discrete spectrum of $L_{*,w}$ is a subset of $i(-\kappa,\kappa)$, and $0 \in \sigma_{\mathrm{d}}\big(L_{*,w}\big)$ is a simple eigenvalue.

The essential spectrum of a non-moving kink is a subset of the imaginary axis; this is because the spectra of the left- and right-asymptotic operators of $L_{*,w}$, namely $L_- = L_O$ and $L_+ = L_{0,K}$, are all on the imaginary axis. This can be seen from (5.2.2) and (5.2.4). In fact:

$$\sigma(L_O) = \mathrm{i}\mathbb{R} \setminus \mathrm{i}(-1,1), \quad \sigma(L_{0,K}) = \mathrm{i}\mathbb{R} \setminus \mathrm{i}(-K,K) \tag{8.2.2}$$

Therefore to prove THEOREM 8.3, it suffices to locate the discrete spectrum, since the essential spectrum is the union of $\sigma(L_O)$ and $\sigma(L_{0,K})$ given by (8.2.2). We consider the eigenvalue problem

$$L_{*,w}\tilde{B} = \lambda\tilde{B} \tag{8.2.3}$$

and $\lambda \in \mathbb{C} \setminus \sigma_{\mathrm{e}}\big(L_{*,w}\big)$ and $0 \neq \tilde{B} \in H^1$ satisfies (8.2.3). From (5.1.5) and (5.1.3) we have and equivalent formulation of (8.2.3):

$$L_{*,w}\tilde{B}(x) \equiv \begin{bmatrix} 0 & 1 \\ 1 & 0 \end{bmatrix} \big(\partial_x - w'(x)\big) + \begin{bmatrix} 0 & \mathcal{N}_0 \\ -\mathcal{N}_0 - 2\mathcal{N}_p & 0 \end{bmatrix} \tilde{B}(x) = \lambda\tilde{B}(x), \tag{8.2.4}$$

where

$$\mathcal{N}_0(x) := \mathcal{N}\big(r_0(x)^2\big), \ \mathcal{N}_p(x) := \mathcal{N}'(s)\Big|_{s=r_0(x)^2} r_0(x)^2 \tag{8.2.5}$$

Note that $v_* = 0$ for kinks with speed $c = 0$, see (2.2.2) and set $c = 0$ there. Multiplying both sides of (8.2.4) by the Pauli matrix σ_1, we find that (8.2.4) is equivalent to

$$\partial_x \tilde{B}(x) = \begin{bmatrix} \mathcal{N}_0(x) + 2\mathcal{N}_p(x) + w'(x) & \lambda \\ \lambda & -\mathcal{N}_0(x) + w'(x) \end{bmatrix} \tilde{B}(x) \tag{8.2.6}$$

Introducing an integrating factor, we rewrite (8.2.6) as

$$\begin{aligned} &\partial_x \left(\exp\left[-w(x) - \int_{-\infty}^{x} \mathcal{N}_p(y)\,\mathrm{d}y \right] \tilde{B}(x) \right) \\ &= \begin{bmatrix} \mathcal{N}_0(x) + \mathcal{N}_p(x) & \lambda \\ \lambda & -\mathcal{N}_0(x) - \mathcal{N}_p(x) \end{bmatrix} \left(\exp\left[-w(x) - \int_{-\infty}^{x} \mathcal{N}_p(y)\,\mathrm{d}y \right] \tilde{B}(x) \right) \end{aligned}$$

So $B(x) \in C^1$ is a solution of

$$\partial_x B(x) = \begin{bmatrix} \mathcal{N}_0(x) + \mathcal{N}_p(x) & \lambda \\ \lambda & -\mathcal{N}_0(x) - \mathcal{N}_p(x) \end{bmatrix} B(x) \tag{8.2.7}$$

if and only if

$$\tilde{B}(x) = \exp\left(w(x) + \int_{-\infty}^{x} \mathcal{N}_p(y)\,\mathrm{d}y \right) B(x) \tag{8.2.8}$$

is a C^1 solution to (8.2.3). That the eigenvalue problem associated with (8.2.3) is equivalent to the eigenvalue problem associated with equation (8.2.8), is a consequence of the following lemma:

Lemma 8.4. *Let $\lambda \in \mathbb{C}$, and let $B(x)$ and $\tilde{B}(x)$ be related by (8.2.8). Then, $B \in L^2$ if and only if $\tilde{B} \in L^2$.*

Proof. It is equivalent to proving that the weight in (8.2.8) is bounded for all $x \in \mathbb{R}$. Equivalently, the exponent

$$w(x) + \int_{-\infty}^{x} \mathcal{N}_p(y)\,\mathrm{d}y \tag{8.2.9}$$

is bounded uniformly for $x \in \mathbb{R}$. Note that $w(x) = 0$ for $x \leq -1$; also $r_0(x) \to 0$ exponentially as $y \to -\infty$, so $\mathcal{N}_p(x) = \mathcal{N}'\big(r_0(x)^2\big)r_0(x)^2 \to 0$ exponentially as $x \to -\infty$ as well since $\mathcal{N}'(r^2)$ is bounded for all $r^2 \geq 0$. As a result, the expression in (8.2.9) is bounded for all large and negative

x. For $x \geq 1$, there is $w(x) = Kx$. Also, $\mathcal{N}_p(x) = \mathcal{N}'\big(r_0(x)^2\big)r_0(x)^2 \to -K$ exponentially fast as $x \to \infty$, since $\mathcal{N}''(r^2)$ is also bounded near $r^2 = 1$ and $r_0(x)^2 \to 1$ exponentially fast as $x \to \infty$. Thus, for some $X_0 > 0$ and all $x \geq X_0$, we have:

$$w(x) + \int_{-\infty}^{x} \mathcal{N}_p(y)\,\mathrm{d}y = Kx + \int_{-\infty}^{X_0} N_p(y)dy + \int_{X_0}^{x} \left(-K + O(e^{-\gamma X})\right) dX,$$

for some $\gamma > 0$ which is bounded for all $x \geq X_0$. as $x \to \infty$. □

It then follows immediately that:

Corollary 8.5. *The pair* $(\lambda, \tilde{B})$*, with* $0 \neq \tilde{B} \in H^1$ *solves the eigenvalue problem* (8.2.3)*, if and only if* (λ, B) *where* $0 \neq B \in H^1$ *solves the eigenvalue problem* (8.2.7).

Now, it is convenient to write out (8.2.7):

$$\begin{aligned} U_x &= \big[\mathcal{N}_0(x) + \mathcal{N}_p(x)\big]U + \lambda V \\ V_x &= \lambda U - \big[\mathcal{N}_0(x) + \mathcal{N}_p(x)\big]V \end{aligned} \tag{8.2.10}$$

We are now able to reduce the problem of finding eigenpairs of $L_{*,w}$ to finding bound state and bound state energies of some linear Schrödinger operator on the real line, as shown in the following lemma:

Lemma 8.6. *Assume that the pair* $(\lambda, B(x))$ *where*

$$0 \neq \lambda \in \mathsf{C} \quad \text{and} \quad 0 \neq B(x) \equiv \begin{bmatrix} U(x) & V(x) \end{bmatrix}^{\mathsf{T}} \in L^2$$

solves (8.2.7)*. Then,* $(\mathcal{E} = -\lambda^2, U(x))$ *with* $0 \neq U \in L^2$ *and* $-\lambda^2 \in \mathbb{R}$*, is an eigenpair for the eigenvalue problem:*

$$\left(-\partial_x^2 + \mathcal{V}(x)\right) U(x) = \mathcal{E}U(x), \quad U(x) \in L^2,$$

with the real-valued potential

$$\mathcal{V}(x) = \big[\mathcal{N}_0(x) + \mathcal{N}_p(x)\big]_x + \big[\mathcal{N}_0(x) + \mathcal{N}_p(x)\big]^2.$$

Moreover, $\mathcal{E} = 0$ *is the ground state of operator* $-\partial_x^2 + \mathcal{V}(x)$.

Proof. From (8.2.10), it is easy to see in fact U is twice continuously differentiable. Now, differentiate the first equation with respect to x and using the second to eliminate V_x:

$$U_{xx} = \big[\mathcal{N}_0(x) + \mathcal{N}_p(x)\big]_x U + \lambda^2 U + \big[\mathcal{N}_0(x) + \mathcal{N}_p(x)\big]^2 U$$

or

$$\big[-\partial_x^2 + \mathcal{V}(x)\big]U(x) = \mathcal{E}U(x),\ \mathcal{E} = -\lambda^2$$

where is a time-independent Schrödinger equation with a real-valued potential

$$\mathcal{V}(x) = \big[\mathcal{N}_0(x) + \mathcal{N}_p(x)\big]^2 + \big[\mathcal{N}_0(x) + \mathcal{N}_p(x)\big]_x.$$

Let $\mathcal{L} = -\partial_x^2 + \mathcal{V}(x)$. We observe that $U \neq 0$ if $\lambda \neq 0$; otherwise if $\lambda \neq 0$ and $U = 0$, it would follow from (8.2.10) that $V = 0$, which contradicts the assumption that $B \neq 0$.

Now we prove that $\mathcal{E} = 0$ is an eigenvalue of $-\partial_x^2 + \mathcal{V}(x)$. From the definition of $\mathcal{N}_0$ and $\mathcal{N}_p$ in (8.2.5),

$$\mathcal{N}_0(-\infty) + \mathcal{N}_p(-\infty) = 1 > 0 > \mathcal{N}_0(\infty) + \mathcal{N}_p(\infty) = -K$$

so there is an $x' \in \mathbb{R}$ at which hold that $\mathcal{N}_0(x') + \mathcal{N}_p(x') = 0$ and that its derivative is negative. At x', there is

$$\begin{aligned}\mathcal{V}(x') =& \big[\mathcal{N}_0(x') + \mathcal{N}_p(x')\big]^2 + \Big(\partial_x\big[\mathcal{N}_0(x) + \mathcal{N}_p(x)\big]\Big)_{x=x'}\\ =&0 + \Big(\partial_x\big[\mathcal{N}_0(x) + \mathcal{N}_p(x)\big]\Big)_{x=x'} < 0\end{aligned}$$

Therefore $\min_{x\in\mathbb{R}} \mathcal{V}(x) < 0$.

Now $\mathcal{E} = -\lambda^2 = 0$ is an eigenvalue of $\mathcal{L}$. In fact, in this case, $\lambda = 0$ and from (8.2.10) we see

$V(x) \equiv 0$ since as $x \longrightarrow \infty$,

$$-\mathcal{N}_0(-\infty) - \mathcal{N}_p(-\infty) = -1$$

so V cannot be bounded as $x \longrightarrow -\infty$, unless it vanishes for all $x \in \mathbb{R}$, and there is a unique $U(x)$ given by (up to a constant):

$$U(x) = U_0(x) = \exp\left(\int^x \mathcal{N}_0(x) + \mathcal{N}_p(x)\right) \tag{8.2.11}$$

that solves the first of the (now decoupled) equations in (8.2.10). In fact, direct differentiation yields:

$$U_{0,xx}(x) = \left[\left(\mathcal{N}_0 + \mathcal{N}_p\right)U_0\right]_x = \left(\mathcal{N}_0 + \mathcal{N}_p\right)_x U_0 + \left(\mathcal{N}_0 + \mathcal{N}_p\right)^2 U_0$$

Now for any $x \in \mathbb{R}$ there is $U(x) \neq 0$, otherwise, there would be $U \equiv 0$. So $U(x)$ has *no nodes* and thus it is the ground state of $\mathcal{L}$, and $\mathcal{E} = 0$ is the (nondegenerate) ground state energy. □

We are ready to prove THEOREM 8.3

Proof of THEOREM *8.3*. Part (i) follows Part (i) of THEOREM 6.2 and Part (ii) of THEOREM 6.3, with $\sigma(L_\pm)$ given by (8.2.2)

It follows from LEMMA 8.6, by self-adjointness of $-\partial_x^2 + \mathcal{V}$ that $-\lambda^2 \in \mathbb{R}$ and therefore,

$$\lambda \text{ is either real or purely imaginary.}$$

We may contrain λ further. Indeed, note that $\mathcal{N}_p(x) = \mathcal{N}'\left(r_0^2(x)\right)r_0^2(x)$ approaches 0 as $x \longrightarrow -\infty$ (since $r_0(-\infty) = 0$) and approaches $-K = \mathcal{N}'(1)$ as $x \longrightarrow +\infty$ (since $r_0(\infty) = 1$). Hence, $\mathcal{V}(-\infty) = 1$, and $\mathcal{V}(\infty) = K^2 > 0$. It follows that $-\lambda^2 = \mathcal{E} < \min\{1, K^2\}$. It follows that

$$\lambda \text{ is either real or purely imaginary with } \left|\mathtt{Im}\lambda\right| < \min\{1, K\} = \kappa. \tag{8.2.12}$$

Now we claim there is no real eigenvalues of $L_{*,w}$. This implies it does not has an eigenvalue with a nonzero real part, and the non-moving kink is neutrally spectrally stable in L_w^2. Should there exist

$\lambda \in \mathbb{R}$ and $\tilde{B} \in H^1$ that solves (8.2.3), then from COROLLARY 8.5 and LEMMA 8.6 there would be an eigenpair $\mathcal{E} = -\lambda^2 < 0$ and $U \in L^2$ of the operator $-\partial_x^2 + \mathcal{V}(x)$. In fact, this is impossible since $\mathcal{E} = 0$ is the ground state energy of $-\partial_x^2 + \mathcal{V}(x)$.

Therefore there is no real eigenvalues of $L_{*,w}$, and proof of THEOREM 8.3 is concluded. ◻

Remark 8.7. We remark that $\sigma(L_{*,w})$ has no embedded eigenvalues in the essential spectrum, see statement (8.2.12), and that $\sigma_{\mathrm{d}}(L_{*,w})$ and is a finite subset of the imaginary interval $(-\mathrm{i}\kappa, \mathrm{i}\kappa)$, since otherwise it would imply $-\partial_x^2 + \mathcal{V}(x)$ has infinite bound states; it is straightforward to see $\mathcal{V}(x)$ asymptotes to $\mathcal{V}(\pm\infty)$ exponentially fast so this contradicts the Faddeev criterion, which says it has only finitely many bound states if $\int (1 + |x|)\mathcal{V}(x) < \infty$.

8.3 Spectral stability of moving kinks $(0 \leq c < 1)$

Introduce the smooth weight $W_c(x) = e^{w_c(x)}$, where

$$W_c(x) = e^{w_c(x)} = \begin{cases} 1 & \text{for } x \leq -1 \\ e^{\frac{\kappa}{\sqrt{1-c^2}}x} & \text{for } x \geq 1 \end{cases} \tag{8.3.1}$$

We furthermore require the nonlinearity satisfies the following **concavity** condition:

$$\mathcal{N}''(s) \leq 0, \quad \text{for } s \in [0, 1] \tag{8.3.2}$$

Theorem 8.8. *Assume the nonlinearity satisfies the concavity condition* (8.3.2). *Then,*

1. *Any kink* $b_* = b_{c,0}$ *(speed* $c \in [0, 1)$*) is spectrally stable in* $L^2_{w_c}$ *given by* (8.3.1)*. That is, the spectrum of weighted operator* L_{*,w_c} *is a subset of the closed left-half complex plane.*

2. *In particular,* $0 \in \sigma_{\mathrm{d}}(L_{*,w_c})$ *and the corresponding zero energy eigenspace is spanned by* $\partial_x b_{c,0}(x)$*, arising from translation invariance of* (2.0.1).

Remark 8.9. The neutral mode by translation invariance which corresponds to the neutral eigenvalue 0, is always in the spectrum, since $e^{\frac{Kx}{\sqrt{1-c^2}}}\partial_x b_*(x) \longrightarrow 0$ as $x \longrightarrow \infty$. In fact, the rate $a = \frac{K}{\sqrt{1-c^2}}$ in THEOREM 8.8 satisfies

$$a \leq \frac{2K}{\sqrt{1-c^2}}$$

where $\frac{2K}{\sqrt{1-c^2}}$ comes from the decay rate of the kink as $x \longrightarrow \infty$, namely (2.3.8). This is in contrast to the case of supersonic pulses, see PROPOSITION 7.4 and the discussion which follows it.

Remark 8.10. We can improve the result a bit by merely requiring that the parameter a in $e^{w(x)} = e^{ax}$ for $x > 1$ to satisfy

$$K\sqrt{\frac{1-c}{1+c}} \leq a \leq K\sqrt{\frac{1+c}{1-c}}$$

However for simplicity we made the restriction $a = \frac{K}{\sqrt{1-c^2}}$ above. This restriction does not affect our understanding of the "big picture". Moreover, with this weight, when $c = 0$, the results in THEOREM 8.3 are recovered.

Recall for $c = 0$ we transformed eigenvalue problem (8.2.3) to (8.2.7), through transformation (8.2.8). We proceed in an analogous manner. We begin with the eigenvalue problem:

$$L_{*,w_c}\tilde{B}(x) = \lambda \tilde{B}(x), \quad \tilde{B} \in L^2 \tag{8.3.3}$$

Explicitly, L_{*,w_c} defined in (5.1.5) is the (weight-conjugated) linearized operator about a kink of speed $0 < c < 1$:

$$L_{*,w_c} = \Sigma\Big(\partial_x - w_c'(x)\Big) + A_*(x),$$

where $\Sigma = c\sigma_0 + \sigma_1$ and

$$A_*(x) = \begin{bmatrix} \mathcal{N}'\big(r_*(x)^2\big)r_*(x)^2 \sin 2\theta & \mathcal{N}_*\big(r_*(x)^2\big) + 2\mathcal{N}'\big(r_*(x)^2\big)r_*(x)^2 \sin^2\theta \\ -\mathcal{N}\big(r_*(x)^2\big) - 2\mathcal{N}'\big(r_*(x)^2\big)r_*(x)^2 \cos^2\theta & -\mathcal{N}'\big(r_*(x)^2\big)r_*(x)^2 \sin 2\theta \end{bmatrix}$$

The expression for $A_*(x)$ is the general expression (5.1.3) where set set $(u_*, v_*) = b_*$ satisfying (2.2.2) with speed c; the kink profile which tends to $(0,0)$ as $x \to -\infty$ and to $(\cos(\theta), \sin(\theta))$ as $x \to +\infty$. Here, $\theta = \theta_{c,0} = -\frac{1}{2}\arcsin c$ is defined in (2.3.2) and setting $E = 0$, or can be read-off directly from the ODE for kinks' profiles (2.2.2). Moreover, since the profile equations for kinks $b_{c,0}$ and $b_{0,0}$ only differ by a factor of $\sqrt{1-c^2}$, there is a simple scaling relating their amplitudes which we will derive below.

Eigenvalue problem (8.3.3) is rather complicated, in view of the expression of A_* above. However, it is possible to reduce it to a simpler form:

Proposition 8.11. *Assume eigenvalue problem* (8.3.3) *is satisfied by* $\lambda \in \mathbb{C}, \tilde{B} \in L^2$. *Let* $B = \begin{bmatrix} U & V \end{bmatrix}^\mathsf{T}$ *satisfying*

$$B(X) = e^{-c\Lambda X} e^{w_c\left(\sqrt{1-c^2}X\right) + \int_{-\infty}^{X} \mathcal{N}_p(Y)\,\mathrm{d}Y} \beta(X) \tag{8.3.4}$$

where the intermediate $\beta(X)$ *is related to* $\tilde{B}$ *by*

$$\tilde{B}\left(\sqrt{1-c^2}X\right) = \left(\sigma_0 \cos\theta + \sigma_1 \sin\theta\right)\beta(X) \tag{8.3.5}$$

where $\sigma_j,\ j = 0, 1, 2, 3$ *are Pauli matrices. See* (1.7.2). *Then,*

$$\begin{aligned} U_X &= \left(\mathcal{N}_0 + \mathcal{N}_p\right)U + \left(\Lambda - 2c\mathcal{N}_p\right)V \\ V_X &= \Lambda U - \left(\mathcal{N}_0 + \mathcal{N}_p\right)V \end{aligned}, \tag{8.3.6}$$

where $\mathcal{N}_0 = \mathcal{N}\left(r_0(x)^2\right)$ *and* $\mathcal{N}_p = \mathcal{N}'(r_0(x)^2)r_0(x)^2$, *defined in* (8.2.5), *where* $r_0(x)$ *is the amplitude of the non-moving kink profile satisfying* (8.2.1); *and* $\Lambda = \frac{\lambda}{\sqrt{1-c^2}}$.

Note that setting $c = 0$, transformation (8.2.8) is recovered from (8.3.5) and (8.3.4).

Remark 8.12. We remark on the intuition behind the transform (8.3.7) above. Consider the ODE (2.2.2) which the profiles of kinks and antikinks satisfy (without the restriction on the second line of (2.2.2)). For $c = 0$, the orbits of possible kinks lie on the u-axis, and those of possible antikinks lie on the v-axis. In general, however, the kink $b_{c,0}$ and $\mathcal{P}b_{c,0}$ lie on the line parallel to vector $\begin{bmatrix}\cos\theta & \sin\theta\end{bmatrix}$, and the antikinks $C\mathcal{P}b_{c,0}$ and $Cb_{c,0}$ lie on the line parallel to the vector $\begin{bmatrix}\sin\theta & \cos\theta\end{bmatrix}$, see FIGURE 2.1a; note that for $c > 0$, $\theta = -\frac{1}{2}\arcsin c < 0$. We would like to express the perturbation in terms of coordinates along these two vectors, hence the transform (8.3.7).

Proof. We will express formulas with Pauli matrices in this proof. See (1.7.2) and (1.7.3).

We conduct an intermediate transform on the unknown function $\tilde{B}$:

$$\tilde{B}\left(\sqrt{1-c^2}X\right) = \left(\sigma_0\cos\theta + \sigma_1\sin\theta\right)\beta(X) \tag{8.3.7}$$

for $X \in \mathbb{R}$, which is exactly (8.3.5).

We must take care when plug (8.3.7) into (8.3.3). For a generic differential equation of the form $\partial_x f(x) = g(x)$ which holds for all $x \in \mathbb{R}$. Consequently we have

$$\frac{1}{\sqrt{1-c^2}}\partial_X f\left(\sqrt{1-c^2}X\right) = g\left(\sqrt{1-c^2}X\right)$$

for all $X \in \mathbb{R}$. So write $L_{*,w}\left(\partial_x, x\right)$, (8.3.3) is equivalent to

$$L_{*,w}\left(\frac{1}{\sqrt{1-c^2}}\partial_X, \sqrt{1-c^2}X\right)\tilde{B}\left(\sqrt{1-c^2}X\right) = \lambda\tilde{B}\left(\sqrt{1-c^2}X\right) \tag{8.3.8}$$

For convenience we further define

$$\psi(X) = \sqrt{1-c^2}w_c'(x)|_{x=\sqrt{1-c^2}X} = \frac{\mathrm{d}w_c\left(\sqrt{1-c^2}X\right)}{\mathrm{d}X}, \quad \Lambda = \frac{\lambda}{\sqrt{1-c^2}} \tag{8.3.9}$$

The kink $b_*(x) = \begin{bmatrix}u_*(x) & v_*(x)\end{bmatrix} = b_{c,0}(x)$ satisfies (2.2.2) which we repeat here:

$$r_*'(x) = \frac{r_*(x)\mathcal{N}\left(r_*(x)^2\right)}{\sqrt{1-c^2}} \tag{8.3.10}$$

Note that for $c = 0$,

$$r_0'(x) = r_0(x)\mathcal{N}\left(r_0(x)^2\right) \tag{8.3.11}$$

and $r_0\Big(\frac{x}{\sqrt{1-c^2}}\Big)$ satisfies

$$\frac{\mathrm{d}}{\mathrm{d}x} r_0\Big(\frac{x}{\sqrt{1-c^2}}\Big) = \frac{1}{\sqrt{1-c^2}} r_0'\Big(\frac{x}{\sqrt{1-c^2}}\Big) \tag{8.3.12}$$

Combining (8.3.11) and (8.3.12), we see $x \mapsto r_0\Big(\frac{x}{\sqrt{1-c^2}}\Big)$ satisfies (8.3.10) and have value $r_0(0/\sqrt{1-c^2}) = r_0(0) = 1/2$ at $x = 0$. Therefore for all $x \in \mathbb{R}$,

$$r_*(x) = r_0\Big(\frac{x}{\sqrt{1-c^2}}\Big)$$

and equivalently for all $X \in \mathbb{R}$,

$$r_*\big(\sqrt{1-c^2}X\big) = r_0(X) \tag{8.3.13}$$

Now we transform (8.3.3) according to (8.3.8). In the first identity below we used (8.3.13):

$$\begin{aligned}
&L_{*,w}\Big(\frac{1}{\sqrt{1-c^2}}\partial_X, \sqrt{1-c^2}X\Big) = \big(c\sigma_0 + \sigma_1\big)\Big(\frac{1}{\sqrt{1-c^2}}\partial_X - w_c'(x)|_{x=\sqrt{1-c^2}X}\Big)\\
&+ \begin{bmatrix} \mathcal{N}'\big(r_*(x)^2\big)r_*(x)^2 \sin 2\theta & \mathcal{N}_*\big(r_*(x)^2\big) + 2\mathcal{N}'\big(r_*(x)^2\big)r_*(x)^2 \sin^2\theta \\ -\mathcal{N}\big(r_*(x)^2\big) - 2\mathcal{N}'\big(r_*(x)^2\big)r_*(x)^2\cos^2\theta & -\mathcal{N}'\big(r_*(x)^2\big)r_*(x)^2 \sin 2\theta \end{bmatrix}_{x=\sqrt{1-c^2}X}\\
=&\frac{\big(c\sigma_0+\sigma_1\big)}{\sqrt{1-c^2}}\big(\partial_X - \psi(X)\big)\\
&+ \begin{bmatrix} \mathcal{N}'\big(r_0(X)^2\big)r_0(X)^2 \sin 2\theta & \mathcal{N}\big(r_0(X)^2\big) + 2\mathcal{N}'\big(r_0(X)^2\big)r_0(X)^2 \sin^2\theta \\ -\mathcal{N}\big(r_0(X)^2\big) - 2\mathcal{N}'\big(r_0(X)^2\big)r_0(X)^2\cos^2\theta & -\mathcal{N}'\big(r_0(X)^2\big)r_0(X)^2 \sin 2\theta \end{bmatrix}\\
=&\frac{\big(c\sigma_0+\sigma_1\big)}{\sqrt{1-c^2}}\big(\partial_X - \psi(X)\big) - \sigma_1\mathcal{N}_p(X)\cos 2\theta + \mathrm{i}\sigma_2\big[\mathcal{N}_0(X) + \mathcal{N}_p(X)\big] + \sigma_3\mathcal{N}_p(X)\sin 2\theta\\
=&\frac{\big(c\sigma_0+\sigma_1\big)}{\sqrt{1-c^2}}\big(\partial_X - \psi\big) - \sigma_1\mathcal{N}_p\sqrt{1-c^2} + \mathrm{i}\sigma_2\big(\mathcal{N}_0 + \mathcal{N}_p\big) - \sigma_3\mathcal{N}_p c
\end{aligned} \tag{8.3.14}$$

In the last line we have used $\theta = -\frac{1}{2}\arcsin c$. Functions $\mathcal{N}_0$ and $\mathcal{N}_p$ are defined in (8.2.5). Using (8.3.14) above, plug the transformation (8.3.7) relating $\tilde{B}$ with β into (8.3.8), (8.3.3) is equivalent to

$$\begin{aligned}
&\frac{c\sigma_0+\sigma_1}{\sqrt{1-c^2}}\big(\partial_X-\psi\big)\big(\sigma_0\cos\theta+\sigma_1\sin\theta\big)\beta-\sigma_1\mathcal{N}_p\sqrt{1-c^2}\big(\sigma_0\cos\theta+\sigma_1\sin\theta\big)\beta\\
&\quad+\mathrm{i}\sigma_2\big(\mathcal{N}_0+\mathcal{N}_p\big)\big(\sigma_0\cos\theta+\sigma_1\sin\theta\big)\beta-\sigma_3 c\mathcal{N}_p\big(\sigma_0\cos\theta+\sigma_1\sin\theta\big)\beta\\
=&\frac{c\sigma_0+\sigma_1}{\sqrt{1-c^2}}\big(\partial_X-\psi\big)\big(\sigma_0\cos\theta+\sigma_1\sin\theta\big)\beta-\sigma_1\mathcal{N}_p\sqrt{1-c^2}\big(\sigma_0\cos\theta+\sigma_1\sin\theta\big)\beta\\
&\quad+\mathrm{i}\big(\mathcal{N}_0+\mathcal{N}_p\big)\big(\sigma_0\cos\theta-\sigma_1\sin\theta\big)\sigma_2\beta-c\mathcal{N}_p\big(\sigma_0\cos\theta-\sigma_1\sin\theta\big)\sigma_3\beta\\
=&\lambda\big(\sigma_0\cos\theta+\sigma_1\sin\theta\big)\beta
\end{aligned}\tag{8.3.15}$$

In the last identity we have used the fact *that* σ_i *and* σ_j *anti-commute for* $i,j\in\{1,2,3\}$ *and* $i\neq j$. See (1.7.3). We would like to obtain a differential equation in which there is no coefficient in front of ∂_X. For this, we multiply on both sides (on the left) by

$$\sqrt{1-c^2}\big(\sigma_0\cos\theta+\sigma_1\sin\theta\big)^{-1}\big(c\sigma_0+\sigma_1\big)^{-1}\tag{8.3.16}$$

Note that $\sigma_0\cos\theta+\sigma_1\sin\theta$ and $c\sigma_0+\sigma_1$ commute, therefore so does their inverses. Explicitly, we have:

$$\big(c\sigma_0+\sigma_1\big)^{-1}=\frac{-c\sigma_0+\sigma_1}{1-c^2}$$

and, note that $\cos^2\theta-\sin^2\theta=\cos 2\theta=\sqrt{1-c^2}$, there is also

$$\big(\sigma_0\cos\theta+\sigma_1\sin\theta\big)^{-1}=\frac{\sigma_0\cos\theta-\sigma_1\sin\theta}{\sqrt{1-c^2}}$$

Now multiplying to the left by (8.3.16) on both sides of the last identity of (8.3.15):

$$\begin{aligned}
&\big(\partial_X-\psi\big)\beta-\big(-c\sigma_0+\sigma_1\big)\mathcal{N}_p\sigma_1\beta\\
&+\mathrm{i}\frac{-c\sigma_0+\sigma_1}{1-c^2}\big(\sigma_0\cos\theta-\sigma_1\sin\theta\big)^2\big(\mathcal{N}_0+\mathcal{N}_p\big)\sigma_2\beta\\
&-\frac{-c\sigma_0+\sigma_1}{1-c^2}\big(\sigma_0\cos\theta-\sigma_1\sin\theta\big)^2 c\mathrm{N}_p\sigma_3\beta\\
=&\frac{-c\sigma_0+\sigma_1}{\sqrt{1-c^2}}\lambda\beta=\big(-c\sigma_0+\sigma_1\big)\Lambda\beta
\end{aligned}\tag{8.3.17}$$

The second term of LHS of (8.3.17) is

$$-\big(-c\sigma_0+\sigma_1\big)\mathcal{N}_p\sigma_1\beta=\big(-\sigma_0+c\sigma_1\big)\mathcal{N}_p\beta \tag{8.3.18}$$

the third term:

$$\begin{aligned}
&\mathrm{i}\frac{-c\sigma_0+\sigma_1}{1-c^2}\big(\sigma_0\cos\theta-\sigma_1\sin\theta\big)^2\big(\mathcal{N}_0+\mathcal{N}_p\big)\sigma_2\beta\\
=&\mathrm{i}\frac{-c\sigma_0+\sigma_1}{1-c^2}\big(\sigma_0-\sigma_1\sin 2\theta\big)\big(\mathcal{N}_0+\mathcal{N}_p\big)\sigma_2\beta\\
=&\mathrm{i}\frac{-c\sigma_0+\sigma_1}{1-c^2}\big(\sigma_0+\sigma_1 c\big)\big(\mathcal{N}_0+\mathcal{N}_p\big)\sigma_2\beta=\mathrm{i}\sigma_1\big(\mathcal{N}_0+\mathcal{N}_p\big)\sigma_2\beta\\
=&-\big(\mathcal{N}_0+\mathcal{N}_p\big)\sigma_3\beta
\end{aligned} \tag{8.3.19}$$

where again $\sin 2\theta=-c$. The fourth term is

$$\begin{aligned}
&-\frac{-c\sigma_0+\sigma_1}{1-c^2}\big(\sigma_0\cos\theta-\sigma_1\sin\theta\big)^2 c\mathcal{N}_p\sigma_3\beta\\
=&\frac{c\sigma_0-\sigma_1}{1-c^2}\big(\sigma_0+\sigma_1 c\big)c\mathcal{N}_p\sigma_3\beta\\
=&-\sigma_1 c\mathcal{N}_p\sigma_3\beta=\mathrm{i}c\mathcal{N}_p\sigma_2
\end{aligned} \tag{8.3.20}$$

Combining (8.3.17), (8.3.18), (8.3.19) and (8.3.20):

$$\big(\partial_X-v\big)\beta+\big(-\sigma_0+c\sigma_1\big)\mathcal{N}_p\beta-\big(\mathcal{N}_0+\mathcal{N}_p\big)\sigma_3\beta+\mathrm{i}c\mathcal{N}_p\sigma_2=\big(-c\sigma_0+\sigma_1\big)\Lambda\beta$$

which is

$$\partial_X\beta=\sigma_0\big(\psi-c\Lambda+\mathcal{N}_p\big)\beta+\Lambda\sigma_1\beta-c\mathcal{N}_p\big(\sigma_1+\mathrm{i}\sigma_2\big)\beta+\big(\mathcal{N}_0+\mathcal{N}_p\big)\sigma_3\beta \tag{8.3.21}$$

Further, we let

$$\begin{aligned}
B(X)&:=e^{-c\Lambda X}\exp\left(\int_{-\infty}^{X}\psi(Y)+\mathcal{N}_p(Y)\,\mathrm{d}Y\right)\beta(X)\\
&=e^{-c\Lambda X}\exp\left(w_c\big(\sqrt{1-c^2}X\big)+\int_{-\infty}^{X}\mathcal{N}_p(Y)\,\mathrm{d}Y\right)\beta(X)
\end{aligned} \tag{8.3.22}$$

which is exactly (8.3.4). Plugging (8.3.22) into (8.3.21) we get rid of the first term on the RHS of (8.3.21):

$$\partial_X B = \Lambda\sigma_1 B - c\mathcal{N}_p\big(\sigma_1 + \mathrm{i}\sigma_2\big)B + \big(\mathcal{N}_0 + \mathcal{N}_p\big)\sigma_3 B$$

Equivalently, $B = \begin{bmatrix} U & V \end{bmatrix}^\mathsf{T}$ satisfies

$$\begin{aligned} U_X &= \big(\mathcal{N}_0 + \mathcal{N}_p\big)U + \big(\Lambda - 2c\mathcal{N}_p\big)V \\ V_X &= \Lambda U - \big(\mathcal{N}_0 + \mathcal{N}_p\big)V \end{aligned}. \tag{8.3.23}$$

which is exactly (8.3.6), and the proof of PROPOSITION 8.11 is done. □

The following result states that to preclude *unstable* discrete spectrum, it suffice to prove that there are no eigenpairs (B, Λ) of (8.3.6).

Lemma 8.13. *Assume* (8.3.3) *is satisfied by* $\mathtt{Re}\lambda > 0$ *and* $\tilde{B} \in L^2$. *Then* B *defined through* (8.3.4) *satisfying* (8.3.6) *with* $\Lambda = \frac{\lambda}{\sqrt{1-c^2}}$ *is in* L^2 *as well.*

Proof. By assumption $L_{*,w}\tilde{B}(x) = \lambda\tilde{B}(x)$. Since the coefficients of $L_{*,w}$ are all bounded and smooth with respect to x, $\tilde{B}(x)$ is actually smooth. Moreover, λ with $\mathtt{Re}\lambda > 0$ is not in the essential spectrum of $L_{*,w}$ since $a = \frac{K}{\sqrt{1-c^2}}$ satisfies the condition in PROPOSITION 8.1. Rewrite Hence there are constants $\mu_\pm$ with $\mathtt{Re}\mu \neq 0$ such that $\big|\tilde{B}(x)\big| = Ce^{\mu x}(1 + o(1))$ as $x \to \infty$; similarly for $x \to -\infty$. As a result, $\tilde{B} \in L^2$ if and only if $\tilde{B}(x) = o(1)$ as $|x| \to \infty$. From the transform (8.3.7) relating $\tilde{B}$ and β, $\tilde{B} \in L^2$ if and only if $\beta \in L^2$, if and only if $\beta(X) = o(1)$ as $|X| \to \infty$.

Now assume $\beta \in L^2$ and rewrite (8.3.22) as

$$B(X) = e^{g(X)}\beta(X)$$

where

$$g(X) = -c\Lambda X + w_c\big(\sqrt{1-c^2}X\big) + \int_{-\infty}^{X} \mathcal{N}_p(Y)\,\mathrm{d}Y$$

For $X \geq \frac{1}{\sqrt{1-c^2}}$, $w_c\big(\sqrt{1-c^2}X\big) = KX$, see (8.3.9); and $\mathcal{N}_p(X) = \mathcal{N}'\big(r_0(X)^2\big)r_0(X)^2$ approaches

$-K$ exponentially fast as $X \to \infty$, because $r_0(X)^2$ approaches 1 exponentially fast. So $g(X) = -c\Lambda X + O(1)$ as $X \to \infty$. Since $\mathtt{Re}\Lambda > 0$, if $\beta \in L^2$, there must be $B(X) \to 0$ (exponentially fast) as $X \to \infty$.

On the other hand $g(X) = -c\Lambda X + o(1)$ as $X \to -\infty$ since $w_c\big(\sqrt{1-c^2}X\big) = 0$ for $X \le \frac{1}{\sqrt{1-c^2}}$, and $\mathcal{N}_p(X) \to 0$ exponentially fast. Since (8.3.23) is also exponentially asymptotically constant, as $X \to -\infty$, $B(X)$ also behaves exponentially. There must be $B(X) \sim e^{\mu X}$ where μ satisfies the following, obtained by taking limits of the coefficients of (8.3.23) (note that $\mathcal{N}_0(-\infty) = 1$ and $\mathcal{N}_p(-\infty) = 0$):

$$\det \begin{bmatrix} 1-\mu & \Lambda \\ \Lambda & -1-\mu \end{bmatrix} = 0$$

namely $\mu = \pm\sqrt{1+\Lambda^2}$. Since $\beta(X) = o(1)$ as $X \to -\infty$,

$$B(X) = o\big(e^{-c\Lambda X}\big), \quad \text{as } X \to -\infty \tag{8.3.24}$$

This forces $B(X) \sim e^{\sqrt{1+\Lambda^2}X}$ since otherwise there must be $B(X) \sim e^{-\sqrt{1+\Lambda^2}X}$. Due to the following relation

$$e^{-c\Lambda X} = o\Big(e^{-\sqrt{\Lambda^2+1}X}\Big), \quad \text{as } X \to -\infty \tag{8.3.25}$$

so condition (8.3.24) is violated. To prove (8.3.25), note that $\mathtt{Re}\big(-\sqrt{1+\Lambda^2}\big) < \mathtt{Re}(-\Lambda)$ since $\mathtt{Re}\Lambda > 0$, by the following elementary fact:

$$\mathtt{Re}\sqrt{z^2+1} > \mathtt{Re}z, \quad \text{for } \mathtt{Re}z > 0 \tag{8.3.26}$$

and thus

$$\mathtt{Re}\big(c\Lambda - \sqrt{1+\Lambda^2}\big) < \mathtt{Re}\big(c\Lambda - \Lambda\big) < 0$$

with $0 \le c < 1$, so $\mathtt{Re}(-c\Lambda) > \mathtt{Re}\big(-\sqrt{\Lambda^2+1}\big)$, and $\mathtt{Re}\big(-c\Lambda X\big) < \mathtt{Re}\big(-\sqrt{\Lambda^2+1}X\big)$ for $X < 0$. As a result (8.3.25) holds.

So $B(X) \sim e^{\sqrt{1+\Lambda^2}X} \to 0$ as $X \to -\infty$. Therefore if $\beta \in L^2$, there must be $B(X) \to 0$

exponentially fast as $|X| \to \infty$, which implies $B \in L^2$.

Now we prove inequality (8.3.26) [1] Note that for any $z \in \mathbb{C}$,

$$\mathtt{Re}z = \frac{1}{2}\left(z + \frac{z\bar{z}}{z}\right). \tag{8.3.27}$$

Write $z = re^{\mathrm{i}\theta}$. Since $\mathtt{Re}z > 0$, where $-\pi/2 < \theta < \pi/2$. Equation (8.3.26) becomes $r\cos\theta < \mathtt{Re}\sqrt{r^2 e^{2i\theta} + 1}$. Dividing by r, we find that (8.3.26) is equivalent to

$$\mathtt{Re}\sqrt{r^{-2} + e^{\mathrm{i}2\theta}} > \cos\theta, \quad -\pi/2 < \theta < \pi/2.$$

Note that the real part of $\sqrt{\cdot}$ is always nonnegative, it is equivalent to prove

$$2\left[\mathtt{Re}\sqrt{s + e^{\mathrm{i}2\theta}}\right]^2 - 2\cos^2\theta > 0, \quad s \equiv r^{-2} > 0, \quad -\pi/2 < \theta < \pi/2.$$

Using (8.3.27), the LHS satisfies

$$\begin{aligned}
&\frac{1}{2}\left[\left(s + e^{\mathrm{i}2\theta}\right)^{1/2} + \frac{\left(s^2 + 1 + 2s\cos 2\theta\right)^{1/2}}{\left(s + e^{\mathrm{i}2\theta}\right)^{1/2}}\right]^2 - 2\cos^2\theta \\
=&2 \times \frac{1}{4}\left[s + e^{\mathrm{i}2\theta} + 2\left(s^2 + 1 + 2s\cos 2\theta\right)^{1/2} + s + e^{-\mathrm{i}2\theta}\right] - 2\cos^2\theta \\
=&s + \cos 2\theta + \left(s^2 + 1 + 2s\cos 2\theta\right)^{1/2} - \cos 2\theta - 1 \\
=&s + \left(s^2 + 1 + 2s\cos 2\theta\right)^{1/2} - 1 > s + |s - 1| - 1 \geq 0
\end{aligned}$$

with $s > 0$ and $\cos 2\theta \neq -1$ since the latter requires $\theta = \pm\pi/2$, contradicting the requirement that $\mathtt{Re}z = r\cos\theta > 0$. Thus we have concluded the proof of (8.3.26).

□

We now show there is no $B \in L^2$ that satisfies (8.3.6) with some $\mathtt{Re}\Lambda > 0$. We proceed with shorthand $F(X) = \mathcal{N}_0(X) + \mathcal{N}_p(X)$ and $f = 2c\mathcal{N}_p(X)$. Acting ∂_X on both sides of the second equation of (8.3.6), then use the first equation for U_X, we obtain a closed equation for V

---

[1] The authors thank Dr. SUN Guanhao of UCSD for pointing out this is not a trivial fact and for providing the following proof.

$$V_{XX} = \left(F^2 - F_X\right)V + \Lambda\left(\Lambda - f\right)V \tag{8.3.28}$$

Lemma 8.14. *Assume* $\mathrm{Re}\Lambda > 0$*, and that the nonlinearity* $\mathcal{N}(r^2)$ *satisfies the concavity condition* (8.3.2)*:*

$$\mathcal{N}''(s) \le 0$$

For $s \in [0,1]$*, along with hypotheses (*$\mathcal{N}$*1) to (*$\mathcal{N}$*4) in* SECTION *1.3. Then, the only* $V \in L^2$ *that satisfies* (8.3.28) *is* $V \equiv 0$.

Proof. Suppose $0 \ne V \in L^2(\mathbb{R})$. Then, V is also smooth. Take L^2-inner product of V with (8.3.28) and obtain

$$\|V\|_{L^2}^2 \Lambda^2 + \left\langle V, -fV \right\rangle_{L^2} \Lambda + \left\langle V, \left(F^2 - F_X\right)V \right\rangle_{L^2} + \|V_X\|_{L^2}^2 = 0 \tag{8.3.29}$$

a quadratic equation in Λ. We claim that the coefficients of this quadratic are all non-negative. Note that the quadratic coefficient of (8.3.29), namely $\|V\|_{L^2}^2 > 0$, and

$$-f = -2c\mathcal{N}_p = -2c\mathcal{N}'\left(r_0(X)^2\right)r_0(X)^2 \ge 0$$

since $\mathcal{N}$ is monotonically decreasing; so the linear coefficient $\left\langle V, -fV \right\rangle_{L^2} \ge 0$ as well. Furthermore, $F_X \le 0$. In fact, since $r_0(X)$ is monotonically increasing in X, and

$$F = \mathcal{N}_0 + \mathcal{N}_p = \mathcal{N}\left(r_0(X)^2\right) + \mathcal{N}'\left(r_0(X)^2\right)r_0(X)^2$$

is monotonically *decreasing* in $r_0(X)^2$. $\mathcal{N}$ is so by definition, and as a result of the concavity condition (8.3.2), there is also $\mathcal{N}' \le 0$ monotonically decreases in $r_0(X)^2$. Therefore $F_X \le 0$ and $F^2 - F_X \ge 0$ whence $\left\langle V, \left(F^2 - F_X\right)V \right\rangle_{L^2} \ge 0$. We conclude that Λ is a root of a quadratic polynomial:

$$c_2\Lambda^2 + c_1\Lambda + c_0 = 0$$

where $c_2 > 0$, $c_1, c_0 \geq 0$. It is easily checked that either Λ is one of two negative real roots or its real part is equal to $-c_1/2c_0 \leq 0$. In all cases, $\mathtt{Re}\Lambda \leq 0$, contradicting the assumption that $\mathtt{Re}\Lambda > 0$. As a result there is no Λ with nonnegative real part such that (8.3.29) holds. This argument carries over for any $V \in L^2$ and we will be done. □

Now we summarize the discussion above and give the proof of THEOREM 8.8:

Proof of THEOREM *8.8*. The essential spectrum of L_{*,w_c} is in the closed left-half plane since $a = \frac{K}{\sqrt{1-c^2}}$, satisfying the condition (8.1.2) in PROPOSITION 8.1.

Assume there was an eigenpair $\lambda, \tilde{B}$ of L_{*,w_c}, where $\mathtt{Re}\lambda > 0$ and $\tilde{B} \in L^2$. Then by LEMMA 8.13, there would be a pair $\Lambda = \frac{\lambda}{\sqrt{1-c^2}}, B = \begin{bmatrix} U & V \end{bmatrix}^{\mathsf{T}} \in L^2$ which would solve the generalized eigenvalue problem (8.3.6). In particular we would have $\mathtt{Re}\Lambda > 0$ and $V \in L^2$. Such V would in fact be smooth since the coefficients in (8.3.6) are bounded and smooth. As a result the pair $\Lambda, V \in L^2$ would solve a generalized eigenvalue problem expressed by a second-order variant coefficient ODE, namely (8.3.28). However such V does not exist by LEMMA 8.14.

Therefore *the assumption does not hold*; namely $L_{*,w}$ does not have any eigenvalue with a positive real part.

Thus $\sigma\left(L_{*,w_c}\right)$ is contained in the closed left-half plane, and by DEFINITION 5.1, moving kinks with nonlinearity concave on $r^2 \in [0, 1]$ are spectrally stable in the weighted space $L^2_{w_c}$ where $w_c(x)$ is given by (8.3.1). □

Conclusions and open problems

We have shown there are a rich family of traveling wave solutions of (1.0.1), in both supersonic ($|c| > 1$) and subsonic ($|c| < 1$) regimes; CHAPTER 2. The bounded traveling wave solutions are the either heteroclinic connections in a 2D phase space between the zero solution and an equilibrium on the unit circle (kinks, antikinks) or heteroclinic connections between distinct equilbria on the unit circle (pulses). We have proved, for saturable nonlinearities, that supersonic pulses are both nonlinearly convectively stable against perturbations (which decay rapidly as $x \to +\infty$. This follows from an a priori bound on general solutions and finite propagation speed property for the semilinear hyperbolic system (1.0.1) (THEOREM 4.1). We have also proved their linear spectral stablility (THEOREM 7.1) in an appropriate weighted L^2 space. For antikinks and subsonic pulses, are no exponential-type weights, with respect to which linearized system is spectrally stable; an instability arises from that of the asymptotic equilibria; SECTION 7.3. Finally, in CHAPTER 8 we demonstrated the spectral stability of kink solutions in suitably weighted L^2 spaces: (a) for the case of non-moving kinks ($c = 0$) (THEOREMS 8.3) and (b) for arbitrary kinks ($|c| < 1$) under a concavity condition on the nonlinearity (THEOREM 8.8).

Appendix A: Numerical schemes for simulation

A.1 Dynamical simulation

In order to numerically compute the solution of the IVP associated with equation (2.0.1), we use the finite difference method [25]. We have used fourth-order discretization of spatial derivative of ∂_x, but to replace for it with other discretization schemes can also be easily done:

$$\partial_x f \approx \frac{-f_{i+2} + 8f_{i+1} - 8f_{i-1} + f_{i-2}}{12\Delta x} \tag{A.1.1}$$

where Δx is the spatial grid size, on a domain $[0, L]$, and the grid points are

$$x_0 = 0;\ x_i = i\Delta x;\ x_N = N\Delta_x = L \tag{A.1.2}$$

to obtain an ODE of $2N+2$ variables. We impose the homogeneous Neumann boundary condition.

We use the Radau-II scheme to solve the discretized ODE, which is a fully implicit RK scheme[26] with Butcher table

$$\begin{bmatrix} c & A \\ & b^{\mathsf{T}} \end{bmatrix} \tag{A.1.3}$$

where

$$A = \begin{bmatrix} \frac{1}{9} & \frac{-1-\sqrt{6}}{18} & \frac{-1+\sqrt{6}}{18} \\ \frac{1}{9} & \frac{88+7\sqrt{6}}{360} & \frac{88-43\sqrt{6}}{360} \\ \frac{1}{9} & \frac{88+43\sqrt{6}}{360} & \frac{88-7\sqrt{6}}{360} \end{bmatrix} \tag{A.1.4}$$

and

$$b^{\mathsf{T}} = \begin{bmatrix} \frac{1}{9} & \frac{16+\sqrt{6}}{36} & \frac{16-\sqrt{6}}{36} \end{bmatrix} \tag{A.1.5}$$

we do not need c here since the discretized ODE is still autonomous.

This in matrix form of the discretized ODE is

$$\frac{\mathrm{d}\vec{b}}{\mathrm{d}t} = \vec{F}(\vec{b}) \tag{A.1.6}$$

where

$$\vec{F}(\vec{b}_m) = \begin{bmatrix} f(\vec{b}_m[0]) \\ f(\vec{b}_m[1]) \\ \vdots \\ f(\vec{b}_m[2i]) \\ f(\vec{b}_m[2i+1]) \\ \vdots \\ f(\vec{b}_m[2N]) \\ f(\vec{b}_m[2N+1]) \end{bmatrix} = (D^{(4)} + N) \begin{bmatrix} \vec{b}_m[0] \\ \vec{b}_m[1] \\ \vdots \\ \vec{b}_m[2i] \\ \vec{b}_m[2i+1] \\ \vdots \\ \vec{b}_m[2N] \\ \vec{b}_m[2N+1] \end{bmatrix} = (D^{(4)} + N)\vec{b}_m \tag{A.1.7}$$

where

$$D^{(4)} = \frac{1}{12\Delta x} \begin{bmatrix} & & & \cdots & & & \\ & & & \vdots & & & \\ \cdots & \sigma_1 & -8\sigma_1 & 0 & 8\sigma_1 & -\sigma_1 & \cdots \\ & & & \vdots & & & \\ & & & \cdots & & & \end{bmatrix} \tag{A.1.8}$$

of which the first two and the last two rows are zero, and N is block diagonal and consists of blocks

$$\begin{bmatrix} 0 & \mathcal{N}\left(\vec{b}_m[2i]^2 + \vec{b}_m[2i+1]^2\right) \\ -\mathcal{N}\left(\vec{b}_m[2i]^2 + \vec{b}_m[2i+1]^2\right) & 0 \end{bmatrix} \tag{A.1.9}$$

for $i = 0, \cdots N$

For the Newton-Raphson [26] root-finding method used in each step of the Radau-II scheme, we need to calculate the Jacobian of $\vec{F}$, which is

$$\vec{F}'(\vec{b}) = D^{(4)} + \mathcal{N} + \left[\sum_{k=0}^{2N+1} \frac{\partial \mathcal{N}(\vec{b})_{ik}}{\partial \vec{b}_j}\vec{b}_k\right]_{ij} \tag{A.1.10}$$

where the last term is a block-diagonal matrix consisting of

$$\frac{N'\left(\sqrt{\vec{b}_m[2i]^2 + \vec{b}_m[2i+1]^2}\right)}{\sqrt{\vec{b}_m[2i]^2 + \vec{b}_m[2i+1]^2}} \begin{bmatrix} \vec{b}_m[2i]\vec{b}_m[2i+1] & \vec{b}_m[2i+1]^2 \\ -\vec{b}_m[2i]^2 & -\vec{b}_m[2i]\vec{b}_m[2i+1] \end{bmatrix} \tag{A.1.11}$$

We exploit the fact that all the matrices encountered (for example $\vec{F}'$) in the numerical scheme that are of size $\mathcal{O}(N) \times \mathcal{O}(N)$ are sparse[27] with only $\mathcal{O}(N)$ nonzero entries on the diagonal as well as a few lower- and upper-diagonals. As a result the numerical scheme runs with time $\mathcal{O}(MN)$ where $M = T/\Delta t$ with T the simulated time and Δt the size of each time-step.

References

[1] Y. Hadad, V. Vitelli, and A. Alu, “Solitons and propagating domain walls in topological resonator arrays,” *ACS Photonics*, vol. 4, pp. 1974–1979, 2017.

[2] Y. Hadad, A. B. Khanikaev, and A. Alu, “Self-induced topological transitions and edge states supported by nonlinear staggered potentials,” *Physical Review B*, vol. 93, no. 15, p. 155 112, 2016.

[3] W. P. Su, J. R. Schrieffer, and A. J. Heeger, “Solitons in polyacetylene,” *Physical Review Letters*, vol. 42, p. 1698, 1979.

[4] W.-P. Su, J. Schrieffer, and A. Heeger, “Soliton excitations in polyacetylene,” *Physical Review B*, vol. 22, no. 4, p. 2099, 1980.

[5] W. Su and J. Schrieffer, “Soliton dynamics in polyacetylene,” *Proceedings of the National Academy of Sciences*, vol. 77, no. 10, pp. 5626–5629, 1980.

[6] N. Batra and G. Sheet, “Understanding basic concepts of topological insulators through su-schrieffer-heeger (ssh) model,” *arXiv preprint arXiv:1906.08435*, 2019.

[7] J. K. Asbóth, L. Oroszlány, A. Pályi, J. K. Asbóth, L. Oroszlány, and A. Pályi, “The su-schrieffer-heeger (ssh) model,” *A Short Course on Topological Insulators: Band Structure and Edge States in One and Two Dimensions*, pp. 1–22, 2016.

[8] P. A. M. Dirac, *The principles of quantum mechanics*. Oxford university press, 1981.

[9] Q. Du, H. Li, M. Weinstein, and L. Zhang, “Discontinuous galerkin methods for a first-order semi-linear hyperbolic continuum model of a topological resonator dimer array,” *arXiv preprint arXiv:2305.00072*, 2023.

[10] R. L. Pego and M. I. Weinstein, “Asymptotic stability of solitary waves,” *Communications in Mathematical Physics*, vol. 164, no. 2, pp. 305–349, 1994.

[11] Y. Martel and F. Merle, “Asymptotic stability of solitons for subcritical generalized kdv equations,” *Archive for rational mechanics and analysis*, vol. 157, pp. 219–254, 2001.

[12] R. L. Pego and M. I. Weinstein, “Convective linear stability of solitary waves for boussinesq equations,” *Studies in Applied Mathematics*, vol. 99, no. 4, pp. 311–375, 1997.

[13] J. R. Miller, “Spectral properties and time decay for an airy operator with potential,” *journal of differential equations*, vol. 141, no. 1, pp. 102–121, 1997.

[14] R. A. Fisher, “The wave of advance of advantageous genes,” *Annals of eugenics*, vol. 7, no. 4, pp. 355–369, 1937.

[15] A. Kolmogorov, “Étude de l’équation de la diffusion avec croissance de la quantité de matière et son application à un problème biologigue,” *Moscow Univ. Bull. Ser. Internat. Sect. A*, vol. 1, p. 1, 1937.

[16] G. Schneider and H. Uecker, *Nonlinear PDEs*. American Mathematical Soc., 2017, vol. 182.

[17] G. B. Folland, “Introduction to partial differential equations,” in *Introduction to Partial Differential Equations*, Princeton university press, 2020.

[18] M. Reed, *Abstract nonlinear wave equations*. Springer, 1976.

[19] R. Goodman, M. Weinstein, and P. Holmes, “Nonlinear propagation of light in one-dimensional periodic structures,” *J. Nonlinear Sci.*, vol. 11, pp. 123–168, 2001.

[20] J. K. Hunter and B. Nachtergaele, *Applied analysis*. World Scientific Publishing Company, 2001.

[21] J. R. Miller and M. I. Weinstein, “Asymptotic stability of solitary waves for the regularized long-wave equation,” *Communications on pure and applied mathematics*, vol. 49, no. 4, pp. 399–441, 1996.

[22] T. Kapitula and K. Promislow, *Spectral and dynamical stability of nonlinear waves*. Springer, 2013, vol. 457.

[23] D. E. Edmunds and W. D. Evans, *Spectral theory and differential operators*. Oxford University Press, 2018.

[24] H. Hanche-Olsen and H. Holden, “The kolmogorov–riesz compactness theorem,” *Expositiones Mathematicae*, vol. 28, no. 4, pp. 385–394, 2010.

[25] J. W. Thomas, *Numerical partial differential equations: finite difference methods*. Springer Science & Business Media, 2013, vol. 22.

[26] D. F. Griffiths and D. J. Higham, *Numerical methods for ordinary differential equations: initial value problems*. Springer, 2010, vol. 5.

[27] G. Allaire, S. M. Kaber, K. Trabelsi, and G. Allaire, *Numerical linear algebra*. Springer, 2008, vol. 55.